THE UNIVERSITY OF OKLAHOMA

GRADUATE COLLEGE

DEVELOPMENT AND VALIDATION OF METRICS TO EVALUATE ROBOTICS OPERATOR PERFORMANCE

A DISSERTATION

SUBMITTED TO THE GRADUATE FACULTY

in partial fulfillment of the requirements for the degree of

DOCTOR OF PHILOSOPHY

By

TAMY L. FRY

Norman, Oklahoma

2003

UMI Number: 3107292

INFORMATION TO USERS

The quality of this reproduction is dependent upon the quality of the copy submitted. Broken or indistinct print, colored or poor quality illustrations and photographs, print bleed-through, substandard margins, and improper alignment can adversely affect reproduction.

In the unlikely event that the author did not send a complete manuscript and there are missing pages, these will be noted. Also, if unauthorized copyright material had to be removed, a note will indicate the deletion.

UMI®

UMI Microform 3107292

Copyright 2004 by ProQuest Information and Learning Company.

All rights reserved. This microform edition is protected against unauthorized copying under Title 17, United States Code.

ProQuest Information and Learning Company
300 North Zeeb Road
P.O. Box 1346
Ann Arbor, MI 48106-1346

© Copyright by Tamy L. Fry 2003

All Rights Reserved.

DEVELOPMENT AND VALIDATION OF METRICS

TO EVALUATE ROBOTICS OPERATOR PERFORMANCE

A DISSERTATION

APPROVED FOR THE SCHOOL OF INDUSTRIAL ENGINEERING

BY

Robert E. Schlegel

Dr. Robert E. Schlegel (Committee Co-Chair)

Randa L. Shehab

Dr. Randa L. Shehab (Committee Co-Chair)

Mary C. Court

Dr. Mary C. Court (Committee Member)

Teri Reed Rhoads

Dr. Teri Reed-Rhoads (Committee Member)

Kirby Gilliland

Dr. Kirby Gilliland (Committee Member)

ACKNOWLEDGEMENTS

It has been a very long journey. Along the way, I made new friends, parted from old friends, and made a few wrong turns. However, having reached the end of this road, I am eager to start along another path. I end this journey much wiser. Looking back, I realize that my quest could never have been accomplished without the aid and support of many people. In particular, I would like to express my gratitude to my committee members for their contributions to my education and to my progress along the way. The journey was made possible through research funding provided under NASA Grant NAG 9-1486, for which I am truly thankful. I must also express my sincere gratitude for the kind support of the NASA personnel who generously provided the vital information, training, and administrative and technical support needed to conduct this research. Special thanks go to Daniel Walker for the long hours he spent on software development for the study. I would also like to thank the other members of the NASA research team at OU: Teryn Bray, Tyler Akagi, and Laura Deaton, who were unfailingly supportive and helped me in many ways. I have greatly enjoyed their company. Similarly, my fellow students John Eichman and Kash Barker lightened my load and my spirits many times, and I am grateful to call them friends. I will think of them fondly each day at lunchtime. Although he was not here in person, my friend Byeong-Cheol Hwang was a constant companion on my journey. His correspondence never failed to brighten my day. Most of all, I am forever grateful to my family, Chester, Briana, Chuck, and Sean, who deserve the bulk of credit for my completion; they carried me when I was weary, led me when I was lost, and loved me unconditionally.

TABLE OF CONTENTS

LIST OF TABLES

Table **Page**

LIST OF TABLES

Table **Page**

LIST OF FIGURES

Figure **Page**

LIST OF FIGURES

Figure **Page**

ABSTRACT

Remote Manipulator Systems (RMS) aboard the International Space Station and the Space Shuttle assist in payload management, crew movement, retrieval of objects from space, and station construction. Safe, accurate, and efficient use of the robot arm requires accurate interpretation of visual cues (visual/spatial perception), an awareness of the position of the arm relative to structures (situation awareness), and appropriate controller inputs (psychomotor control). Errors in RMS operation can be catastrophic, leading to huge monetary losses or loss of life.

Generic Robotics Training (GRT) uses the Basic Operational Robotics Instructional System (BORIS) graphics simulator to teach basic robotics concepts and skills that are transferable to any of the on-orbit RMS systems. Currently, operator competency is assessed on a five-point scale by an "expert" observer. There is a need for quantitative performance metrics that would achieve an objective, reliable, and sensitive evaluation of RMS operator capabilities.

Toward these efforts, the objectives of this dissertation were to develop and validate objective performance metrics for RMS operators to facilitate operator screening, provide training feedback, and examine performance changes over time. The development of the research methodology represents a major contribution of the dissertation. Preliminary investigation identified smooth hand controller inputs (ramping) and multi-axis commanding as skills that are critical to the safe, effective operation of the RMS robotic arm. Theoretical models of expert performance were developed that helped to identify critical aspects of these skills. Performance metrics were selected that quantified the differences observed during comparisons of actual operator performance with the theoretical models. Observed control strategies were discussed from a human factors standpoint.

Validation of the metrics was achieved in an empirical study during which twelve novice operators performed a series of targeted movement tasks designed to evaluate ramping performance and the use of multi-axis control. Ramping performance was assessed by examining velocities and accelerations, R-square values (representing smoothness of the commanded inputs), completion times, and distances traveled during the ramp-in, travel, ramp-out, and correction phases of the task. Multi-axis control was assessed by examining percentages of control usage (single, dual, and triple-axis), lag times, completion times, accelerations, and correction times. A combination of univariate and multivariate statistical techniques was used to evaluate the sensitivity of the metrics to differences between task characteristics, operators, and changes in performance over time. MANOVA results indicated that ramping performance was significantly affected by movement distance ($F_{7,5} = 333.02$, $p < .0001$) and operator ($F_{77,103.32} = 6.86$, $p < .0001$), and multi-axis performance varied significantly due to task distance ratios ($F_{4,8} = 22.63$, $p = .0002$), replicate ($F_{4,8} = 35.87$, $p < .0001$), and operator ($F_{44,1727.4} = 19.85$, $p < .0001$). A select subset of the metrics was successful in providing a reasonable classification of RMS operator performance.

DEVELOPMENT AND VALIDATION OF METRICS TO EVALUATE ROBOTICS OPERATOR PERFORMANCE

CHAPTER 1

INTRODUCTION

The history of human spaceflight covers a relatively short span of time, with the first successful orbit of the earth by an American astronaut occurring on February 20, 1962. Over the past twenty years, the additions of the Space Shuttle program and the International Space Station (ISS) have resulted in an increase in human-flight frequency and duration of stay in space. At the end of 2001, the average duration of a shuttle flight was 12 days, and continuous human presence onboard the ISS had exceeded one full year. The inhabitants of the space station included five Russian cosmonauts and four American astronauts who resided in-orbit for durations of four to six months each. During 2001, the space station hosted seventy additional visitors who arrived on six Shuttle flights and three Soyuz flights to bring supplies, exchange crewmembers, and help in assembly tasks [NASA, 2002b]. Despite the increases in frequency and duration of space travel, mission demands continue to strictly limit the availability of astronaut time. Because of the limited opportunities for in-flight research and limitations of in-flight research protocols, there is little research available that addresses the impact of the environmental and task demands that astronauts must face during spaceflight.

1.1 Performance Shaping Factors in Space

The space environment is extremely hostile to humans, with potential exposure to high radiation levels, extreme temperatures, vacuum, lack of oxygen, and zero gravity. Known physiological effects include postural changes, decreased dexterity, space sickness, disorientation, loss of equilibrium, decreased bone mass, and muscle atrophy [Smart, 2000]. Some of the factors that have the potential to affect astronaut cognitive performance include the microgravity environment, high stress due to the criticality of errors, heavy workload, sleep deficits, time pressures, isolation, fatigue, and shift changes. To date, substantially more research has been devoted to determining the physiological effects rather than evaluating the cognitive or psychological effects of these factors. However, considering the complexity and criticality of tasks facing today's astronauts, the increasing length of shuttle missions, and the near-completion of the International Space Station, a more global understanding of the factors that affect astronaut performance, both physical and cognitive, has become increasingly important.

Microgravity effects on cognitive and psychomotor performance have been the focus of several studies. Significant effects have been reported for movement time, time perception, time-sharing, and tracking performance, while reaction times, accuracy, memory, and logical reasoning were relatively unaffected [Eddy, Schiflett, Schlegel, & Shehab, 1998]. These conclusions were supported by Manzey, Lorenz, and Poljakov [1998] in an investigation of the long-term effects of microgravity on a Russian cosmonaut during a 438-day mission aboard the MIR space station. The authors reported that basic cognitive processes such as memory and logic were unaffected, but significant impairments were exhibited in attention and motor control (tracking and simultaneous tracking with memory search). Decrements in motor control (tracking ability) were most pronounced during transitional phases of flight: just after entering orbit and again upon returning to earth. Manzey et al. [1998] believed these effects to be an indicator of the high sensitivity of the tracking task to the effects of astronaut fatigue and adaptation to the change in gravitational conditions. While tracking performance was shown to stabilize over time after these transitional shifts, dual-task performance (tracking with simultaneous memory search) showed increasing decrements over time in zero gravity [Manzey et al., 1998].

A subsequent examination of performance in microgravity during a 20-day MIR mission focused on identifying the specific causes of the degradations found in tracking performance [Manzey, Lorenz, Heuer, & Sangals, 2000]. The authors identified differences in effective time-delay, gain, and remnant noise in the tracking control at different stages of flight, and suggested that the decrements upon entry into space represent microgravity effects (i.e., slowing of visuo-motor processing), while later performance degradation may be attributed to stress factors such as workload and fatigue.

1.2 Identified Needs

One of the more difficult tasks that astronauts must perform is operation of the remote manipulator systems (RMS), which requires complex cognitive and psychomotor skills. These systems have been placed aboard the International Space Station and the Space Shuttle to assist in space operations such as material management, transportation, loading and retrieval, and construction. The Shuttle Remote Manipulator System (SRMS) is a 50 ft (15.2 m) long telerobotic arm with six-degree-of-freedom (6-DOF) movement capability. Movement of the arm is remotely controlled by an astronaut using two hand controllers (one translational and one rotational) while monitoring the task on closed-circuit video displays [IEEE, 2001]. Control of the RMS system in the complex and dynamic space environment is challenging, even when the operator is highly experienced. In addition, many of the tasks involving operation of the robotic arm are performed under physical and/or psychological pressure. These tasks often require both speed and accuracy, and the consequences for mistakes can be catastrophic, leading to huge monetary losses or loss of life.

The effectiveness of the method used to evaluate expertise and performance capability of an RMS operator is critical. Currently, assessment of skill acquisition is conducted during training by an "expert" observer. While this method may be adequate for determining an "achieved" skill level, it is impractical for evaluating performance outside of the training facility, where the operator may experience uncontrolled conditions and be subjected to a number of stressors. For example, sleep deprivation has been shown to significantly affect performance on a surgical training simulation tool [Shah & Darzi, 2001]. RMS operations would benefit by a more objective means of assessing expertise, which could be extended to enable a quick and effective means of self-assessment of readiness to perform.

In order to be effective, a self-assessment tool should be quick and easy to administer, provide a reliable, objective evaluation of the performance capabilities of the operator, be sensitive to degradations in performance, and furnish timely, easily understood results. Toward this effort, this dissertation presents the results of an effort to develop performance metrics that would achieve an objective, reliable, and sensitive evaluation of RMS operator capabilities.

1.3 Dissertation Genesis

Since 1992, a team of researchers at the University of Oklahoma has conducted several studies to investigate the effects of microgravity on cognitive performance. Simultaneously, members of the team initiated a separate line of research on evaluating a worker's readiness to perform (RTP). "Readiness to Perform" refers to the ability of an individual worker to effectively perform expected tasks with minimal risk of error or injury [Gilliland & Schlegel, 1993]. RTP implies that the individual is not influenced by factors, either internal or external, that would potentially lead to decrements in performance. A measure of an individual's readiness to perform is not an assurance against error; rather, it is an indication of an individual's *potential* to perform relative to that person's *normal* performance.

Evaluation of RTP is generally achieved using computer-based assessment tasks that measure cognitive and psychomotor abilities. Information from these tests is valuable in applications where safety is critical and where human errors would have serious results. For example, RTP tests have been employed in aerospace and aeronautic applications to evaluate the effects of alcohol, antihistamines, sleep loss, and microgravity on the performance of air traffic controllers, pilots, and astronauts. As individual responses to these stressors can vary greatly, RTP tests are typically not intended to evaluate group results, although the measures themselves are generalizable to a larger population. Nor do the tests attempt to isolate or assign cause. Rather, RTP tests are meant to provide a quick, effective means to evaluate the performance of an individual and identify any significant change relative to that individual's normal (baseline) performance. In this way, RTP tests are analogous to the quality control tests used in industry, and to single-subject research designs employed in the clinical and behavioral sciences [Shehab & Schlegel, 2000]. For a comprehensive review describing the development of RTP test batteries, along with details related to specific procedures, tasks, and outputs, refer to the works of Gilliland and Schlegel [1993] and Kane and Kay [1992].

University of Oklahoma researchers have employed RTP test batteries to determine the effects of a number of known "risk factors" including caffeine, alcohol, sleep loss, over-the-counter cold and allergy medications (antihistamines), and microgravity [Schlegel & Gilliland, 1990; Eddy et al., 1998; Gilliland, Schlegel, & Nesthus, 1999]. The NASA Performance Assessment Workstation (PAWS) was used to evaluate microgravity effects on two separate shuttle flights, STS-65 in 1994, and STS-78 in 1996. This task battery included two subjective rating scales that assessed psychological states (mood and fatigue) and six performance tests (Critical Tracking, Sternberg Memory Search, Continuous Recognition Memory, Dual Task – Tracking and Memory Search, Directed Attention – Manikin and Mathematical Processing, and Spatial Matrix Rotation) that measured tracking, short-term memory, dual-task timesharing, attention, and spatial / mathematical reasoning. Significant effects were reported for tracking performance, while reaction times, accuracy, memory, and logical reasoning were relatively unaffected [Eddy et al., 1998]. While fatigue was suggested to contribute to cognitive declines, degraded psychomotor performance was largely attributed to adaptation effects of the visuo-motor system while entering and leaving the microgravity environment.

Currently, two related research efforts are being conducted at the University of Oklahoma. The first effort, titled "*Integrated Crew Performance Assessment and Training*," focuses on the development of adaptive, dynamic-load tasks as a tool for the self-assessment of astronaut cognitive and psychomotor states [Schlegel, Shehab, & Gilliland, 2000]. The second effort, "*The Development and Validation of Remote Manipulator System (RMS) Operator Proficiency and Training Effectiveness Metrics*," parallels the measurement of performance on the dynamic-load tasks with the assessment of performance on a comparable, real-world task — RMS operation. In order to validate the ability of the dynamic-load tasks to predict astronaut performance, the researchers need to show that the tasks provide reliable, sensitive, objective measures that are predictive of complex task performance. To accomplish this goal requires similar measures of RMS operator performance [Schlegel, Gilliland, & Shehab, 2002]. Hence, in support of these efforts, this dissertation outlines the framework for developing RMS performance metrics, and presents the development and validation of potential metrics for two critical aspects of RMS operator performance.

CHAPTER 2

PROBLEM BACKGROUND

2.1 Remote Manipulator System

The Shuttle Remote Manipulator System (SRMS) is a six-degree-of-freedom (6-DOF) telerobotic arm (Figure 1). Built in Canada, the "Canadarm" made its debut on the space shuttle Columbia (STS-2) on November 13, 1981. The SRMS consists of a shoulder joint, an upper boom, an elbow joint, a lower boom, a wrist joint, and an End Effector (i.e., a mechanical hand). The SRMS joints control shoulder pitch and yaw, elbow pitch, and wrist pitch, yaw, and roll. The total length of the arm is approximately 15 m (50 ft). The End Effector (EE) grasps an object by tightening three cables around the object's grapple fixture (a knobbed pin), much like a snare. The SRMS arm is remotely operated, either autonomously by computer control or by manually using two hand controllers that separately control translational and rotational motion. Unloaded motion can achieve a maximum rate of 0.6 m/s (2 ft/s), while loaded motion is constrained to speeds of 0.06 m/s (2.4 in/s) [IEEE, 2001].

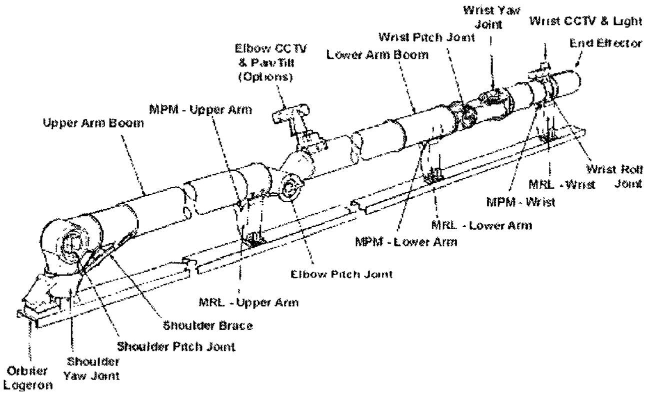

Figure 1. Diagram of the SRMS Robotic Arm [IEEE, 2001].

As one of the robotic arms aboard the international space station, the Space Station Remote Manipulator System (SSRMS, also known as Canadarm2) is a 7-DOF robotic arm with a total length of 17.6 m (57.7 ft). The SSRMS has two Latching End Effectors (LEE) that give it the ability to "self-relocate" or "walk" from point to point on the station. The SSRMS is one of three elements that make up the Mobile Servicing System (Figure 2). Representing Canada's contribution to the ISS, the Mobile Servicing System was delivered during the STS-100 shuttle mission in April 2001. The other two elements in the Mobile Servicing System are the Mobile Base System (MBS), a movable work platform, and the Special Purpose Dexterous Manipulator (SPDM), a two-fingered robotic hand [NASA, 2002a].

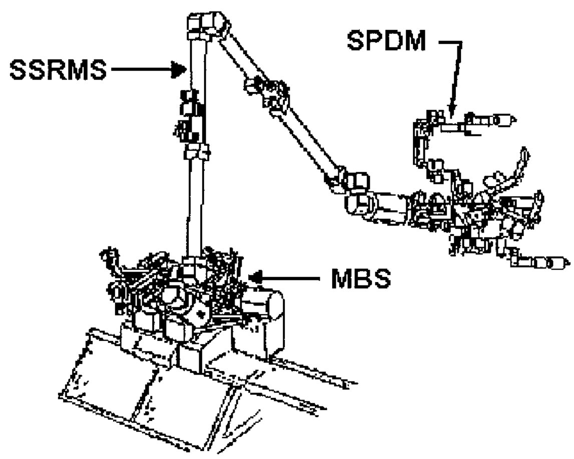

Figure 2. Mobile Servicing System [Adapted from Bloomer, 2001].

The operator interface for control of the SSRMS system is provided by the Robotic Workstation (RWS), whose main components include two hand controllers, three video monitors, a portable computer system, and a display and control panel (Figure 3) [Bloomer, 2001]. Control of the RMS arms – which includes all translations and rotations – occurs with respect to the Point of Resolution (POR), the center point at the distal end of the EE. The POR can be equated to a cursor in three-dimensional space. The RMS operator controls the position of the POR, and the orientation of the EE about the POR. The hand controllers operate using first-order (rate) control, so that displacement of the controller in a given direction is mapped to the velocity of the POR in that direction (i.e., POR position is the integral of controller displacement over time). Hence, movement of the hand controllers controls the direction and rate of movement of the POR [Nguyen & Hughes, 1994].

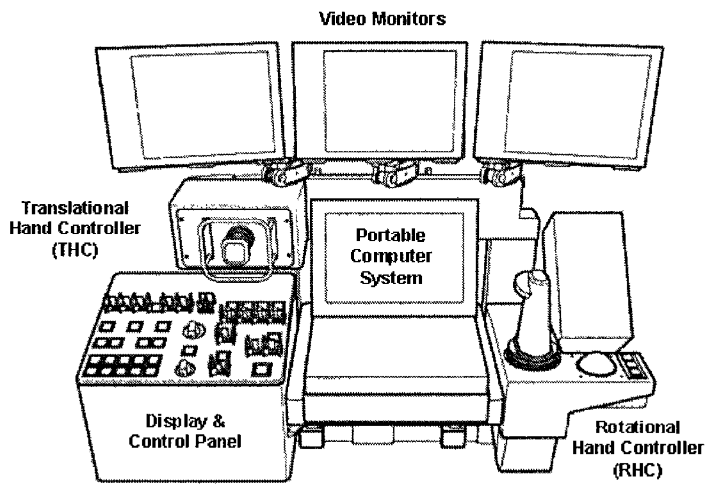

Figure 3. Robotic Workstation (RWS) Console [Adapted from Bloomer, 2001].

Monitoring of the arm maneuver is achieved through direct vision (out-the-window sighting) or through closed-circuit video displays of views transmitted by external cameras. Six cameras are accessible to SRMS operators: four cameras mounted at different locations in the payload bay, a camera attached to the lower arm boom just below the elbow joint, and a camera located on the EE. Four cameras are mounted on the SSRMS: one on each LEE, and one on each boom to either side of the elbow joint [Bloomer, 2001]. The operator has the ability to control lighting, camera selection, and camera adjustment (pan, tilt, and zoom). Unfortunately, despite the availability of these cameras, optimal viewing conditions are rarely achieved.

The RMS arms are employed for manipulation of payloads, ISS construction, payload deployment and retrieval, extra-vehicular activity (EVA) support, and inspection tasks. RMS operator teams are employed to help distribute the demands of the task and increase the safety of the operation. Typically, one astronaut operates the hand controllers while the other controls the camera views, verifies procedures, and provides support.

2.2 Critical Factors in RMS Operation

Morphew, Balmer, and Khoury [2001] performed a cognitive task analysis of RMS operation in order to understand the factors that might affect the performance of the task in space. Cognitive task analysis (CTA) is a method in which detailed knowledge of a task is obtained and analyzed to determine the cognitive demands required to produce skilled performance. Expert performance is characterized by automatic behavior achieved through extensive training and practice. Experts may not be aware of the extent of their knowledge, or have the ability to verbalize that knowledge, since automatic processes occur on a subconscious level. Hence, CTA seeks to elicit and document the knowledge of experts as it relates to task performance.

The researchers focused on several critical RMS tasks that included grappling an object, berthing and unberthing a payload, transporting astronauts at the end of the arm, handing-off between two manipulators, and recovering an object tumbling in space. Subject-matter experts were interviewed to identify and evaluate the most challenging physical and cognitive demands of these complex tasks [Khoury, Morphew, & Balmer, 1999]. Morphew et al. [2001] suggested that the psychomotor aspect of the RMS task is the most critical, requiring psychomotor and information processing skills that are easily compromised by time pressure, fatigue, stress, workload, and anxiety. Additional critical demands identified by the authors include situation awareness, spatial rotation, distance estimation, shifting / focusing attention, and assimilation and interpretation of environmental cues. Cognitive requirements associated with these demands include perception, memory, attention allocation, projection of future status, and visual-spatial processing. Morphew et al. [2001] identified translation of environmental cues into hand controller inputs as the most challenging aspect of RMS operation and postulated that this activity required a high level of situation awareness. The authors recommended the development of a means to assess these factors to improve training and evaluate operator performance.

The available research seems to suggest that human factors issues associated with the safe, accurate, and efficient use of the robot arm include accurate interpretation of visual cues from the environment (visual/spatial perception), an awareness of the movement capabilities and position of the arm relative to structures in the environment (situation awareness), and application of appropriate inputs to the manual controllers (psychomotor control). A more thorough discussion of the impact of these elements on RMS performance is included in the following sections.

2.2.1 Visual / Spatial Perception

Achieving proficiency in the operation of the RMS requires high levels of skill, training, and practice. To be successful, operators must first be able to perceive and interpret visual cues from the environment. The visual information provided by the environment, and the ability to accurately process that information, greatly affects RMS operator performance. However, in-orbit viewing conditions are often less than optimal. While performing arm maneuvers, the RMS operator must deal with low light, shadows, occluded vision, and interpreting cues from multiple camera views to estimate distances, depths, and clearances. In addition, the operator must adapt to continual changes in lighting conditions due to the dynamics of the orbiting system.

In microgravity conditions, the orientation and movement of objects in the environment can be dizzying. Because of the close relationship between the visual and motor processes in RMS operation, orientation of the controls and the operator with respect to the visual display is likely to affect performance. Visual-motor compatibility has been shown to have significant effects on teleoperator performance. High visual-motor compatibility is achieved when the motion direction of the cursor on a display, as viewed by the operator, matches the motion direction of the control device. Misalignments of the control and display axes that reduced visual-motor compatibility significantly increased RMS error on a tracking task [Macedo, Kaber, Endsley, Powanusorn, & Myung, 1998]. For this reason, selection of appropriate camera views is very important to successful operation. Unfortunately, camera selection is limited to available sites whose vantage points are not always adequate. Therefore, astronauts must have the ability to spatially rotate and orient themselves and the view within the environment, and to mentally map and predict spatial translations and orientations in three dimensions. Some researchers have provided evidence that this ability can be improved with training and practice [Macedo et al., 1998].

Van Erp and Oving [2002] conducted two experiments to investigate control accuracy in three dimensions (X, Y, and Z). Previous research had found differences in accuracy for movements made in the horizontal and vertical dimensions, and a greatly decreased accuracy for the depth dimension. However, it was suggested that the differences might be due to varying attentional priorities during learning, since the differences appear to be reduced with training. In effect, participants tended to favor motions in certain directions, particularly those that were more familiar. To investigate these differences more thoroughly, the first experiment utilized a cursor-positioning task to examine control-display compatibility and attentional priority. To determine the effects of relative controller-display orientation on motion in three dimensions, the researchers coupled the control motion to one of two different visual display orientations (Figure 4). In the spatial-motion mapping condition, motion of the hand controller was parallel to the motion displayed on the monitor (X horizontal, Y depth, and Z vertical). In the reference-plane mapping condition, the reference plane of the display matched the reference plane of the controller (X horizontal, Y vertical, and Z depth).

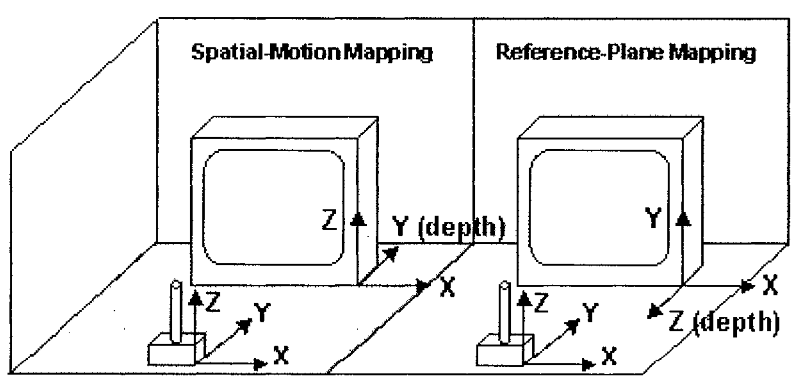

Figure 4. Control-Display Mappings Used by Van Erp & Oving [2002].

In order to determine whether differences in accuracy were due to attentional priority, early error correction was examined. Results showed no significant differences between the two control mappings. However, since the mappings were tested using two different groups (between-subjects design), no conclusions could be made regarding crossover in learning or first-response tendencies. While priority for the horizontal dimension was indicated when attention demands were high (as when first learning the task), the authors suggested that differences in accuracy between the horizontal and vertical dimensions might diminish with increased proficiency (as was found in the later trials of the study). As in previous studies, accuracy was lowest in the depth dimension.

The second experiment employed two tracking tasks to isolate visual effects (mapping differences) from psychomotor effects (axis differences) on accuracy. In the standard pursuit-tracking task, the operator input controlled the cursor to pursue a moving target, while in the modified tracking task, a disturbance input to the cursor required compensation by the operator in order to maintain the cursor position on the stationary target. In both tasks, the operator was instructed to minimize the error between the target and the cursor. RMS error was not affected by control mapping or type of tracking task. Tracking errors for the X (horizontal) dimension were significantly smaller. RMS errors in the depth dimension were nearly four times larger, suggesting a large effect of the visual depth component of the task. Control along the Z-axis was associated with consistently higher error than the error along the Y-axis regardless of mapping, suggesting psychomotor differences between these axes. The authors concluded that the quality of visual information, particularly in the depth dimension, is critical to maximizing performance [Van Erp & Oving, 2002].

The results of these experiments have several implications related to RMS task performance. Since performance is known to differ by axis, measurements of control performance should be examined separately for each dimension. These results also affect and are affected by camera selection. Cameras should be chosen to provide the maximum depth information. Since performance in the depth dimension was shown to improve over time, sufficient training and practice should help to reduce performance errors.

2.2.2 Situation Awareness

Situation awareness has been identified as a critical factor in RMS operation. Mica Endsley is most often credited with the term "situation awareness", which she defined as "*the perception of the elements in the environment within a volume of time and space, the comprehension of their meaning, and the projection of their status in the near future*" [Endsley, 1995b, p. 36]. In effect, situation awareness is the extent of a person's knowledge and understanding of the current state of the system. Endsley's theoretical model attempts to define the construct of situation awareness (SA) and explain the role that it plays in decision-making and human performance. A simplified version of this model is shown in Figure 5, in which SA is portrayed as the prerequisite for decision-making and subsequent performance.

In Endsley's theory, situation awareness occurs on three levels: **Perception** of elements in the environment (Level 1), **Comprehension** of the current situation (Level 2), and **Projection** of future status (Level 3). The state of SA is affected by external system factors such as interface design, system complexity, stress, and workload. Additional effects on SA are attributed to individual capabilities, goals and expectations, experience, and training. For example, the allocation of attention to elements in the environment is greatly influenced by an individual's goals and past experience, which in turn affects perception, understanding, and choice of response.

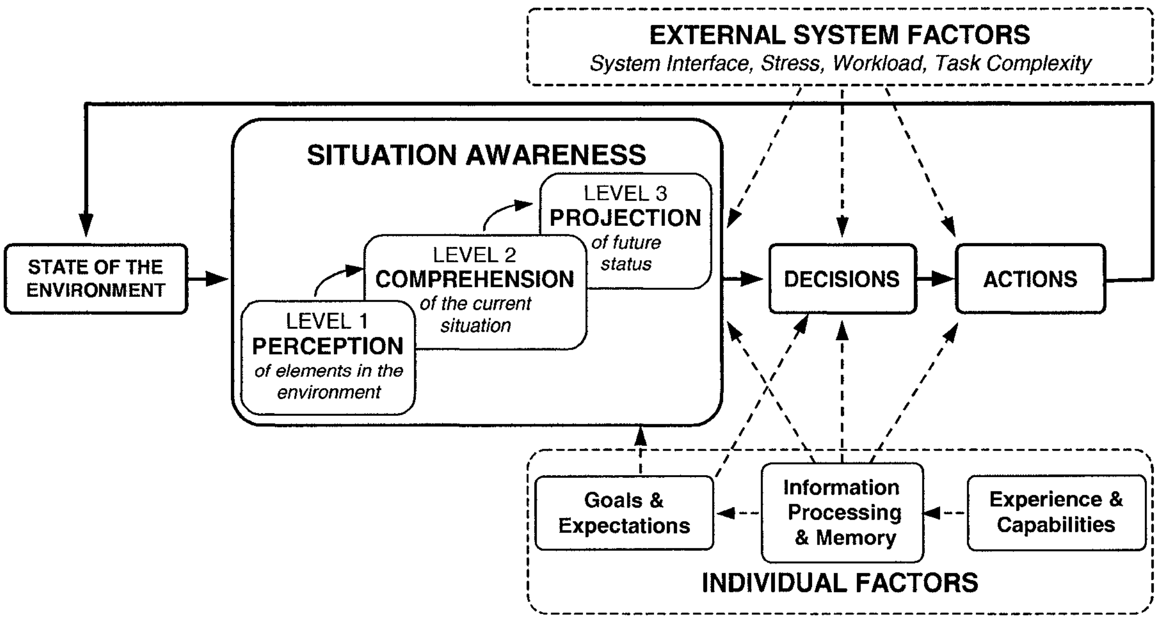

Figure 5. Stage Model of Situation Awareness [Adapted from Endsley, 1995b].

While situation awareness is generally acknowledged to be a factor in human performance, the relationship is complex and largely unknown, although several explanatory theories exist. This complex relationship contributes to the difficulty in precisely defining situation awareness. To date, there is no single, accepted definition. A large portion of the debate centers on the point where situation awareness should be evaluated within the model. Some researchers consider situation awareness to be a product or an outcome of the processing of information. Others describe SA as encompassing both the process of achieving awareness and the resulting state attained, while another group views SA as a phenomenon rather than a behavior. A criticism of many of the definitions of SA comes from their reliance on other psychological constructs that are themselves not fully understood. For example, Endsley borrows heavily from theories on information processing, and her definition is based on an understanding of the psychological constructs of attention and memory [Uhlarik & Comerford, 2002].

Endsley describes SA as a *state of knowledge*, and is careful to differentiate it from the process by which SA is achieved. Further, she cautions that SA should be regarded as a separate and independent construct within the decision-making cycle to reliably and accurately portray its influence on human performance. Achieving a high level of SA does not guarantee a high level of performance, but it does increase its likelihood. For example, performance may suffer due to poor decision-making or an erroneous response. Similarly, a lower level of SA may be compensated by applying a different problem-solving strategy to result in good performance. Because of the complex interplay of the numerous performance-shaping factors, the exact effect of SA on performance is difficult to predict [Endsley, 1995b].

Situation awareness is important in situations that require high levels of human performance while completing complex tasks in dynamic environments. Dynamic environments are often characterized by high information content, uncertainty, risk, time pressures, complexity, and constant changes that the human must perceive, understand, and address. It is important that the operator be able to anticipate some of these changes, and make appropriate plans. Hence, SA not only involves an awareness of the present state of the system, but also implies an ability to predict the future state based on knowledge of the past and present. For example, situation awareness is important when direct view of the task is obstructed or unavailable, requiring the robotics operator to estimate distances and clearances based on camera views alone [CSA, 1999].

Attention is a critical factor affecting SA. Attentional demands in complex, dynamic environments can often exceed human capacity, and constrain perception, information processing, and decision-making. Additionally, poor allocation of attention resources due to improper prioritization by the operator will lead to degraded SA. Attentional narrowing is a phenomenon in which attentional priority is given to certain elements in the environment (often due to stress or a perception of danger) leading to the exclusion of other elements, sometimes with disastrous results. For example, a pilot in a combat situation may be so preoccupied with enemy planes that he fails to monitor his fuel level, resulting in a crash landing [Endsley, 1995b]. Training crewmembers to anticipate multiple system failures can help reduce the occurrence of attentional narrowing [Morphew et al., 2001].

Some of the operational domains that are particularly concerned with understanding and evaluating situation awareness are aviation (design of display and control systems, piloting, air traffic control), security (firefighting, police), medicine (emergency medicine, surgery), military (combat tactics, munitions), robotics (teleoperation), and heavy equipment operation (shipping, construction, forestry). In these domains, failure to respond correctly to system stimuli can result in large monetary losses, injury, and death. Effective control of these systems requires assessment of the current state and an understanding of the system dynamics that will allow monitoring changes and predicting the future state of the system based on knowledge of those changes. Processing and decision-making requirements increase with the complexity and dynamics of the system.

A number of methods have been proposed and employed to measure SA. As with other psychological constructs such as workload, SA cannot be directly observed and measured. Therefore, researchers often attempt to assess SA through indirect means [Vidulich, 2003]. Uhlarik and Comerford [2002] describe three categories of SA measures: explicit measures, implicit measures, and subjective measures. Explicit measures compare self-reports of SA information in memory with the true state of the system to provide a pseudo-objective measure. Implicit measures infer SA based on performance. Unfortunately, although these measures may provide an objective assessment, changes in performance cannot reliably be attributed to differences in SA. Subjective measures solicit ratings of SA based on the opinion of the subject or an observer. Although self-ratings of SA provide a more direct assessment, they are subject to individual bias and temporal effects, and may actually measure the subjects' *confidence* in their SA, rather than SA itself. Observer ratings are more objective, but cannot ascertain the extent of the subject's internal knowledge of the situation [Endsley, 1995a]. Uhlarik and Comerford [2002] suggest that concurrent validity may be achieved by employing several measures of SA.

A widely used method of assessing SA in aircraft simulation studies is the Situation Awareness Global Assessment Technique (SAGAT), an explicit measure that reduces temporal effects by employing a freeze technique. In this technique, task simulation is suspended at random points in time to allow researchers to question the operators regarding their perceptions of the current system state. Operator responses can then be compared with the true current state to objectively evaluate the level of SA. Endsley [1995a] conducted two separate studies to determine (1) the effects of freeze duration on memory of SA, and (2) the effects of the freeze method (intrusiveness) on resumed performance of simulated air combat. Results showed that operators were able to provide accurate responses for five to six minutes following the freeze with no memory decay, and that the freeze method produced no significant effects on pilot performance. Advantages of SAGAT are that it provides measures that are timely, global, objective, and possess face validity [Vidulich, 2003]. This measure also has several drawbacks, including the amount of effort and knowledge required to develop the question set, the need to pause the simulation (intrusiveness), and the fact that the data collected are binomial (scored as correct or incorrect) and must be transformed before using standard statistical models [Uhlarik & Comerford, 2002].

The emphasis on the importance of SA to human performance in complex systems is reflected in the NASA RMS training program, which includes SA among the most critical skills when evaluating operator competency. However, the difficulties of accurately and objectively measuring SA underscore the need for the development of more effective metrics to assess SA in RMS operations.

2.2.3 Psychomotor Control

Maneuvers of the RMS arm are often made in extremely close confines that require precise movements made under strict time pressures. The operator must understand and consider the RMS system constraints during operation. For example, it is critical that the operator be aware of clearances from structure, and movement limitations and reach capabilities of the robotic arm to avoid potential collisions. Flight rules and programmed system stops are designed to help reduce errors or accidents due to induced oscillations in the arm or to exceeding physical or mechanical reach limits.

In addition to the demanding cognitive requirements, the psychomotor aspect of the RMS operation task is important to the safe and efficient operation of the arm. Psychomotor control refers to the human stimulus-response loop in which the subject responds to a perceived visual or auditory signal based on schema accessed from long-term memory. Example psychomotor tasks include tracking and moving or positioning a cursor. As mentioned previously, control of the RMS arm is analogous to controlling the POR, or to controlling a cursor in three-dimensional space. Hence, inputting motion commands to the hand controllers is a psychomotor task.

The microgravity environment causes unique problems. Physiological effects of weightlessness include decreased dexterity and posture changes that reduce operator performance accuracy [Smart, 2000]. In microgravity, even a small force can displace an astronaut who is not anchored. For this reason, the system designers placed a metal "cage" around the translational controller knob to stabilize the operator and to counteract the momentum resulting from the forces needed to displace the controller knob. Control performance may also be affected by differences in motion capabilities in the various directions due to the physiology of the hand and wrist [Van Erp & Oving, 2002]. As mentioned previously, Eddy et al. [1998] attributed degraded psychomotor performance of the astronauts in their study to changes in gravity. Hence, this dissertation seeks to include measures of psychomotor performance that are sensitive to the effects of microgravity in order to assess astronaut performance state.

The difficulties and challenges involved in controlling movement utilizing 6-DOF input devices have been a topic investigated by researchers at the University of Toronto in Ontario, Canada. Zhai and Milgram [1998] evaluated the extent to which an operator is able to coordinate control among multiple degrees of freedom. The authors defined a perfectly coordinated motion (in three-dimensional space) as one in which all DOF were simultaneously controlled. Coordination of translational and rotational movements was quantified separately by measuring translational and rotational efficiency based on deviation from a "shortest" path. A third measure was used to evaluate the coordination between the control of the translational and rotational movements (i.e., whether they were performed at the same time). Using the author's measures, a perfectly coordinated motion would have a coordination coefficient of zero.

Two single-handed 6-DOF input devices were evaluated: the Fingerball (a position control device), and the EGG (Elastic General-purpose Grip; a rate control device). The experiment employed a 3-D docking task that required participants to align a 3-D cursor (tetrahedron) with an identically-shaped target placed at various locations and orientations. The researchers reported that while the position control device provided significantly faster completion times, the rate control device provided significantly greater efficiencies in mean translation and rotation, coordination between translation and rotation, and coordination among all six degrees-of-freedom.

Efficiency was significantly improved for both devices after participants were specifically instructed to complete the trials as quickly as possible using the smoothest and shortest path. After an initial increase on the first trial under the new instructions, completion times were also improved. Rotational performance was found to be significantly less efficient than translational performance. The authors confirmed that this result supported previous research findings suggesting that humans have only a limited ability to perform mental rotations in three-dimensions, particularly when the axis of rotation is arbitrarily oriented as shown in Figure 6.

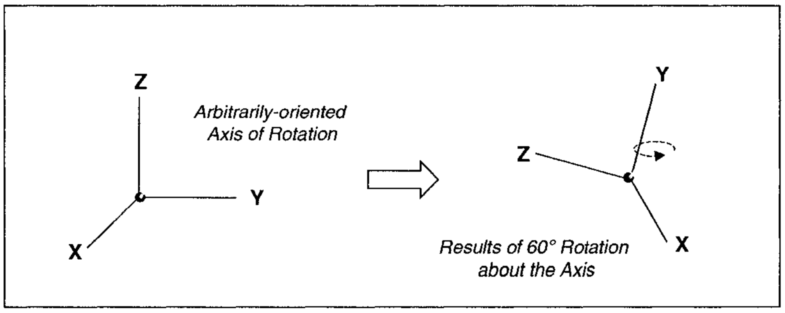

Figure 6. Rotation of Coordinate Axes about an Arbitrary Axis.

A subsequent study by Masliah and Milgram [2000] discussed the development and utility of a metric to measure coordination (or allocation of control) in a 6-DOF docking task. The authors discussed the problems associated with several alternative coordination measures, including time-on-target, the coordination index, measures of spatial and temporal invariance and inefficiency, cross-correlations, and integrality. Although it is easy to compute the time-on-target for each DOF, the measure provides no information about overall error, or an idea of average closeness to the target. To account for the tradeoff between accuracy and speed, the coordination index is calculated as the product of the two measures.

The degree of invariance in repeated movements can be analyzed using cross-correlations and phase analysis, which are designed mainly to measure repeated, rhythmic limb motions. Cross-correlations can indicate coordination between DOF, but fail to indicate whether the coordination is appropriate or erroneous. The authors' proposed M-metric is designed to account for both efficiency and simultaneity in docking tasks requiring the control of multiple degrees of freedom. The product of a measure of simultaneity of control and a measure of control efficiency, the M-metric results in a value between zero and one, where one indicates perfectly simultaneous and efficient control. However, the M-metric is a task-dependent measure that can only be calculated for successfully completed tasks.

Two single-handed 6-DOF input devices were evaluated: the Fingerball (a position control device) and the Spaceball (a rate control device). No significant differences were found in the mean completion times for the two devices. Although the participants' ability to control multiple degrees of freedom increased with extended practice, the participants demonstrated a preference to allocate control along rotational axes and translational axes separately, switching control between the two rather than attempting to control translations and rotations simultaneously. The authors suggested that this was a strategy employed by the participants to reduce the complexity of the task.

Both of the Canadian studies show a clear preference and improved performance for the rate control device, a single 6-DOF device operated using one hand. Similarly, the RMS hand controllers employ rate control. Unfortunately, the RMS system is operated using two-handed controls, which changes the complexity of the input task since rotations are commanded separately from translations. Further, the manipulation of the THC and RHC are made using different motions in different planes. To understand how these differences might affect performance, an analogous exercise might be to try to rub your stomach while patting your head, or vice versa. The exclusive use of novice operators and the small number of trial sessions in the studies raises questions regarding the stability and utility of the results, since the data demonstrate learning across all trials. A potential flaw lies in the assumption by the authors that the "shortest-path" is optimal, and that completely simultaneous control is best. A discussion in Section 3.3.7 of this dissertation explains why this assumption may not be supported when considering the capabilities and limitations of the human operator.

2.3 RMS Operator Training

Extensive training and practice can lead to expertise, which is characterized by increased automatic behavior and a reduced demand on cognitive / attention resources. When encountering highly familiar or repetitive information, processing becomes nearly effortless. Appropriate schema and their associated scripts are automatically retrieved from long-term memory to trigger predetermined responses based on stored decisions. This automaticity can be important in complex, dynamic environments, since it reduces the information-processing burden on working memory. Unfortunately, this increased efficiency in information processing can be problematic. Since responses are made with less conscious effort, situation awareness for familiar stimuli may be reduced. Subsequently, new environmental elements that deviate from the old, rehearsed conditions may be disregarded, (i.e., the operator may miss salient cues) which could lead to erroneous actions or failures to respond [Endsley, 1995b]. For example, a driver accustomed to traveling along a particular route may fail to heed a new stop sign placed along the route.

Sauerwein and Molino [1993] found that training significantly improved the mean task completion time of industrial robot operators by almost 40 percent, but was less effective in improving performance quality and reducing errors. An effective training program must be able to produce operators possessing the sufficient information and understanding of the system to safely and efficiently operate under a vast number of potential situations. To this end, simulation has been employed as an efficient and effective training tool in many applications, including surgical and dental procedures, heavy equipment operation, aviation, astronautics, driving, air traffic control, and robotics operation.

2.3.1 Use of Simulation in Training

The use of simulation has long been advocated in situations where real-world training is infeasible or costly, or where the criticality of errors is extremely high. Military training missions have traditionally relied on simulated scenarios when training military personnel to deal with complex, risk-filled situations. Technological advances have increased the need for additional training to update performance skills and the knowledge required to use increasingly sophisticated equipment and devices. Fortunately, these same advances in technology have provided the ability to simulate scenarios with ever-increasing fidelity and realism. For example, the STAR simulation generates a 360° virtual ship bridge or engine room to train voyager-class ship operators. The simulator can accurately and realistically represent a large variety of water and weather conditions, ship traffic, and sea and land elements [Wilkinson, 2002]. A virtual-reality simulation employed in the training of forestry machine operators has been shown to increase wood harvesting by 23% over traditionally trained operators [Lapointe & Robert, 2000].

Computer-based simulations can be used to visualize unknown or imagined environments to evaluate efficiency, estimate potential performance and probabilistic behaviors, and predict problems. This allows virtual testing of proposed designs to help designers select the best alternatives. The use of simulations in training programs can provide trainees with realistic practice on a wide variety of tasks that may be required under different scenarios. The trainee is able to experience and train for improbable but critical events where failure to respond correctly would be costly in real life. An added benefit is that the simulation provides trainers the ability to record objective data to reliably assess trainee performance and to produce timely feedback. It is even possible that these assessments could be generated automatically.

Virtual reality simulations have recently been employed in training and evaluating surgical skills. With the increased precision, dexterity, and skill required in minimally invasive (e.g., laparoscopic) surgical procedures, simulation allows greater opportunities for "hands-on" practice while reducing training costs, medical errors, and the cost associated with the use of the hospital equipment and facilities while training. One method being employed in the medical training arena involves assessing dexterity through motion analysis using measurements of the number of movements, distance and speed of movements, and completion times. This computer-based system, called the Imperial College Surgical Assessment Device, has accurately identified differences in levels of surgical experience [Shah & Darzi, 2001]. A similar methodology for assessing perioperative skills based on comparison of performance against acceptable criteria is currently in the development stages [Witzke et al., 2001]. This criterion-referenced approach can be applied to the RMS training evaluation. Expert performance could be used to establish a criteria set against which trainee competence would be evaluated.

Simulation is also useful in robotics operator training, since the operator can learn to safely and effectively operate the system without risk. Several robotics simulation software packages are available that require only a single computer with a small number of accessories for learning to maneuver a robot. The Interactive Graphics Robot Instruction Program (IGRIP) simulation software program from Deneb Robotics provides CAD-based model building and workcell layout, motion path planning and simulation, and collision detection [Kim, 1993]. An interesting technique available through the World Wide Web provides the opportunity to learn robot operation by working with a physical robot [Taylor & Trevelyan, 1998]. The robot is in a remote location that the trainee may access through an Internet connection (http://telerobot.mech.uwa.edu.au/).

Training to maneuver the SSRMS is conducted by the Canadian Space Agency on the Robotics Operations and Training Simulator. The simulator realistically represents the space environment through complex 3-D visual models in a display arrangement identical to that found onboard the Shuttle and the International Space Station. Software tools are included that permit the collection and analysis of command, telemetry, and performance data [Belanger, Jaar, & Cyril, 2000]. This "hands-on" approach to training has been shown to improve operator performance in complex control tasks and leads to greater understanding of the system dynamics [Goonetilleke, Drury, & Sharit, 1995].

2.3.2 NASA Generic Robotics Training

The BORIS / Trick Simulation

Astronauts typically undergo a series of training programs to qualify them to operate the shuttle or space station robot arms. The initial training program, Generic Robotics Training (GRT), utilizes the Basic Operational Robotics Instructional System (BORIS) software that simulates operation of a 6-DOF jointed robotic arm in a rectangular 'room' (3000 cm L x 1500 cm W x 1500 cm H) referred to as the Virtual

Environment for Generic Arms (VEGA) [McCartney, 2001]. The VEGA includes four walls (forward, starboard, aft, and port) and a floor. Gridlines dissect the VEGA in 100 cm increments to help provide the operator with visual cues to estimate positions and orientations. The BORIS arm can be positioned at either of two base locations, centered on the forward and the port walls. A window for viewing arm maneuvers is located in the forward wall. The aft and starboard walls contain large, irregularly shaped "meteor collision holes." The simulation provides an optional table that can be placed in one of three pre-determined locations within the room. Six payload berths are located on the tabletop. Two additional payload berths are located near the center of the aft wall and on the floor near the port wall. The BORIS simulation provides the operator access to six cameras: one positioned in each of the four corners of the room, a boom camera, and an End Effector (EE) camera. Figure 7 is a view of the BORIS arm and payload table viewed through the camera located at the starboard-aft corner of the room (Camera 2). The arm is positioned on the port base in this view, but the forward base can be seen under the window to the right. The platform for Camera 4 can also be seen in the port-forward corner of the room, at the center of the display.

The BORIS simulation runs within the Trick environment, a simulation operating system developed by the NASA Johnson Space Center (JSC) Automation, Robotics, and Simulation Division [McCartney, 2002]. The Trick environment provides the ability to record data from the simulation that may be extracted for analysis or stored and analyzed internally. In November 2001, NASA developed a PC version of the BORIS software and the Trick operating system that was made available for research purposes. Access to this system made the current research feasible.

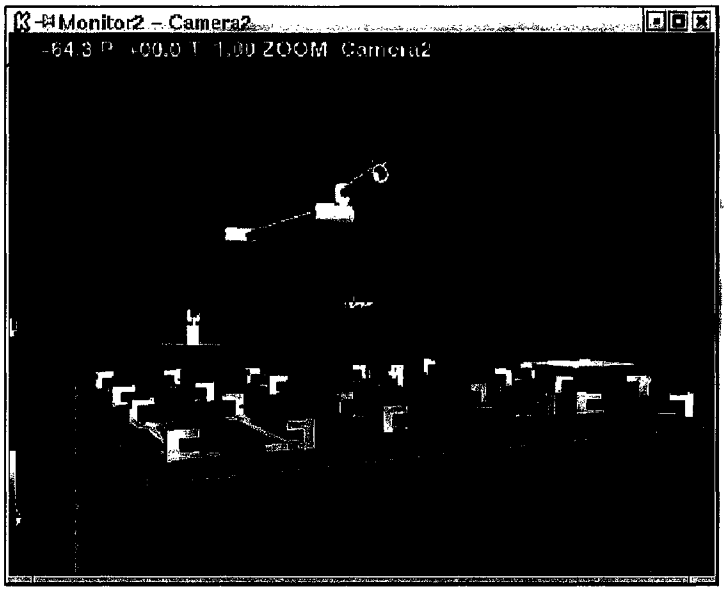

Figure 7. Camera Monitor View of the BORIS Arm and Payload Table.

RMS Concepts and Terminology

One of the most difficult concepts to master in RMS operation is that of "coordinate frames," a term that refers to individual coordinate systems used to describe position, orientation, and motion in three dimensions. The BORIS simulation utilizes four separate frames: a Frame of Resolution (FOR), a Display Frame, a Hand Controller Frame, and a Command Frame. The Display Frame and FOR combine to describe the relative position and orientation of an object, while the Hand Controller Frame and Command Frame are used to determine the direction of motion of the arm.

The Frame of Resolution (FOR) is a fixed coordinate axis system (X, Y, and Z) that is used to define the position and orientation of the EE or attached payload. The POR is the origin of the FOR, and is the point commanded by the hand controller inputs. When no payload is attached to the EE (unloaded condition), the POR is located at the center of the distal end of the EE. When a payload is attached to the EE (loaded condition), the POR is shifted to a location on the payload. Hence, this point becomes the new reference point about which all rotations and translations are made [McCartney, 2002].

The Display Frame is fixed with respect to some VEGA structure, usually at the base of the BORIS arm. Position and orientation of the FOR are measured as the difference in position and orientation of the FOR relative to the Display Frame. In effect, the Display Frame can be thought of as the origin of the coordinate frame system, or the reference position and orientation in this three-dimensional environment. The simulation digitals display the current position and orientation of the FOR with respect to this origin [McCartney, 2002].

The coordinate axes of the Hand Controller Frame are fixed with respect to the controllers, and define the way BORIS translates the mechanical inputs to the hand controllers into displayed motion. The orientation of the HC Frame coordinate axes is illustrated in Figure 8.

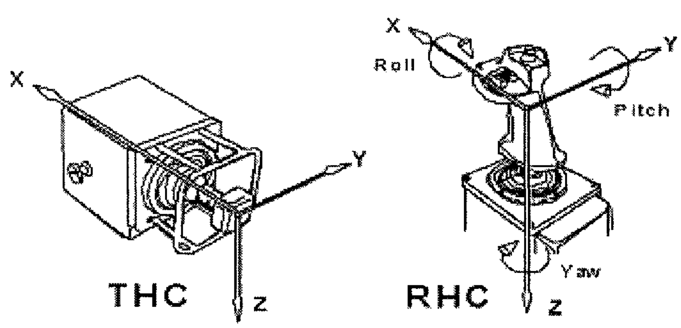

Figure 8. RMS Hand Controllers [NASA, 2002c]**.**

The final frame that the RMS operator must consider is the Command Frame. The direction of commanded motion resulting from the movement of the hand controllers is defined by the Command Frame. Orientation of the Command Frame axes depends on the type of command frame being used, either external or internal. An *external* command frame is fixed with respect to structure, while an *internal* command frame is co-located with the FOR. Hence, an internal command frame moves and rotates with the FOR (i.e., an internal command frame is co-aligned with the FOR) while an external command frame has a fixed orientation with respect to some VEGA structure [McCartney, 2002]. Since arm maneuvers made using an internal command frame are likened to "flying the EE camera," the internal command frame is typically used for tasks that require use of the EE, such as grappling, inspection, or tracing maneuvers.

The position and orientation of objects in BORIS is represented by a set of six values that specify X, Y, Z, P(itch), Y(aw), and R(oll), respectively. Space-robotics convention defines orientations by an Euler sequence, which specifies three sequential rotations about the Y (pitch), Z (yaw), and X (roll) axes of a particular frame that result in the described attitude [McCartney, 2002]. Understanding the relationships of these frames is critical to the effectiveness of RMS operation. Due to the system dynamics, the RMS operator must have a clear understanding of these frames to successfully perform the "mental gymnastics" that can be required during arm maneuvers.

During training, three-dimensional models of the BORIS arm, the VEGA, the coordinate frames, the EE, and the payload are provided to help the operator visualize and predict the motion of the arm and to determine the required commands to achieve a desired maneuver. The arm model is particularly useful in demonstrating the movement capabilities and limitations of the arm, such as reach limits and singularities. A singularity is a configuration of the arm that results in the loss (or restriction) of one or more degrees of freedom for a particular joint. For example, an elbow singularity occurs when the internal angle between the upper and lower booms gets close to 180 degrees.

When this occurs, the arm loses the ability to make a pure (straight-line) translational motion along either the Y-axis or Z-axis - the subsequent motion becomes an arc. Figure 9 is an illustration of some of the 3-D models that are used by the trainees in the GRT program.

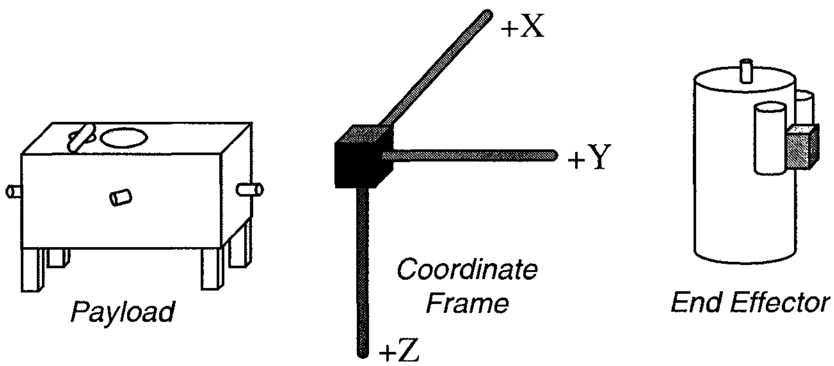

Figure 9. 3-D Models Used in NASA's Generic Robotics Training.

BORIS Controls and Displays

The BORIS training setup consists of a workstation with two high-resolution display screens, two specialized hand controllers (Figure 8), a mouse, and a keyboard. The translational hand controller (THC) is operated with the left hand to command motion along the X, Y, and Z axes, while the right hand operates the rotational hand controller (RHC) to control Pitch, Yaw, and Roll. As mentioned previously, the hand controller displacement determines both velocity and direction of arm motion. Positive rotations are defined using the "right-hand-rule," such that when the thumb of the right hand is pointing in the direction of the positive translational axis, the curl of the fingers around the axis represents a positive rotation about that axis.

Four virtual control panels (Camera Control, Arm Control, Configuration Control, and GUI Select) are presented on the left display, and three "monitors" (camera or window views) are presented on the right display (Figure 10). The Camera Control panel allows the operator to assign the camera view to be displayed in each of the three monitors (windows). Monitors 1 and 2 may each be multiplexed (split in half) to provide a total of five camera views simultaneously. Specification of the forward window view is made using the computer keyboard. The Camera Control panel provides control of camera adjustments (movement rate, pan, tilt, and zoom), camera lights, and the display of camera crosshairs and rate overlay graphics. The Arm Control panel allows the operator to select between several manual and automatic control modes, and the panel displays the joint angles, movement rates, and the digital information that relates the position and orientation of the FOR with respect to the Display Frame. This panel also controls the payload latches, EE grappling mechanism, and system brakes, and provides frame selection and single-joint controls. The Configuration Control Panel allows the user to set operational constraints (joint and rate limits, motion stops, etc.) and to control payload table location and visibility of the FOR and Display Frame axes. The GUI Select control panel is used to activate a specific panel, or to exit the simulation [McCartney, 2002].

GRT Training Sequence and Rationale

The GRT program is designed to teach basic robotics concepts and skills that will be transferable to operation of any of the on-orbit RMS systems on the shuttle or the ISS. The lesson sequence consists of eight two-hour, one-on-one training sessions that provide the operator basic knowledge of relevant robotics terminology, robotics technologies, kinematics, system capabilities and constraints, and operational rules, procedures, and strategies. Each lesson in the sequence has clearly defined goals and objectives. In

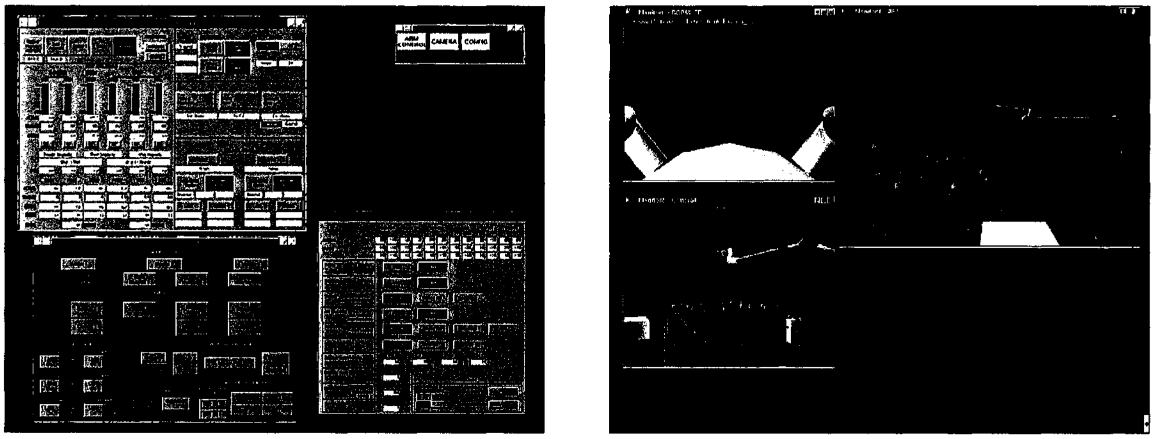

Figure 10. BORIS Display Screens Showing Control Panels and Camera Monitors.

addition, two final sessions are included to evaluate operator proficiency. Trainees are typically scheduled for two to three lessons per week. The GRT flow presents trainees with increasingly complex scenarios and maneuvers to build on previously learned concepts, to provide practice, and to perfect skills. GRT was designed to provide the prerequisite skills needed for subsequent training, and to facilitate the selection of those individuals who would be most adept at RMS operations. Standard test scenarios are used to evaluate specific skills and to provide an opportunity to compare proficiencies among individuals. This process can help differentiate potential RMS operator candidates when making important crew assignment decisions.

2.3.3 Assessment of RMS Operator Performance

Currently, the evaluation of RMS skill acquisition is made by "expert" observers during a timed performance of specific task scenarios. As mentioned, the trainees attend two evaluation sessions after completion of the eight GRT lessons. The first session is a "practice" evaluation that is used to identify potential deficits and predict the ability of the trainee to pass the final evaluation. The practice session allows the trainee to become comfortable with the test conditions, and provides time to work on skills that may need further development. The operator is allotted 2.5 hours to complete eight specified tasks. The GRT instructor provides the trainee with feedback after each task is completed. In the final evaluation, independent assessments are made by a certified instructor and an expert operator. The eight task scenarios in the evaluation sessions include an unloaded fly-to, an unloaded camera inspection, a grapple approach without using the EE camera, a payload grapple and unberth, two loaded fly-to tasks, a payload berth, and a single-joint task. A fly-to is a targeted movement wherein the trainee is given a set of terminal position and orientation coordinates. Final position and orientation values that fall within 2 meters and 30 degrees of the target coordinates are considered successfully completed.

Although assessed subjectively by the expert observer / instructor, the GRT assessments are guided by pre-defined criteria. Trainees are evaluated based on their competency on nine skill categories utilizing a five-point rating scale (from 1 = Unsatisfactory to 5 = Outstanding) for each category. The nine skill categories include situational awareness, arm maneuvers, hand controller techniques, application of frames, grapple alignment with no EE camera, single-joint techniques, spaceflight resource management (SFRM), target usage, and camera technique. Each skill category is assigned a weight based on its contribution to the safe and effective operation of the RMS. Category 1 skills are given the highest priority by the GRT evaluators, as shown in Table 1. The trainee's overall score is the sum of the weighted totals achieved during the performance of the eight tasks in the final GRT evaluation (multiplied by 0.05 to transform the weighted score to a 5-point scale). Astronauts who achieve an overall average score of at least 4.0 on the GRT evaluation are qualified to proceed to NASA's mission-specific robotics training programs.

Table 1. Skill Assessment Criteria Used in the GRT Evaluation.

	Skill Assessed	Assessment Criteria	Relative Importance
Category 1	Situation Awareness	Scan pattern, clearances, avoids limits, follows flight rules, camera selection	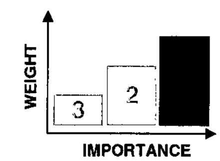
	Arm Maneuvers	Smooth / controlled motion, correct direction, steady closing rate, appropriate command frame	
	Hand Controller Techniques	Good grip, ramped commands, concurrent inputs, slow / deliberate multi-axis inputs	
	Application of Frames	Determines proper attitude based on Euler sequence	
Category 2	Grapple Alignment (No EE Camera)	Uses appropriate camera views, EE in grapple envelope	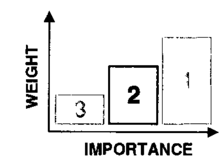
	Single-Joint Techniques	No pulsing, joint selection / strategy, direction of movement	
	Spaceflight Resource Management (SFRM)	Clear communication, appropriate responses, adequate preparation	
Category 3	Target Usage	Correct interpretation of visual cues, correct alignment / pre-grapple	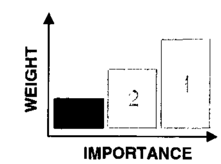
	Camera Technique	Proper zoom / pan / tilt, multiplexing, real-time tracking	

Criticizing the RMS training program for lacking consistent, appropriate, objective feedback, or quantitative measures of performance, Zak and Das [1995] developed and validated the Task Acquisition Training (TAST) method to achieve a more consistent level of teleoperation skill during the performance of critical tasks. This method differed from the traditional astronaut training approach in its use of quantitative performance measures and in the application of concepts derived from human factors research. The data collected and analyzed included six position and orientation values, six force and torque values, and total task completion time. The data were summarized into Knowledge of Results and Knowledge of Performance measures and a total task score, which provided the trainee with feedback on performance. The effectiveness of the method was evaluated by comparing performances of TAST-trained subjects with those trained using the traditional methods. The TAST method was shown to accelerate learning and enhance retention of teleoperation skill.

NASA's robotics training program would benefit from the development of objective, quantitative performance metrics that could be obtained from the BORIS simulator. These metrics should be indicators of both cognitive and psychomotor skills associated with proficient operation of the RMS arm. Traditional measures of human performance can provide a basis for selection of appropriate metrics. Many existing computer-based cognitive performance tests attempt to assess abilities and functions that are important predictors of human performance in complex systems. These elements include attention, perception, psychomotor control, psychological / emotional state, working memory, information processing, logic, spatial reasoning, and timesharing ability.

2.4 Dissertation Rationale and Objectives

As discussed previously, the training and evaluation of RMS operators would benefit greatly from the development of quantitative performance metrics. These measures would aid training by providing objective, timely feedback to both instructors and trainees. By allowing for quicker detection and correction of performance errors, overall training time can be reduced. As a training tool, performance criteria can be displayed graphically to demonstrate desirable and acceptable performance levels. Finally, quantitative performance metrics would permit a more precise evaluation of proficiency that would facilitate operator selection and crew assignment.

In summary, the development of these metrics will benefit RMS training and assessment by providing a more reliable, objective indicator of operator proficiency and by enabling a quick and effective means of self-assessment. Additionally, the metric development will support current research efforts at the University of Oklahoma in validating the ability of adaptive, dynamic-load tasks to assess astronaut functional state. Toward these efforts, this dissertation had the following overall objectives:

- to define the methodology for the development and validation of objective performance metrics for RMS operators based on NASA's Generic Robotics Training,
- to develop a select subset of measures that satisfy several critical skill categories used in the NASA GRT evaluation,
- and to extract and validate the selected performance metrics from the BORIS / Trick simulation.

This dissertation served as the initial investigation into the development of the NASA RMS operator performance metrics. Performance characteristics of twelve novice operators were examined. The novice data were then used to evaluate the ability of a set of proposed metrics to differentiate among operators. Specific goals of the dissertation are listed below.

- Investigate the differences / similarities in the input patterns (i.e., the order and manner in which each of the axes is entered and commanded) of novice operators. These differences might suggest important performance characteristics that indicate operator skill. Select performance metrics that quantify the differences observed in performance patterns.

- Compare the performance of novice operators to the rational models of expert performance developed for this dissertation. Differences between the rational model and the performance of the novice operators might suggest critical aspects of performance. Focusing on the development of these critical skills in training could reduce training time.

- Compare hypothesized and observed control strategies (patterns of input) and discuss the advantages and disadvantages of the control strategies from a human factors perspective. A preliminary hypothesis presented in this dissertation is that minimizing the number of axes simultaneously being commanded reduces cognitive workload and the potential for error.

2.5 Organization and Chronology

To meet the objectives outlined above, the dissertation research was completed in two stages that resulted in (1) metric development, and (2) metric extraction and validation. Figure 11 illustrates the organization and chronology of the two dissertation stages.

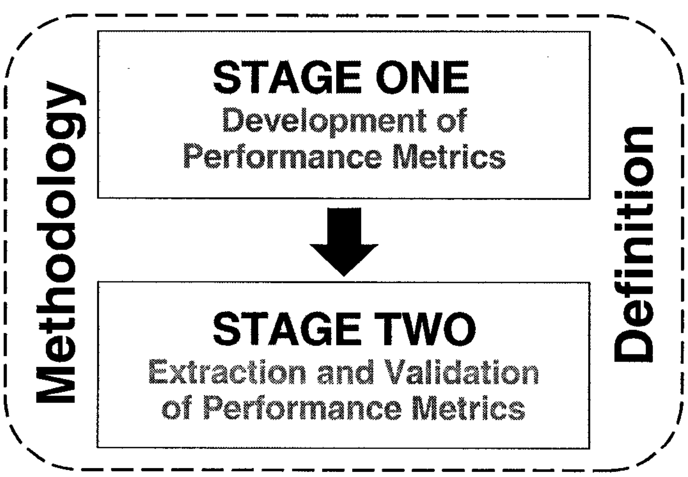

Figure 11. Organization and Chronology of the Dissertation.

Stage One (Development of Performance Metrics) and Stage Two (Extraction and Validation of Performance Metrics) were completed in sequential order. The nature of this dissertation dictated that much of the research methodology be defined as the work progressed. Therefore, the information gathered in the course of the research guided decision-making and led to the development of new alternatives that formed the basis for (and affected the direction of) subsequent work. This process of exploration and change was difficult to manage, and even more difficult to describe. Hence, the research methodology developed and employed in these stages represents a major contribution and satisfies the first objective of this dissertation – to define the methodology for development and validation of the performance metrics. Objectives and activities conducted in each stage of the dissertation work are discussed in the following chapters.

CHAPTER 3

STAGE ONE: DEVELOPMENT OF PERFORMANCE METRICS

Stage One activities were designed to achieve the first objective of the dissertation: to develop objective performance metrics for RMS operators based on NASA's Generic Robotics Training. Development of the performance metrics required a clear and thorough understanding of BORIS, task demands, training procedures, and evaluation criteria. Hence, meeting the Stage One objective required the completion of three major activities: examining the NASA robotics training program, performing an analysis of the RMS task, and proposing potential performance metrics. Figure 12 illustrates the flow of the activities completed during Stage One that resulted in the development of potential metrics to evaluate RMS operator performance. Examination of the NASA GRT program provided the information needed to understand the demands of RMS operation and to identify a critical RMS task. Subsequently, a task analysis resulted in the identification of critical elements of RMS performance. A thorough examination of the critical aspects of performance was achieved through an iterative process that consisted of defining the potential metrics and developing theoretical models of expert performance through investigation and comparison of the differences observed in plots of actual performance data.

One of the major contributions of this dissertation was the development and documentation of the methodology used to develop and validate the performance metrics. As mentioned, the methodology was developed integrally with the Stage One and Stage Two activities and was based on the information acquired as the research progressed.

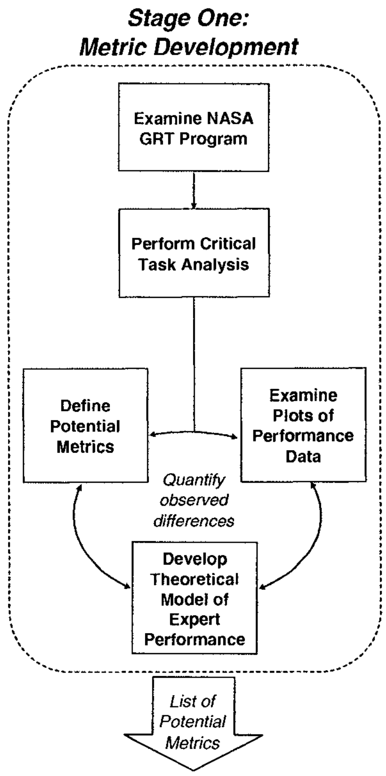

Figure 12. Flowchart Diagram of the Stage One Activities and Output.

Table 2 provides a summary of the goals, methodology, and outputs of the Stage One activities. Details of the Stage One methodology and activities are discussed in the remainder of this chapter.

3.1 Examination of the NASA Robotics Training Program

Producing reliable, sensitive performance metrics required a comprehensive understanding of the factors that affect RMS operation. Hence, it was critical to review NASA's current robotics training procedures, particularly those employed in the GRT program. Since empirical testing would be utilized to validate the effectiveness of the developed metrics, it was crucial that the researchers not only learn to properly and effectively operate BORIS, but also learn to train others to operate BORIS. It was necessary to understand the instructor evaluation process in order to identify the skills

Table 2. Summary of Stage One Activities and Outputs.

Activity	Goals	Methodology	Outputs
Examine NASA robotics training program	• Learn general robotics terminology • Learn to properly and effectively operate BORIS • Learn to train others to operate BORIS • Understand physical and cognitive activity involved • Understand instructor evaluation process	• Review existing literature and documentation • Interview SMEs • Participate in NASA GRT program at JSC (Houston, TX)	• Understanding of RMS task (operation, demands, and evaluation) • Information input to task analysis
Perform task analysis	• Identify critical task elements • Define Task Analysis Methodology	• Select a critical operational task • Determine task demands on operator • Identify critical demand elements (psychomotor / cognitive) • Prioritize categories of skills required	• Input needed for metric development • Task Analysis Methodology

Propose potential performance metrics	• Develop reliable, sensitive, objective (quantitative) metrics to assess RMS operator performance
	• Define Metric Development Methodology
		• Identify critical task measures
		• Describe each measure in general terms
		  * Identify importance / utility of the measure
		  * Identify important measure characteristics
		  * Propose potential measurement solutions
		• Operationally define measure
		• Identify ramifications / constraints
		• Determine performance criteria and limits
		  * Interviews with instructors
		  * Demonstrations of various levels of performance
		• Set numerical limits
		• Identify data acquisition procedure
			• List of potential performance metrics
			• Metric Development Methodology

that the instructor-experts consider important indicators of operator competence. Understanding the relative importance of the identified skills helped guide the metric selection and development process.

Acquiring the essential information to achieve the Stage One objective was accomplished through perusal of available literature related to NASA's robotics training, interviews of subject-matter-experts (SMEs) including GRT instructors and RMS operators, and, most importantly, participation in the GRT program at NASA's Johnson Space Center in Houston, Texas. During an intensive week in the summer of 2002, the researchers completed the entire GRT lesson sequence and the practice evaluation session. To provide insight into training and evaluation procedures and techniques, the researchers were also permitted to observe a NASA astronaut trainee during the first three GRT training lessons and an experienced astronaut crewmember performing an advanced mission-specific lesson that simulated installation of an additional element to the ISS.

Actively experiencing the RMS operator training through on-site, hands-on participation provided greater insight into the task demands than could be obtained through external reviews alone. It also served to build a knowledge base that permitted a more profound understanding of the information acquired from external sources. Section 2.3 presents much of the information learned through participation in the GRT program.

To ensure that comparable training would be provided to the participants in the study to validate the proposed measures, the NASA JSC robotics personnel graciously provided access to lesson plans, evaluation materials, and support documents used in the GRT sequence. Interviews of the instructors and GRT evaluation personnel were conducted to obtain instruction, guidelines, and advice on evaluating RMS operator skills. Training aids were constructed to match (as closely as possible) those used at JSC. The BORIS simulation and Trick operational environment were installed and configured to operate on a PC workstation in laboratory space located in Carson Engineering Center on the Norman Campus of the University of Oklahoma. A set of hand controllers comparable to those used in the NASA RMS training (and similar to the ISS and Shuttle RMS controllers) was purchased and subsequently received in January 2003.

3.2 RMS Task Analysis

Examination of the RMS training program and completion of the on-site GRT training provided detailed knowledge of the physical and cognitive activities involved in the operation of the RMS. The next step in the methodology development process involved the use of task analysis methods to identify the critical performance elements to be incorporated in the metrics. As discussed previously, Khoury et al. [1999] and Morphew et al. [2001] attempted to identify the most challenging physical and cognitive demands of RMS operation with a cognitive task analysis based on interviews of subject-matter experts and a literature review. The researchers suggested that the psychomotor aspect, or translation of environmental cues into hand controller inputs, was the most challenging RMS task, and postulated that this activity required a high level of situation awareness. Unfortunately, the researchers provided few details on the processes and inputs that were used to obtain their results. Further, their findings were presented in very general terms that were insufficiently detailed to be of practical use in this dissertation. Hence, in order to meet the Stage One objective, a separate task analysis of the RMS operation was conducted. The task analysis was designed to determine task demands on the RMS operator, identify critical demand elements (psychomotor/ cognitive), and define the skills required to efficiently and effectively operate the RMS.

As listed in Table 2, the task analysis process began with the selection of a critical RMS task. Although a complete analysis of the RMS task was beyond the scope of this dissertation, a task analysis was performed on a representative portion that demonstrated several critical demand elements. With a focus on representing the GRT Category 1 skills, the translation element of an unloaded fly-to was chosen for analysis. This task is a critical RMS psychomotor task that requires perceptual-motor skill. Tendick et al. [2000] reported that performance in these types of targeted movements depends on the quality and use of visual depth cues and the accuracy of the operator's mental model of the 3-D environment. Hence, performance of this task requires three of the four Category 1 skills: situation awareness, arm maneuvers, and hand controller techniques. Additional skills that might be assessed include SFRM and camera techniques.

The task analysis methodology was developed as a logical extension of the basic model of a cognitive process depicted in Figure 13. This model illustrates the relationships between elements involved in perceptual, cognitive, and psychomotor aspects of human performance.

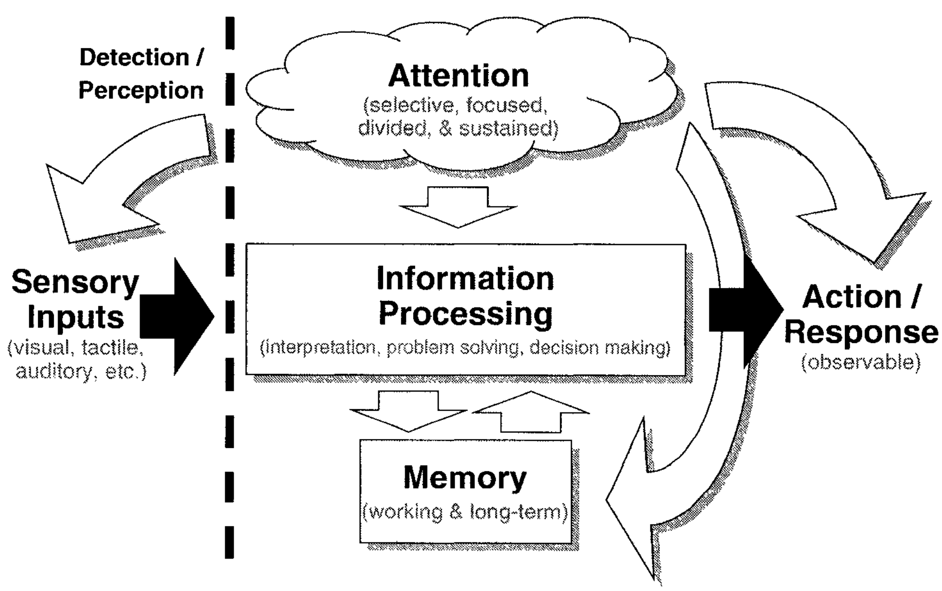

Figure 13. Model of a Cognitive Process [Adapted from Sanders & McCormick, 1992].

The task analysis process continued by constructing a detailed list of all activities involved in performing the task to determine the task demands on the operator. Then, the critical perceptual, cognitive, and psychomotor demands of each of the activities were identified. During the course of this process, the relationship of the task analysis process to the cognitive process model was recognized, resulting in an organization of the task demands into Task, Planning, and Execution elements, corresponding to the Input, Information Processing, and Response elements of the cognitive process model. The resulting Task Analysis Model for the chosen translation task is shown in Figure 14.

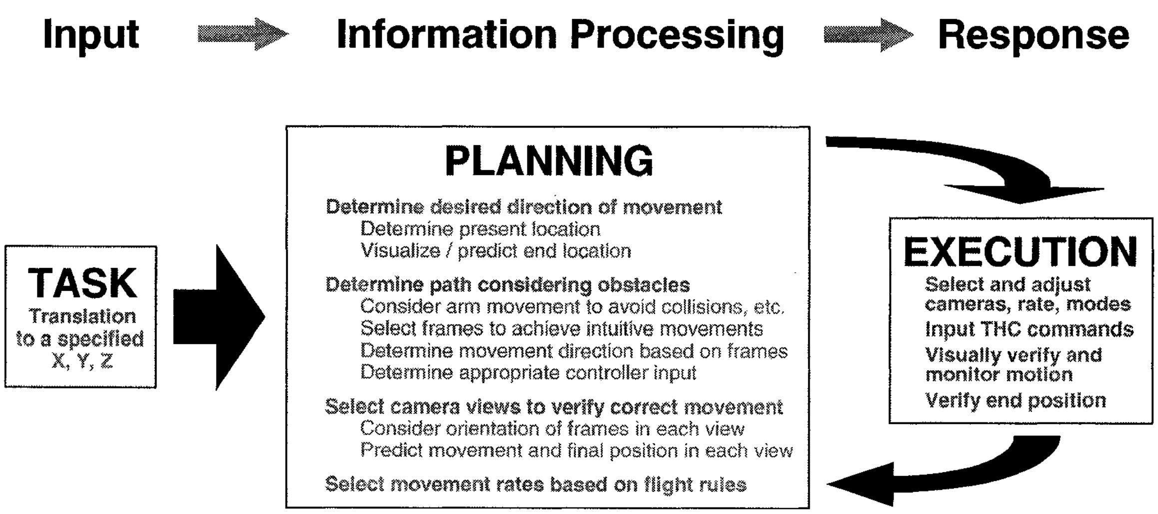

Figure 14. Task Analysis Model of a Critical RMS Task.

Once the critical skills associated with the task were identified, these skills were prioritized with respect to their relative contribution to overall performance. This was done by considering the amount of time required, and the potential for (and impact of) making errors while performing the task. Additionally, the GRT evaluation criteria were considered since they represent the consensus of experts regarding the impact of the skills on RMS task performance. As seen in the task analysis model, the majority of demands were related to planning the task. Hence, the most important skill required by the task was determined to be situation awareness (perception, comprehension, and projection). This finding supports the GRT categorization of SA as a Category 1 skill.

Safe, effective, and efficient performance of the translation task requires the operator to utilize all available information to develop sufficient SA. Selection of camera views is important to provide perception cues that reduce the necessary spatial processing / mapping to result in intuitive movement. In this manner, good camera views can increase the task speed and reduce errors. Spatial-perceptual skills are required to predict and recognize proper positioning. The operator must possess a good understanding of frames in order to select the frames that will facilitate performance. In the event that intuitive frames are not available, the operator must be able to perform the "mental gymnastics" required to achieve the goals of the task.

As mentioned previously, the translation task inherently contains a large psychomotor element, so motor control was also determined to be very important to the performance of the task. The most critical psychomotor skills involved in the execution of the task are related to the hand controller inputs. Improper inputs can result in errors in speed or direction of movement that could reduce the efficiency of the operation, impose oscillations in the arm, or result in collisions with structure. While the greatest potential for error exists in the cognitive processes, there is a chance that errors can occur in the transference from thoughts to actions. This is the case where the operator decides to input a command in a particular direction (such as +Y), but physically commands a different direction (such as +X). Further, two of the Category 1 skills (arm maneuvers and hand controller techniques) are concerned with control skills. Based on the results of the task analysis, two control skills were identified as critical task elements: smooth inputs and multi-axis commands.

Smooth ramping of commands is critical to reduce arm oscillations that can affect the safety of the task. Multi-axis commands also reduce arm oscillations, and provide smooth and efficient movement. While both of these elements demonstrate psychomotor skills, multi-axis commands also require situation awareness and spatial skills. Multi-axis commands are appropriate for general fly-to tasks, and are essential when aligning the EE with the grapple pin, but may not be appropriate when too close to structure, or when grappling, berthing, or unberthing a payload. In these cases, movements should be restricted along one axis for safety purposes.

3.3 Metric Development

The task analysis was designed to identify critical task elements that were used to guide further development of the metrics. As a result, two critical task elements were identified: smooth hand controller inputs (ramping) and multi-axis commanding. The identified elements require psychomotor skills, situation awareness, and spatial skills, thereby satisfying the focus on measuring Category 1 skills (arm maneuvers, hand controller techniques, and situation awareness). Defining the requisite knowledge, skills, and abilities (KSAs) for the critical task elements helped suggest potential performance measures that assess the skills required to perform those elements. The activities and reasoning presented in this section provided the foundation that led to the definition of the metric development methodology.

Table 3 shows the application of the metric development methodology to the critical task elements identified by the task analysis. Each element was operationally defined to provide the transition from a qualitative description to a quantifiable measure. Then, ramifications and constraints were identified to help establish the criteria that might indicate various levels of performance. Criteria bounds were dictated by specified system constraints or based on acceptable and unacceptable levels of performance exhibited by expert operators. When combined with knowledge of the recordable variables in the BORIS simulation, performance data can be isolated and extracted.

Table 3. Application of the Metric Development Methodology.

Methodology	Smooth HC Inputs	Multi-Axis Commanding
Describe measure in generai terms	• Smoothness in rate of change of controller displacement over time • Smoothness in rate of change of arm movement rates over time	• Simultaneous input along two or more HC axes • Simultaneous input to both hand controllers
Operationaily define the measure	• Change in commanded rate along or about a specified axis divided by change in time (elapsed time)	• Percentage of time that multi-axis control is applied • Minimal travel time based on maximum rates and optimal path
Identify ramifications / constraints	• Maximum rate (speed) in specified direction • Design limits of the arm, flight rules, task requirements	• Starting and ending positions and orientations • Obstacles and structural interference • Available views (orthogonal, compatible, triangulation) • Selection of command frame
Determine performance criteria and limits	• Steepness of rate change slope • Smoothness of rate change slope • Detection of sudden instantaneous changes • Lower limit (affects completion time) • Upper limit (affects safe use of arm)	• Percentage of time using multi-axis commanding • Lower limit (affects completion time) • Upper limit (affects task difficulty)

Set numerical limits	• Objective
	  * Physically determined limits
	  * Maximum acceptable oscillation
	• Subjective
	  * Sample several participants (use mean / median)
		• Subjective
		  * Construct theoretical models of expert performance
		  * Compare expert & novice to select measure(s) that maximize group differences

Identify data acquisition procedure	• HC inputs and robot arm movements • BORIS / Trick data files and output plots	• HC inputs and robot arm movements • BORIS / Trick data files and output plots

The remainder of this chapter provides a detailed account demonstrating the application of the methodology that led to the development of the metrics that were selected to measure ramping performance and the use of multi-axis commanding. A description of the methodology used to validate the metrics is given in the next chapter.

3.3.1 Determination of Performance Criteria

One of the challenges involved in the development of metrics to assess operator performance is determining the criteria that demonstrate skilled performance. While some aspects of a performance standard can be developed using theoretical methods, the resulting criteria limits may represent "idealistic" performance. However, theoretical models can be used to determine the performance limits that can be achieved given the physical limits of the RMS system. These theoretical performance limits may be dictated by the mechanical joint reach and rate limits of the arm within the constraints of the VEGA environment. Once these limits are identified, one must attempt to define a more realistic performance "standard" and determine how to assess differences from the standard. In other words, what is the acceptable deviation from the standard that delineates "expert" from "good" or "fair" performance?

One of the most practical methods for determining realistic values is to investigate the characteristics of "expert" operators. Comparing the performance characteristics of novice operators with those of operators considered "expert" by NASA standards could help to provide the basis for determining RMS performance metric gradations that define the different levels of skill. However, in the absence of actual data from expert operators, this dissertation examined performance differences between novice operators and made comparisons with the rational models presented in the following sections.

3.3.2 A Theoretical Model of Ramping

As mentioned previously, the RMS hand controllers control the rate of movement of the POR. Deflection of the controller in a given direction results in a corresponding change in the velocity of the POR in that direction limited by the velocity constraints at the joints and overall along a given axis. Ramping refers to making gradual, controlled displacements (inputs) of the hand controllers to smoothly increase and decrease the POR velocity over time. Smoothness of hand controller inputs during ramping can be depicted by an idealized plot of the system velocity as a function of time, as shown in the diagram in Figure 15. The positively sloped line from t_0 to A shows a smoothly ramped increase in velocity from time t_0 to time t_1 (ramp-in). Line AB depicts movement at a constant maximum rate (not necessarily the system maximum) from time t_1 to time t_2 (travel time). The negatively sloped line from B to t_3 represents a smoothly ramped decrease in velocity from time t_2 to time t_3 (ramp-out). Final input adjustments are made between time t_3 and time t_4, the task completion time, in order to accurately align the POR with the target point. The slope of each line represents the rate of change (acceleration) of the commanded input velocity.

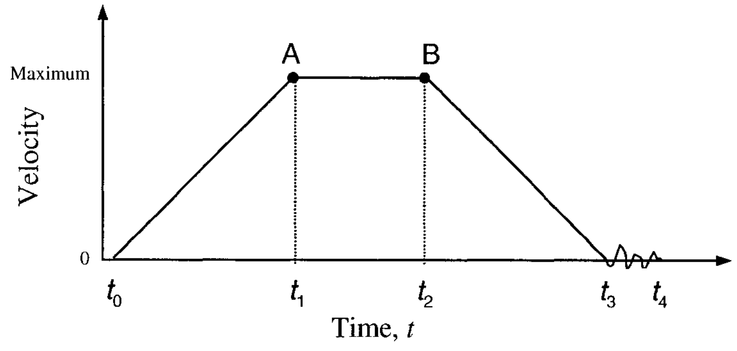

Figure 15. Rational Model of a Smoothly Ramped Hand Controller Input.

The model portrayed in Figure 15 can be used to theoretically determine the minimum total time it would take to complete a movement along one axis considering the system capabilities and physical constraints of the RMS system. The total movement time is given by the sum of the required ramp-in time (t_{rin}), travel time (t_{trav}), ramp-out time (t_{rout}), and correction time (t_{corr}). Expressed mathematically, the total time to complete a movement is given by the equation

$$\text{Total Movement Time (TMT)} = t_{rin} + t_{trav} + t_{rout} + t_{corr}.$$

Ramp-in time is defined as the time taken to accelerate from zero to a constant maximum velocity (not necessarily the system-imposed maximum). Travel time is defined as the interim time between ramp-in and ramp-out. Ramp-out time is defined as the time taken to decelerate from the constant maximum velocity to zero. Correction time is the amount of time used to acquire the target beyond the time when motion is initially ramped out. With reference to the diagram above, these times can be expressed by the following equations:

$$\text{Ramp-In Time } (t_{rin}) = t_1 - t_0,$$

$$\text{Travel Time } (t_{trav}) = t_2 - t_1,$$

$$\text{Ramp-Out Time } (t_{rout}) = t_3 - t_2, \text{ and}$$

$$\text{Correction Time } (t_{corr}) = t_4 - t_3.$$

For known velocities and constant accelerations, the distance traveled during a specified time period (i) is given by the equation

$$d(t)_i = v_0 t_i + \tfrac{1}{2} a\, t_i^2.$$

Based on design specifications, the BORIS system can achieve a maximum commanded translational velocity (in coarse rate) of 30 cm/s. If the velocity transition from 0 to 30 cm/s^2 occurs within 0.08 seconds (the sampling interval of the data recording), the maximum acceleration provided by the system is 375 cm/s^2. However, empirical observations show that the acceleration to maximum velocity typically requires a time span of 0.24 s (three sampling periods), producing realistic maximum acceleration of 125 cm/s^2. Hence, the minimum ramp-in time (to achieve maximum velocity) is 0.24 s, during which time the arm moves a distance of $d(t)_{\text{rin}} = v_0\, t_{\text{rin}} + \frac{1}{2}\, a\, t_{\text{rin}}^2 = (0)(0.24) + \frac{1}{2}(125)(0.24)^2 = 3.6$ cm. Travel time is minimum for $t_{\text{trav}} = 0$ s, during which time the arm moves a distance of $d(t)_{\text{trav}} = v_0\, t_{\text{trav}} + \frac{1}{2}\, a\, t_{\text{trav}}^2 = 30(0) + \frac{1}{2}(125)(0)^2 = 0$ cm. Minimum ramp-out time is 0.24 s, during which time the arm moves a distance of $d(t)_{\text{rout}} = v_0\, t_{\text{rout}} + \frac{1}{2}\, a\, t_{\text{rout}}^2 = 30(0.24) + \frac{1}{2}(-125)(0.24)^2 = 3.6$ cm. Therefore, the minimum time required to achieve maximum velocity and then decelerate to zero would be 0.48 s, during which time the arm would move a total distance of 7.2 cm. Clearly, any task requiring a total translation distance of less than 7.2 cm would not allow the operator to achieve maximum velocity while maintaining efficiency and precision.

It is important to note that the minimum total movement time calculated above would only be achieved under a scenario in which the movements were not truly "ramped." Rather, the example illustrates "full throttle" hand controller inputs. These abrupt accelerations and decelerations are undesirable because they have the potential to produce oscillations in the arm. In the model above, ramping performance can be assessed by the slope and smoothness (linearity) of the ramp-in and ramp-out velocities. The steepness of the slope, which represents the acceleration of the movement, has an upper bound defined by the "full-throttle" condition, such that the maximum slope (acceleration) is 375 cm/s^2.

One of the goals of the larger research project within which this dissertation work was conducted is to determine the slope (or range of slopes) that defines "expert" ramping and, from there, define the ranges of deviation from the "expert" that delineate lesser performance levels. The range of acceptable accelerations can be determined by analyzing the performance of operators with varying skill levels. Hence, a comparison of the performance characteristics of novice and expert operators will be conducted at a later date to define the statistical properties of the metric distribution (mean and variance) and demonstrate the ability of each metric to differentiate among operators with varying levels of skill.

3.3.3 Critical Aspects of Ramping Performance

The ramp-out performed by the operator is very important to the overall efficiency and accuracy of the task. One of the questions investigated in this research is the extent to which operators generally plan and control the ramp-out in advance of approaching the target. It was hypothesized that the ramp-in may be a more consciously-guided open-loop task, and that ramp-out may be a less-planned closed-loop task. Ramp-in occurs at the beginning of the task when there are fewer events that need attention, while ramp-out begins during the course of the task, perhaps in the midst of events that compete for the operator's physical and mental resources. If the ramp-out can be accurately planned and controlled by the operator, the ramp-out rate would be consistent with the ramp-in rate. To perform in the most efficient manner possible, both speed and accuracy must be high. Therefore, the operator would ramp-in at the maximum acceptable acceleration and move at the maximum speed until beginning ramp-out. The operator would then ramp-out at the maximum acceptable deceleration and precisely meet the target. Hence, with precise initiation of the ramp-out, the commanded deceleration rate would mirror the commanded acceleration rate. Skilled control of movement requires the ability to make accurate spatial and temporal judgments. A critical measure of performance may be indicated by the operator's ability to determine when to begin ramp-out (point B on the diagram) based on visual feedback and to control the ramp-out deceleration so that the target is precisely met. Failure to recognize this point would require the operator to change the rate of deceleration and/or may result in a loss of accuracy that requires further adjustment and, hence, additional time. Comparison of accelerations and decelerations within and between operators should show how well operators are able to plan motions, and whether differences are indicative of skill level.

While there may be individual differences in operators' commanded acceleration, ramping performance is largely determined by the physical constraints of the system and NASA guidelines. On a graph of commanded velocity vs. time, the slope of the ramped input (acceleration) and the smoothness of the line (straightness representing steadiness of the acceleration) are the critical measures that might demonstrate differences in performance. Both of these characteristics may be determined by performing separate linear regressions of the commanded hand controller input data for the ramp-in and ramp-out periods. Least-squares linear regression provides the equation of the "best fit" line determined by the data. Typically, the corresponding R^2 value is calculated to represent the percent of the variation in the data explained by the equation, and its square-root, r, indicates the strength of the linear relationship. The value of R^2 ranges from zero to one, with values closer to one suggesting a closer "fit" of the linear model to the data. The linear regression line is in the form

$$y = \beta_1 x + \beta_0,$$

where y is the dependent variable, x is the independent variable, β_1 is the slope of the line (change in y for each unit change in x), and β_0 is the y-intercept (value at which the line crosses the y axis).

A plot of the commanded velocity and position data for a "full throttle" movement along the X-axis is provided in Figure 16 to illustrate the example discussed in the previous section and to demonstrate how linear regression can be used to evaluate ramping performance. The linear regression line equations associated with the ramp-in and ramp-out periods express the commanded velocity (v) as a function of time (t). As mentioned previously, the slope (acceleration) of the ramped input and the smoothness (linearity) of the line are hypothesized to be critical measures that demonstrate differences in performance. The slope of the line represents the average rate of change of the commanded velocity over time (acceleration), while the value of R^2 can provide a measure of the smoothness of the commanded inputs. Figure 16 also contains a plot of the position in X with respect to time. Note that the slopes for the regression lines of the commanded velocity and position over time represent the average acceleration and average velocity achieved, respectively.

Based on the discussion in the previous section, perfectly smooth and linear "full-throttle" inputs would achieve average accelerations of $\pm$ 125 cm/s^2 over the 0.24 s ramp-in and ramp-out time periods. However, as illustrated by the changes in the slope of the ramp-in line in Figure 16, the ramp-in acceleration was not consistent, with slower accelerations at the beginning and ending of the ramp-in period. Due to the inconsistency in the rate of the commanded inputs, the average ramp-in acceleration was 143.69 cm/s^2 rather than the theoretical 125 cm/s^2 that would have been achieved if the inputs were

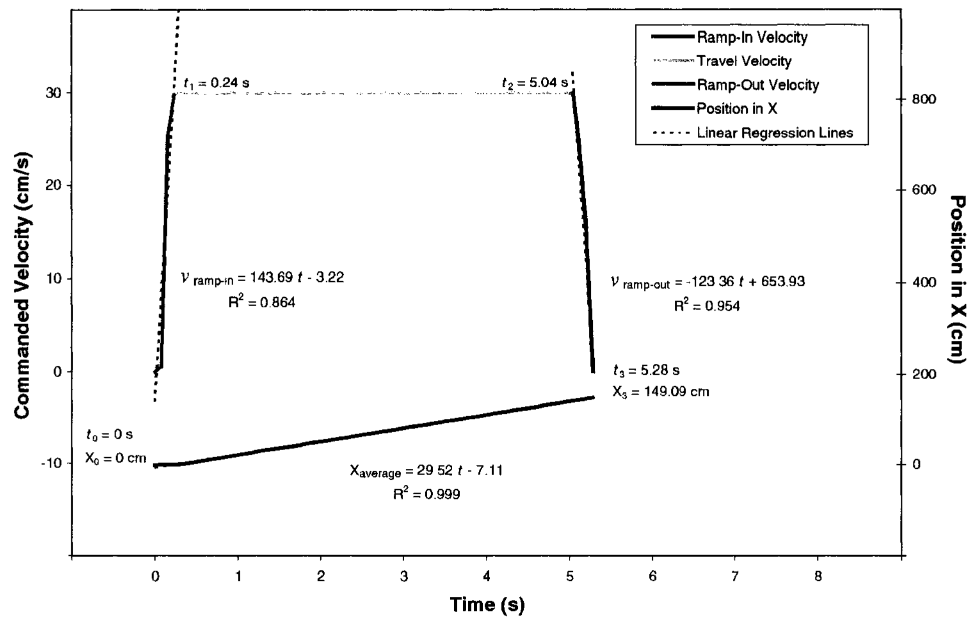

Figure 16. Evaluation of "Full-Throttle" Ramping Using Linear Regression.

completely linear. Further, if the commanded inputs were smooth and linear, the R^2 value, which suggests the degree of deviation from pure linearity (smoothness), would be close to a value of 1.0. Therefore, the inconsistency in the commanded inputs is also indicated by the lower R^2 value of 0.864. In contrast, the ramp-out performance is more smooth and linear, as seen by the plotted line and indicated by the associated linear regression equation. The average deceleration achieved by the ramp-out (-123.36 cm/s^2) is very close to the theoretical -125 cm/s^2, and the R^2 value of 0.954 is much closer to 1.0.

Although GRT instructors encourage operators to ramp commands in and out, there is no precise formal recommendation regarding the appropriate or "optimal" accelerations to apply. As mentioned above, determining the range of acceptable accelerations will require analysis of performance data from acknowledged "expert" operators and comments from NASA instructors. Novice operators may benefit from a training tool that would allow them to trace an optimal ramp pattern. This exercise could help to remove some of the ambiguity from the instruction and reduce the potential to learn bad hand controller techniques.

3.3.4 Potential Metrics to Assess Ramping Performance

Identification of the preliminary set of potential metrics to assess ramping performance was accomplished by examining the critical aspects of ramping: accelerations during ramp-in and ramp-out, smoothness of hand controller inputs, and the ability to determine when to begin ramp-out so that the target is precisely met (i.e., accuracy / efficiency). These critical aspects were determined through the iterative study of the rational model and plots of previous data and pilot data collected for the ramping tasks. As mentioned, linear regression of the commanded velocity data was employed to provide the potential ramping performance metrics that represent accelerations (slope of the regression line) and smoothness of hand controller inputs (R^2 value). Comparison of the ramp-in and ramp-out accelerations and R^2 values within and between operators could indicate differences in performance that may be used to differentiate levels of skill. It was hypothesized that one of the most critical measures of operator skill would be indicated by the ramp-out performance. Specifically, the operator's ability to control the ramp-out so that the target is precisely met may be highly indicative of skill level. Differences in accelerations between the ramp-in and ramp-out may indicate a lack of planning, so that the deceleration is dictated by the upcoming target rather than planned by the operator. Inadequate planning can lead to inefficiency (undershooting the target) and / or failure to accurately meet the target (overshooting the target). These can be indicated by changes in the slope of the ramp-out or by control reversals. The methodology employed in identifying the potential metrics to evaluate ramping performance is illustrated in the example below.

Plots of the commanded velocity over time were generated using performance data from tasks that demonstrated ramping. The plots were divided into four segments that represented ramp-in, travel, initial ramp-out (Ramp-Out 1), and ramp-out plus corrections (Ramp-Out 2). These segments were identified manually by examining the commanded velocity data values provided in the BORIS output data. "Ramp-In" was defined from the initialization of commanded input until some constant maximum velocity was reached. Movement at this constant maximum velocity was defined as "travel." The initial ramp-out (Ramp-Out 1) was defined from the initial decrease in velocity after the travel segment until velocity first reached zero. The overall ramp-out (Ramp-Out 2) includes all of the initial ramp-out plus any corrections required to complete the task. The four segments can be seen in Figure 17, which illustrates the linear regression analysis approach on a ramping task in which the operator was instructed to move the POR as quickly as possible while using smoothly ramped commands along the +Y axis to a target (a gridline with a width of 5 cm) located at a distance of 100 cm from the start position.

The inconsistency in hand controller inputs over the ramp-in period, as evidenced by the "stepped" appearance of the ramp-in segment, produced a lower R^2 value (0.799) in the linear regression of the ramp-in data. The travel segment was performed at a maximum constant velocity of 19.9 cm/s for 1.5 seconds. Notice that the ramp-out deceleration was initially too large, such that the motion would have stopped far short of the target. Subsequently, the operator adjusted the deceleration rate and completed the task at a slower pace. The operator then stopped short of the target, and had to provide additional input before coming to rest within the target boundaries. Although the target was eventually met (within a tolerance of ± 2.5 cm, or the width of a gridline), the ramp-out performance was not smooth or consistent. Further, the overall efficiency of the task suffered since the need to make corrections added to the task completion time.

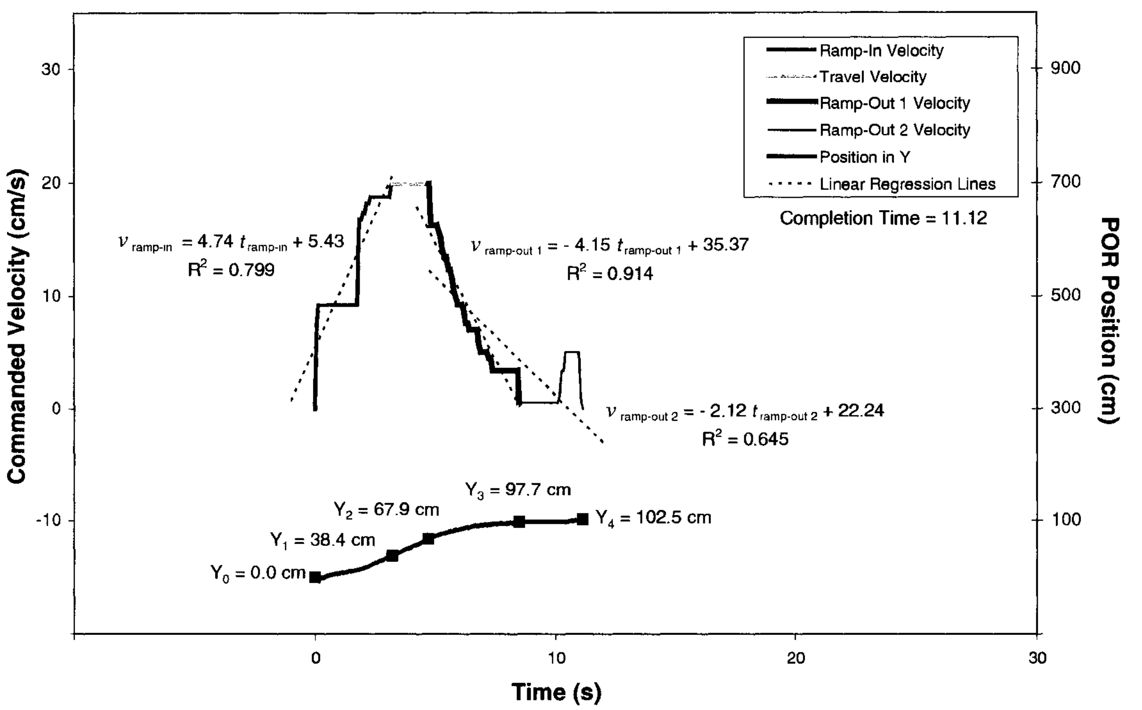

Figure 17. Evaluation of a Task Demonstrating Inconsistent Ramping Performance.

While the average Ramp-In acceleration (4.74 cm/s^2) was only slightly higher than the average Ramp-Out 1 deceleration (–4.15 cm/s^2), the corrections further reduced the average deceleration for Ramp-Out 2 to –2.12 cm/s^2 and dropped the R^2 value for the overall ramp-out from 0.914 to 0.645. Ramp-in was completed in 3.2 s, during which time the POR moved 38.4 cm. If the operator had been consistent, the ramp-out period would have covered the same time and distance. This means that the operator should have begun ramp-out at a point 38.4 cm from the target location, or at the point Y = 61.6 cm. As seen in Figure 17, the operator started ramp-out later, at the point Y = 67.9 cm, and then decelerated more slowly in order to meet the target. Ramp-Out 1 took 3.8 s, during which time the POR moved a distance of 29.8 cm. Then, corrections added an additional 2.6 seconds. Because of this, the total ramp-out period took twice as long (6.4 s) as the ramp-in period (3.2 s), causing a loss in overall task efficiency. Travel time would have required about 1.2 s to cover the remaining 23.2 cm, so the task could have been completed in 7.6 s rather than 11.1 s if the operator had been consistent.

The BORIS simulator output provided raw values of time, movement velocities, and POR positions over the course of the task. Linear regressions on the commanded velocity data acquired from the ramping task were conducted to obtain the metrics for evaluating the accelerations (slope of the regression line) and smoothness of hand controller inputs (R^2 value). Finally, overall efficiency in the ramping performance was assessed by maximum commanded velocities, off-target error, correction times, and task completion times. Table 4 provides a complete listing and descriptions of the ramping metrics that were evaluated in the analysis stage of the dissertation.

3.3.5 Impact of RMS Operator Strategy in the Use of Multi-Axis Commands

The strategy employed by an RMS operator while performing a task is a large determinant of the resulting performance. One aspect of "strategy" refers to the way in which the operator elects to input multi-axis commands (i.e., the order and manner in

Table 4. Preliminary Set of Metrics to Evaluate Ramping Performance.

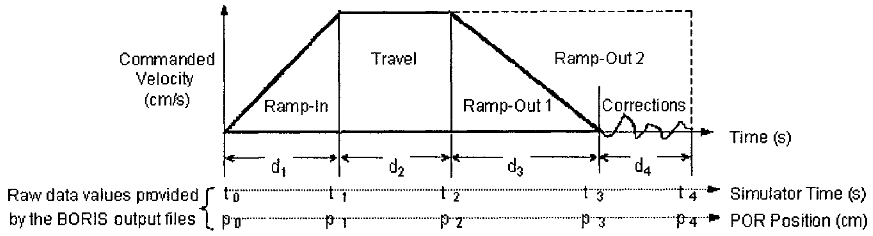

Code	Metric	Units	Description / Comments
A_In	Ramp-In Acceleration	cm/s^2	Slope of the regression line for the ramp-in data. Ramp-in is defined from the initial commanded input until some maximum constant velocity is reached.
R_In	Ramp-In R^2	----	Fit of the linear regression line of the ramp-in data. Intended as a measure of the smoothness (linearity) of the commanded input over the ramp-in period.
A_Out_1	Ramp-Out 1 Deceleration	cm/s^2	Slope of the regression line for the initial ramp-out data. Ramp-Out 1 is defined from the initial decline from the maximum constant velocity until zero velocity is reached.
R_Out_1	Ramp-Out 1 R^2	----	Fit of the linear regression line of the initial ramp-out data. Intended as a measure of the smoothness (linearity) of the commanded input over the initial ramp-out period.
A_Out_2	Ramp-Out 2 Deceleration	cm/s^2	Slope of the regression line for the overall ramp-out data. Ramp-Out 2 is defined from the initial decline from the maximum constant velocity until the task is completed; this includes all corrections.
R_Out_2	Ramp-Out 2 R^2	----	Fit of the linear regression line of the overall ramp-out data. Intended as a measure of the smoothness (linearity) of the commanded input over the overall ramp-out period.
V_Max	Maximum Velocity	cm/s	The maximum velocity achieved during the task. Typically the "travel" velocity.
RIT	Ramp-In Time	s	Time spent during ramp-in; RIT= $(t_1 - t_0)$.
RID	Ramp-In Distance	cm	Distance covered during ramp-in; RID = $d_1 = (p_1 - p_0)$.
TT	Travel Time	s	Time spent during the travel period; TT = $(t_2 - t_1)$.
TD	Travel Distance	cm	Distance covered during the travel period; TD = $d_2 = (p_2 - p_1)$.
RO1T	Ramp-Out 1 Time	s	Time spent during the initial ramp-out; RO1T = $(t_3 - t_2)$.
RO1D	Ramp-Out 1 Distance	cm	Distance covered during the initial ramp-out; RO1D = $d_3 = (p_3 - p_2)$.
CT	Correction Time	s	Time spent making corrections; CT = $(t_4 - t_3)$.
CD	Correction Distance	cm	Error distance from target after initial ramp-out; CD = $d_4 = (p_4 - p_3)$.
TCT	Task Completion Time	s	Time required to complete the task; TCT = $(t_4 - t_0)$.
PRIT	Percent Ramp-In Time	----	Percentage of the total time spent during ramp-in; PRIT = $((t_1 - t_0) / (t_4 - t_0))$ X 100%.
PRID	Percent Ramp-In Distance	----	Percentage of the total distance covered during ramp-in; PRID = $(d_1/(p_4 - p_0))$ X 100%.
PTT	Percent Travel Time	----	Percentage of the total time spent during the travel period; PTT = $((t_2 - t_1) / (t_4 - t_0))$ X 100%.
PTD	Percent Travel Distance	----	Percentage of the total distance covered during the travel period; PTD = $(d_2 / (p_4 - p_0))$ X 100%.
PRO1T	Percent Ramp-Out 1 Time	----	Percentage of the total time spent during initial ramp-out; PRO1T = $((t_3 - t_2) / (t_4 - t_0))$ X 100%.
PRO1D	Percent Ramp-Out 1 Distance	----	Percentage of the total distance covered during initial ramp-out; PRO1D = $(d_3 / (p_4 - p_0))$ X 100%.
PCT	Percent Correction Time	----	Percentage of the total time spent making corrections; PCT = $((t_4 - t_3) / (t_4 - t_0))$ X 100%.

which each of the axes is commanded). One of the research questions in this study is concerned with comparing the differences in the control strategies used by novice operators. An even more important aspect of the question may be "Which strategy is better, from a human factors perspective?" A human factors perspective refers to taking a human-centered approach to viewing tasks and processes (considering the capabilities and limitations of the human) with the objective of reducing effort (workload) and increasing safety and efficiency. Multi-axis commands are encouraged by NASA instructors to reduce undesirable oscillations in the RMS arm and shorten the total task time. However, a human factors perspective might suggest that minimizing the number of axes controlled simultaneously will reduce cognitive workload and the potential for error. Masliah and Milgram [2000] provide support for this theory by observing that the operators in their study employed control strategies that reduced the number of axes being controlled simultaneously in an attempt to reduce task complexity. Hence, operational strategies that consider and accommodate both system and operator needs may produce the safest and most efficient performance.

To illustrate the results of several different control strategies, consider a simple translation task that requires motion along two axes, X and Y, between two points, A and B. The operator has many options with respect to choice of path and speed of movement, which are both commanded using the hand controllers.

Strategy 1: Sequential Single-Axis Control

Travel between the two points could be made by moving the required distance along one axis, coming to a stop, and then moving the required distance along the other axis. This strategy would involve consecutive single-axis movements to arrive at the target location. Figure 18 illustrates the path of movement and velocity inputs over time for this particular strategy (assuming the ability to instantaneously achieve maximum velocity). While this strategy might reduce cognitive workload since it only requires the operator to control one axis at a time, it is undesirable from an arm dynamics (oscillations) standpoint and would take more time to complete. Multi-axis control can improve task efficiency and reduce task completion times and system oscillations when performed by expert operators. However, the performance of novice operators may actually suffer when attempting to control multiple axes simultaneously by increasing the off-target error and, hence, increasing task completion time. An additional advantage of single-axis control is that translational errors are much easier to correct individually than when using multi-axis control. Use of this strategy may be an indicator of unskilled performance.

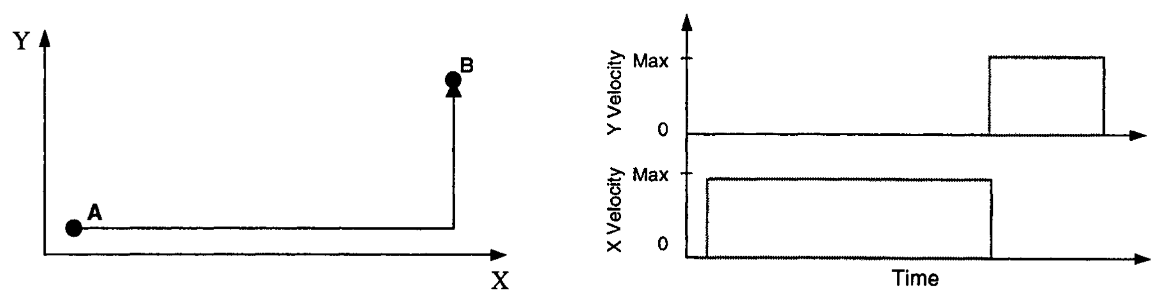

Figure 18. Movement Path and Velocity Inputs for a Sequential Single-Axis Control Strategy.

Strategy 2: Continuous Multi-Axis Control

Geometrically, it is known that the shortest distance between two points is a straight line. However, this may be a difficult path for an RMS operator to follow even in a two-dimensional case. Due to the fact that maximum velocities are defined along individual axes, alternative (longer) paths may be completed in the same amount of time.

Assuming the maximum rates of travel along the two axes are equal, the operator would need to calculate and command rates in exact proportions in X and Y to follow this straight-line path. For example, if the distance in the X direction is twice the distance in the Y direction, the operator would need to maintain a speed exactly twice as fast in the X direction as that in the Y at all times to achieve this path. This strategy, illustrated in Figure 19, would be described as one that maximizes the duration of multi-axis input (100%), so motions in all axes start and end simultaneously. Maximizing the duration of multi-axis input would be more time efficient than Strategy 1, but would be a more difficult task for the operator, both physically and mentally. This strategy appears to be implemented in the Auto Sequence (computer controlled) mode of the BORIS simulation.

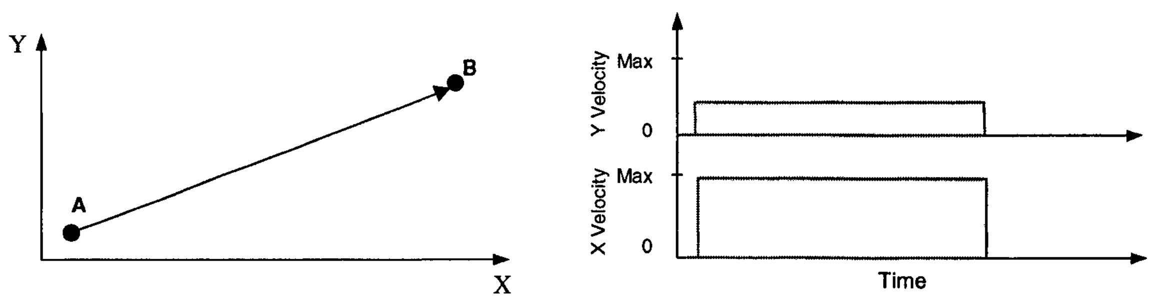

Figure 19. Movement Path and Velocity Inputs for a Continuous Multi-Axis Control Strategy.

Strategy 3: Flexible Multi-Axis Control

An equivalent performance efficiency could be achieved (i.e., total movement time would be equivalent) if the operator chose a strategy such that motion along the non-limiting axes (those requiring shorter distance movements) was input at any time that would allow completion within the time required to move along the axis with the longest distance. This strategy allows the operator more flexibility in choosing the timing, order, and velocity of the inputs along each of the non-limiting axes. As illustrated in Figure

20, the operator can choose to start all movements simultaneously and proceed at full-rate as long as needed to reach the required coordinates along the individual axes, allowing movement along those axes to be discontinued as soon as possible. Alternatively, the operator can wait to begin the movement along the non-limiting axes until a later time (within the shaded boundary region), and still achieve the same efficiency. The operator may also choose to reduce the velocity of the movement along the non-limiting axes to allow more time to evaluate the system state (check camera views, arm position, joint angles, location, precision, etc.). For tasks requiring movements along three or more axes, staggering the non-limiting axes inputs when possible may reduce the cognitive demands of the task.

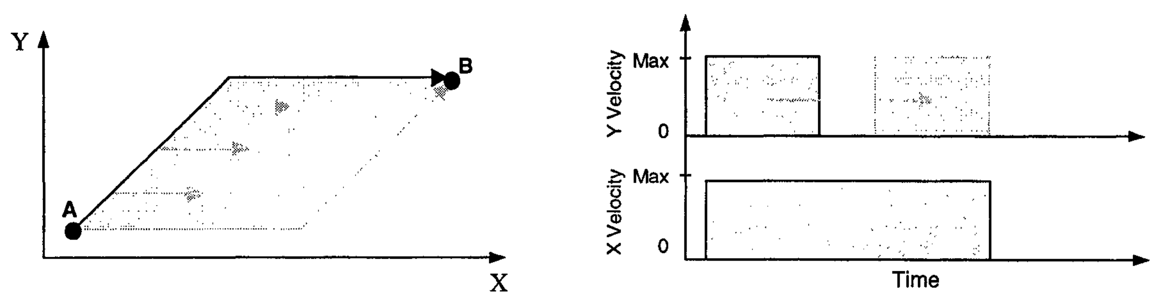

Figure 20. Movement Path and Velocity Inputs for a Flexible Multi-Axis Control Strategy.

3.3.6 Factors Affecting Multi-Axis Control

As mentioned previously, one of the goals of this research was to investigate the differences in control strategy and determine the role that control strategy plays in the performance of operators possessing different experience and ability. Other factors that might affect performance include the number of axes to be commanded, the distance of movement along each axis, and the direction / plane in which the motion is made.

Task workload increases with the number of axes being simultaneously controlled. The control strategy employed by the operator also affects workload. The operator must apportion control along each axis relative to the strategy being employed, while simultaneously keeping track of movement progress and position along each axis. The operator must also determine when the required distance along each axis has been reached and ramp-out control appropriately to avoid the need to make corrections.

Distance effects may occur when distances of travel along each axis are equal, requiring simultaneous attention to each axis that may conflict with the ability to determine when to begin ramp-out. Direction of motion is important because of suggested differences in performance between horizontal / vertical and depth, particularly in novice operators [Van Erp & Oving, 2002]. Hence, camera selection is critical to provide important depth cues and control-display movement compatibility. To balance any effects that number of axes, distances, and directions have on the performance of novice operators, these factors were systematically varied in the creation of the experimental tasks for this dissertation.

3.3.7 Potential Metrics to Assess Multi-Axis Performance

Efficiency in performance of the multi-axis tasks might be represented by the ratio of task completion time to the "optimal" completion time. However, translation time of the RMS arm is constrained by rate limits and the need to ramp commands to reduce oscillations in the arm. Since the criteria that characterize "optimal" ramping have not yet been defined, determination of an "optimal" time becomes more difficult. One might use "expert" performance of the task as the optimal criteria to estimate the skill level attained by the novice in relation to that of the expert. Unfortunately, obtaining expert data was not feasible at this stage of the research. Therefore, a methodology similar to that used for identifying the ramping metrics was employed in the identification of the multi-axis metrics. Identification was based on the determination of the critical aspects of multi-axis performance through an iterative examination of the rational models and plots of previously collected data and pilot data.

Since the shortest path between two points is a straight line, the most efficient translation might require motion along a straight-line. In 3-D environments, this straight-line motion will typically require multi-axis commands. Hence, efficiency might be measured as the percentage of time that the operator uses multi-axis commands. Unfortunately, straight-line motion may not be optimal in actuality due to the workload required in apportioning the command rates in various directions or to limitations of the joints that restrict straight-line movements. Therefore, assuming that maximizing the amount of time that multiple axes are commanded is optimal is the same potentially erroneous assumption made by Masliah and Milgram [2000]. Still, differences in the amount of multi-axis control used might be indicative of differences in skill. A characteristic of expert performance might be that the operator is able to simultaneously control multiple axes throughout much of the task while maintaining a high level of movement precision.

For a particular task, the minimal task completion time can be defined as the time needed to complete the movement along the limiting axis, or the axis with the longest distance to be traveled. The ratio of the distances to be traveled along each axis represents the minimal percentage of multi-axis control required to complete the task efficiently. For example, if a task requires travel distances of 300 cm along one axis and

100 cm along another axis, the task could be completed in the minimal amount of time only if the operator commands both axes simultaneously for at least 33% of the total time taken to complete the task. Any smaller percentage of multi-axis control would extend the task completion time. However, the task can be completed just as efficiently with respect to task completion time for any amount of multi-axis control between 33% and 100%. Lacking the ability to define a specific theoretical model of optimal multi-axis performance, an examination of the strategy employed in performing the task was included to provide additional information in comparisons of performance differences between operators.

Examination of plots of commanded velocity over time helped in the identification of potential metrics to assess multi-axis performance. In particular, observed differences in the plots were isolated and quantified in the belief that these differences might represent critical aspects of performance. To demonstrate the methodology using a practical example, Figure 21 shows the commanded velocities over time for a 3-D multi-axis task in which the operator was instructed to move to a target (a 6 mm white square) located from the start point at a distance of 300 cm along the +X-axis, 300 cm along the +Y-axis, and 300 cm along the +Z-axis (designated by the horizontal lines of the camera crosshairs). This task required 100% multi-axis control (as given by the ratio of distances along the three axes) in order to complete the task in the minimal amount of time. Hence, this particular task was designed to investigate the ability of novice operators to control straight-line motion (Strategy 2), or the ability to simultaneously initiate and control all required axes throughout the task. In order to investigate strategy differences, other task ratios used in the study allowed more flexibility in the choice of when to start and stop motion along each of the axes.

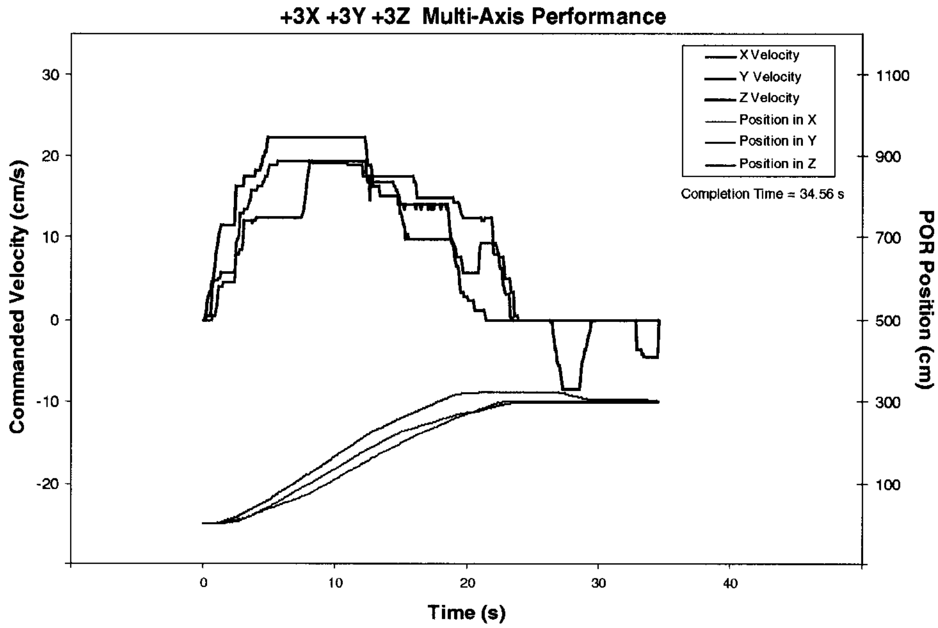

Figure 21. Performance on a Task Requiring 100% Multi-Axis Control.

As shown, the operator initiated movement along the X-axis, followed by inputs to the Z-axis (after a lag time of .08 s) and then the Y-axis (after a lag time of .56 s). All three axes were controlled simultaneously for approximately 22 s, at which point input along the Z-axis was initially terminated (most likely because the operator recognized that the Z target distance had been exceeded). Notice that the commanded Z velocity was higher than the commanded X or Y velocities, which were comparable. Because the distance to be traveled was identical along each of the axes, the operator needed to ramp-out control of the Z-axis at an earlier point to accurately meet the target. The operator continued simultaneous control of X and Y, terminating the X input precisely at the X target distance at 23.5 s, and then terminating the Y input 0.4 s later at the correct Y target distance. At this point in time, motion was stopped along all axes. After approximately 2.5 s, the operator initiated a second Z input in an attempt to correct the off-target error along the Z-axis. The first correction attempt moved the POR Z position from about 323 cm to 306.5 cm, which was still outside of the designated target boundaries. Therefore, a third input was made along the Z-axis that moved the POR position to 301.4 cm, which was within the target boundaries that defined acceptable task completion.

The operator's ability to command multiple axes simultaneously was quantified as the percentage of the total task time during which two or three axes were being input at the same time. In the example above, the operator controlled three axes simultaneously during 59.8% of the task, while dual-axis control accounted for 7.4% of the total task time. Therefore, the percentage of multi-axis input (simultaneous control of two or more axes) employed during performance of the task was 67.2%. Single-axis control accounted for 15.5% of the total task time. The remaining 17.3% of the total task time was spent with no movement of the arm. The task required 34.56 s to complete, with 13.12 s (or 38% of the total time) spent in making corrections along the Z-axis. Clearly, the failure of the operator to maintain similar ratios of input increased the need for additional single-axis inputs and extended the total task completion time.

In the example presented above, the greatest efficiency would have been achieved if the operator had been able to accurately control all axes simultaneously 100% of the time. Hence, in this case the amount of single-axis control is an indicator of inefficiency. However, it is not known whether the use of single-axis control is due to a lack of skill or is a desired movement strategy. The operator strategy may have been to merely get close to the target as quickly as possible, and then make adjustments at the end. Therefore, using the metric to make conclusions about skill may not be reasonable.

As discussed previously, the percentage of multi-axis control employed by an operator is determined not only by operator skill, but also by target distance and location, movement strategy, environmental obstacles, safety requirements, and system constraints such as rate and reach limits. These metrics cannot directly differentiate good performance from bad since the criteria for "optimal" performance are unknown. However, it was sufficient at this early stage to determine if the measures prove to be sensitive to variations that can identify differences in performance between operators and differences in task demands.

Comparisons of the plots of commanded velocity over time helped to identify additional characteristics that may indicate critical aspects of multi-axis performance. Differences in the order of inputs were quantified as "lag times," or the elapsed time between the initial input and the time at which the other axes were initiated. Differences were also observed in the number of times the axes were initiated. The smoothness and magnitude of the accelerations were identified as potentially critical aspects of performance. For the multi-axis case, it was infeasible to use the linear regression analysis due to the number of axes and the multiple number of "starts" along the three axes. Therefore, an attempt was made to quantify the "step-changes" noted in the plots by counting the number of excessive accelerations. The criteria for these excesses were determined through a visual investigation of the plots. Simply, large jumps in the commanded velocity were identified visually, and the accelerations associated with those steps were calculated and noted. The lower limit of the large acceleration jumps was 30

cm/s^2. To narrow the sensitivity of the measure, medium jumps with a lower limit of 15 cm/s^2 were also investigated. Hence, additional potential metrics counted the number of excessive accelerations along each axis throughout the task. Finally, overall efficiency in multi-axis performance was assessed by correction times and task completion times. Table 5 provides a complete listing and descriptions of the multi-axis metrics that were evaluated in the analysis stage of the dissertation.

Table 5. Preliminary Set of Metrics to Evaluate Multi-Axis Performance.

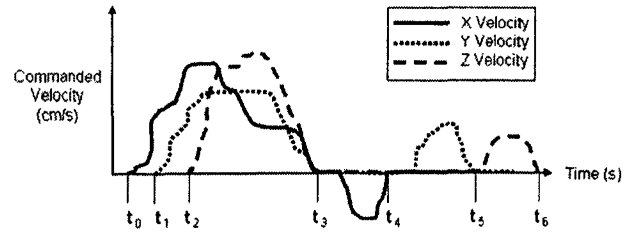

Code	Metric	Units	Description / Comments
P1A	Percent of Single-Axis Control	----	Percentage of total task time during which inputs are made in X, Y, or Z alone.
P2A	Percent of Dual-Axis Control	----	Percentage of total task time during which simultaneous inputs are made along two axes (XY, XZ, or YZ).
P3A	Percent of Triple-Axis Control	----	Percentage of total task time during which simultaneous inputs are made along three axes (XYZ).
PMA	Percent of Multi-Axis Control	----	Percentage of total task time during which multi-axis inputs are made (simultaneous inputs along two or three axes); PMA = P2A + P3A.
X1	X Lag Time	s	Time at which the first input is made along the X axis. In the figure above, X1 = t_0.
Y1	Y Lag Time	s	Time at which the first input is made along the Y axis. In the figure above, Y1 = $t_1 - t_0$.
Z1	Z Lag Time	s	Time at which the first input is made along the Z axis. In the figure above, Z1 = $t_2 - t_0$.
TCT	Task Completion Time	s	Time required to complete the task (acquire the target). In the figure above, TCT = ($t_6 - t_0$).
XS	Number of X Starts	----	Number of times movement is initiated along the X axis.
YS	Number of Y Starts	----	Number of times movement is initiated along the Y axis.
ZS	Number of Z Starts	----	Number of times movement is initiated along the Z axis.
XCT	X Correction Time	s	Time spent making corrections along the X axis. In the figure above, XCT = ($t_4 - t_3$). NOTE: Correction time is the additional time required to acquire the target along a particular axis after the initial input along that axis is terminated (i.e., velocity reaches zero).
YCT	Y Correction Time	s	Time spent making corrections along the Y axis. In the figure above, YCT = ($t_5 - t_3$).
ZCT	Z Correction Time	s	Time spent making corrections along the Z axis. In the figure above, ZCT = ($t_6 - t_3$).
XPC	Percent Correction in X	----	Percent of total time spent making corrections along the X axis; XPC = (XCT / TCT) X 100%
YPC	Percent Correction in Y	----	Percent of total time spent making corrections along the Y axis; YPC = (YCT / TCT) X 100%
ZPC	Percent Correction in Z	----	Percent of total time spent making corrections along the Z axis; ZPC = (ZCT / TCT) X 100%
XA>15	X Accelerations > 15 cm/s^2	----	Count of sampling periods in which X accelerations exceed 15 cm/s^2. NOTE: Acceleration is calculated as the change in commanded velocity / change in time for each sampling period (.08 s).
YA>15	Y Accelerations > 15 cm/s^2	----	Count of sampling periods in which Y accelerations exceed 15 cm/s^2.
ZA>15	Z Accelerations > 15 cm/s^2	----	Count of sampling periods in which Z accelerations exceed 15 cm/s^2.
XA>30	X Accelerations > 30 cm/s^2	----	Count of sampling periods in which X accelerations exceed 30 cm/s^2.
YA>30	Y Accelerations > 30 cm/s^2	----	Count of sampling periods in which Y accelerations exceed 30 cm/s^2.
ZA>30	Z Accelerations > 30 cm/s^2	----	Count of sampling periods in which Z accelerations exceed 30 cm/s^2.

CHAPTER 4

STAGE TWO: PERFORMANCE METRIC EXTRACTION AND VALIDATION

Stage Two activities were designed to accomplish the second objective of the dissertation: to extract and validate the selected performance metrics from the BORIS simulation. The two major activities employed to achieve the Stage Two objective are discussed in this chapter: acquisition and treatment of the specified RMS data, and validation of the proposed performance metrics. Figure 22 illustrates the flow of the activities completed during Stage Two that achieve a validation of the ability of the selected metrics to evaluate RMS operator performance. Examination of the BORIS system provided the information needed to extract the desired performance data. Subsequently, experimental tasks and procedures were developed that required the operator to demonstrate the critical aspects of RMS performance identified in the task analysis. Univariate analysis procedures on the performance data identified metrics that were sensitive to differences in task characteristics, individual differences between operators, and skill acquisition over time. The list of sensitive metrics was reduced further using a methodology designed to achieve a set of measures that was highly sensitive to differences among operators. Results of the multivariate analyses on the reduced metric set was combined with the results of the univariate analyses in a procedure that achieved a reasonable classification of operator performance based on the selected metrics. The illustrated Stage Two activities are discussed in detail in this chapter.

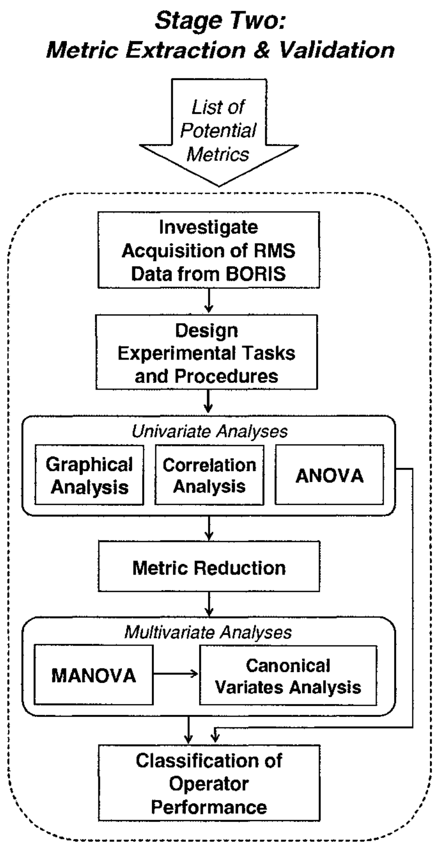

Figure 22. Flowchart Diagram of the Stage Two Activities.

4.1 Data Acquisition and Treatment

Achieving a working familiarity with the BORIS system was necessary to help identify available output variables and to understand exactly what each measure represents. Once the potential performance metrics were identified, the appropriate data needed to be isolated and acquired from BORIS. The TRICK utility used by BORIS provides the ability to capture and store data output from any session of a simulated RMS task. For example, variables that represent the *POR position* in X, Y, and Z can be tracked and recorded over time. As discussed by Van Erp and Oving [2001], these variables could be used to evaluate differences in hand controller inputs for the three axes that might be an indicator of unskilled performance or attentional priority.

4.1.1 Analysis of the BORIS Operating System

Thorough examinations of the BORIS and TRICK user manuals and extensive hands-on exploration of the BORIS simulator were performed to identify the resident variables and determine their units and sampling rates. A major requirement of the data extraction process was the determination of the appropriate variables and data sampling rates to provide the best measure of the designated critical element. To provide good precision while maintaining a reasonable data file size, the data-sampling rate of the system, which can be specified by the user, was set at 0.08 seconds (12.5 Hz).

During this time, the necessary knowledge was also gained to write codes and scripts to adjust system parameters and create custom scenarios for the study. Procedures were identified for specifying and recording the designated variables, and for acquiring the data files from the system memory. Additionally, these investigations helped to identify variables that were most representative of the performance characteristics to be measured for this research, and helped eliminate those that demonstrated excessive instability. In addition to *system time* and *POR position* data, BORIS can provide information on commanded inputs as well as the system response to the commands. Hand controller inputs are recorded by the system in several forms. Some variables represent input values, while others are translated into system outputs. For example, one variable represents the amount of *hand controller deflection* and produces values that range from – 1 to 1. Another variable is merely a scaled version of the hand controller deflections created to represent *commanded velocities*, a prediction of system response based on the maximum velocity allowed for the selected rate mode. Commanded velocity data values range between ± 30 cm/s in coarse mode, and between ±10 cm/s in vernier mode. An additional variable represents the average *POR velocities* achieved by the simulation for each sampling period. The POR velocities are calculated based on the rate of change of the POR position over time and simulate the true system response including any effects of disturbances in the system (oscillations). Therefore, the POR velocity variables can achieve values that exceed the limits that can be commanded by the system, and generally show much more variability than the commanded velocity data.

Ultimately, the decision was made to collect all of the system variables that were thought to be of any potential use, since the additional data might prove valuable in future studies. Table 6 lists the actual system variables designated to be captured and recorded in each of the BORIS output files. Additional details are provided for the variables that were used in this dissertation (designated by bold characters).

4.1.2 Investigation of BORIS System Response and Constraints

A systematic investigation of the BORIS system was conducted to determine whether the simulation response variables were consistent in different parts of the VEGA. A pilot study was designed to determine the variability in maximum translational rates and to delineate the reach envelope of the BORIS arm within the VEGA. Repeated translations of the arm were made in a straight-line fashion along a single axis while holding other axes constant. For example, while holding the Z-elevation at 200 cm and maintaining an orientation of [–90, 0, 0], the arm was moved in a straight line along the Y-axis (pure +Y and –Y commands) at various X coordinates (-100, 100, 300, 500, 800, and 1100 cm). Velocity mean and range values were recorded on grid-charts to show the pattern and range of motion demonstrated by the BORIS arm within each of the planes investigated. A sample grid-chart displaying the results of the runs in the Z = 200 cm

Table 6. BORIS System Variables Recorded in Output Data Files.

Header	Units	TRICK Variable Name	Description
Time	**s**	sys.exec.out.time	**System time.** Time series values in increments of 0.08 s from the start of the simulation.
X	**cm**	*.por_pos_vf[0]	**POR Position (X).** Represents the POR coordinate relative to the origin (base of the BORIS arm). Range: -200 cm to 1300 cm (forward to aft).
Y	**cm**	*.por_pos_vf[1]	**POR Position (Y).** Range: -1500 cm to 1500 cm (starboard to port).
Z	**cm**	*.por_pos_vf[2]	**POR Position (Z).** Range: 500 cm to -1000 cm (floor to ceiling).
P	d	*.por_ang_vf[0]	POR Orientation (Pitch).
Yw	d	*.por_ang_vf[1]	POR Orientation (Yaw).
R	d	*.por_ang_vf[2]	POR Orientation (Roll).
Xv	cm/s	*.por_vel_vf[0]	Translational Velocity (X).
Yv	cm/s	*.por_vel_vf[1]	Translational Velocity (Y).
Zv	cm/s	*.por_vel_vf[2]	Translational Velocity (Z).
Pv	d/s	*.por_ang_vel_vf[1]	Rotational Velocity (Pitch).
Ywv	d/s	*.por_ang_vel_vf[2]	Rotational Velocity (Yaw).
Rv	d/s	*.por_ang_vel_vf[0]	Rotational Velocity (Roll).
Xvc	**cm/s**	*.com_por_rate_vf[3]	**Commanded Velocity (X Translations).** The scaled system response to the hand controller deflection relative to the selected mode (coarse). Range: -30 cm/s to 30 cm/s.
Yvc	**cm/s**	*.com_por_rate_vf[4]	**Commanded Velocity (Y Translations).** Range: -30 cm/s to 30 cm/s (coarse mode).
Zvc	**cm/s**	*.com_por_rate_vf[5]	**Commanded Velocity (Z Translations).** Range: -30 cm/s to 30 cm/s (coarse mode).
Pvc	d/s	*.com_por_rate_vf[1]	Commanded Velocity (Pitch Rotations).
Ywvc	d/s	*.com_por_rate_vf[2]	Commanded Velocity (Yaw Rotations).
Rvc	d/s	*.com_por_rate_vf[0]	Commanded Velocity (Roll Rotations).
Trig	----	ndof.sequencer.hc_trigger_lp	Trigger Flag. Indicates depression of the trigger on the RHC. Used in this study to help identify start and end of performance data for data reduction purposes. Range: 0 (no) or 2 (yes).
HC X	----	**.hardware.Data.Thc[0]	Hand Controller Deflection (X).
HC Y	----	**.hardware.Data.Thc[1]	Hand Controller Deflection (Y).
HC Z	----	**.hardware.Data.Thc[2]	Hand Controller Deflection (Z).
HC P	----	**.hardware.Data.Rhc[0]	Hand Controller Deflection (Pitch).
HC Yw	----	**.hardware.Data.Rhc[1]	Hand Controller Deflection (Yaw).
HC R	----	**.hardware.Data.Rhc[2]	Hand Controller Deflection (Roll).

Note: * = ndof.output.por ** = ui.hc.hw_device_data plane is shown in Figure 23. The reach envelope of the BORIS arm at that elevation is indicated by the dashed line. The results of the investigation provided valuable information regarding the areas of the room in which the response variables were most stable (i.e., least affected by troublesome arm / joint configurations). Despite minor variation in some areas, the results confirmed that constant velocity could generally be assumed within the BORIS arm's reach envelope.

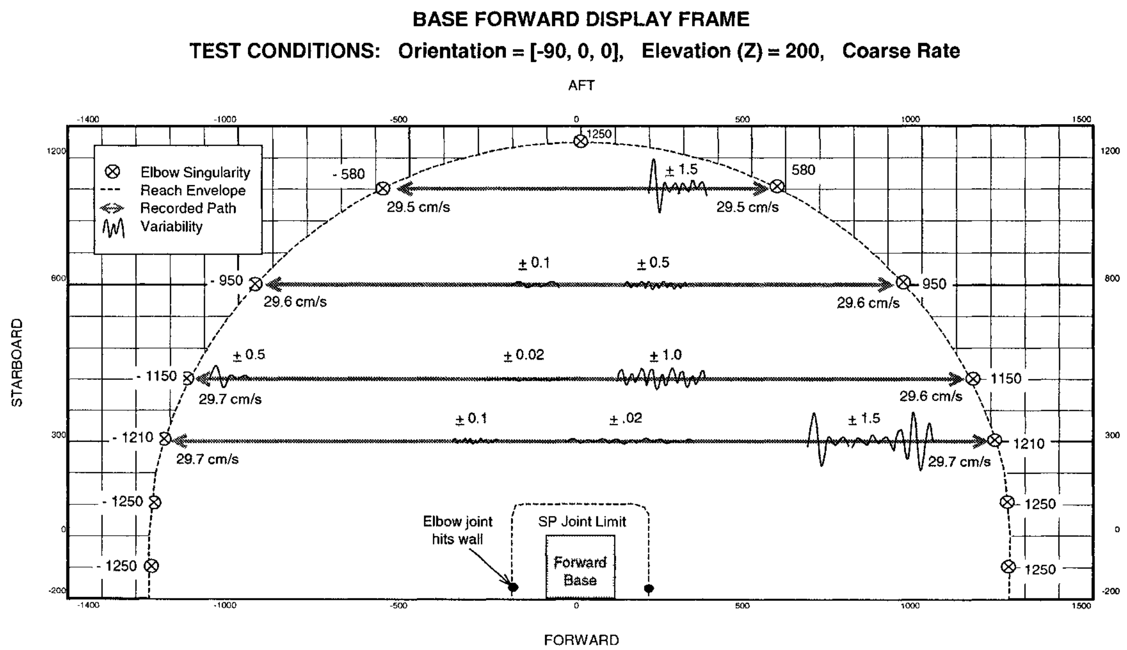

Figure 23. Sample Grid-Chart from Pilot Test Investigating System Constraints.

Additional investigations examined the impact of hand controller deadbands and the behavior of the auto-sequence feature with respect to the response variables. The hand controller deadbands were calibrated and adjusted to minimize inadvertent inputs while maximizing the range of responsiveness. Upper and lower deadband threshold and limit adjustments were set at 10% and 3% of the total available byte range for each axis. The BORIS investigations provided the working knowledge of the system necessary to make informed choices when designing the tasks for the validation study.

4.1.3 Data Treatment

The output files provided by BORIS were saved in a comma-separated format that was easily imported into Excel spreadsheets. The simulation data were sampled at a rate of 12.5 Hz, so each row of the data file contained the observed values of each recorded variable (columns) at 0.08 s time intervals. The variables examined in this dissertation were time, positions, and commanded velocities (represented by bold characters in Table 6). To facilitate the graphing process and to provide a consistent base for comparison of performance across various tasks, the time and position values for each task were transformed to begin at zero and proceed in the positive direction. Macros were used to calculate accelerations and percentages, identify starts and stops, and provide counts that were necessary to produce the selected performance metrics. Once the appropriate data were contained in each spreadsheet, the data were plotted for graphical analysis. The metrics created in the individual data spreadsheets were then transferred to a new spreadsheet where each row contained all of the metric values for one task run. This set of "metric" data was used in the statistical analyses to identify the metrics that were sensitive to differences in performance among operators. Summary statistics for this data set were also calculated.

4.2 Validation of the Proposed Metrics

Chapter 3 described the methodology used to identify a set of potential metrics that represent a range of critical performance skills. Validation of the performance metrics was achieved by conducting an empirical study. The experimental tasks were designed to provide data that demonstrated specific ramping and multi-axis skills. Each of the potential metrics was evaluated for the ability to demonstrate changes in performance over time (skill acquisition) and to indicate differences in performance between operators (skill level). Evaluation of the potential metrics was accomplished through a combination of graphical and statistical techniques, and through comparisons with the rational models of performance developed in this dissertation.

Graphical analysis of performance was employed to identify input patterns and to provide the acceleration and smoothness metrics for the ramping tasks. As mentioned previously, a visual inspection of the input patterns in plots of commanded velocity over time and comparisons against the rational model led to the identification of potential quantitative metrics to assess ramping and multi-axis performance. Plots of each ramping task were generated. Then, the linear regression analysis was applied to each plot to provide the data for the metrics representing acceleration (slope of the regression line) and smoothness (R^2 values).

Summary statistics for each metric (mean, standard deviation, minimum and maximum values, and percent standard error) were also examined. Metrics with little variation might be of little use in differentiating among skill levels. Therefore, metrics with higher variation were selected since they might be more representative of performance aspects that are more difficult to learn or require greater skill.

Analysis of Variance (ANOVA) and Multivariate Analysis of Variance (MANOVA) were used to verify the metrics' ability to indicate differences between operators, and to further suggest the utility of each of the metrics. These statistical techniques were also used to investigate any differences due to the levels of the experimental design variables (i.e., task variables such as axis and direction of motion, distance, and replicate). Correlation analysis was utilized to reduce the number of metrics for the multivariate analyses. The experimental methodology associated with this study is detailed in the following sections.

4.2.1 General Experimental Methodology

This dissertation measured the performance of twelve novice participants during two replicates each of 37 targeted movement tasks. There were twelve 1-D tasks in which the EE was moved along a single axis (X, Y, or Z), eighteen 2-D tasks in which movements were made along two axes (X and Y, or X and Z, or Y and Z), and seven 3-D tasks in which movements were made along three axes (X and Y and Z). These tasks were designed to evaluate the operator's ability to command smooth hand controller inputs and simultaneously control motion along multiple axes.

4.2.1.1 Participant Selection and Training

To examine and isolate individual differences in performance that might indicate differences in level of skill, a group of twelve novice (beginner) operators were selected. Participants were recruited locally from the student population on the Norman Campus of the University of Oklahoma. Because of the heavy spatial requirements of the RMS task, participants were provided training and practice on the BORIS simulator to ensure that they possessed or achieved the appropriate psychomotor and 3-D visualization skills. The training and practice sessions were designed to produce a homogeneous group of participants with respect to the content of GRT training received and the amount of hands-on practice on the BORIS simulator. Half of the participants chosen for this research had participated in a previous study (eight months prior to this study) that provided them with limited training and practice in the operation of the BORIS robotic arm. However, the previous experience with BORIS had been conducted before the acquisition of the NASA hand controllers. These participants were provided with a review of the previous training and hands-on experience with the new hand controllers.

Since the GRT training and testing required a substantial amount of the participants' time, the motivation and commitment of the participants was very important. Therefore, participants who expressed a high interest in the NASA robotics system were sought. Several of the participants were recruited through the OU Robotics Club. All participants were compensated for their time. This compensation was provided as a per-hour fee, with an additional bonus for completion of all trials. All participants had self-reported vision of 20/20 or corrected to 20/20. A summary of the participant characteristics is presented in Table 7.

Table 7. Summary of Participant Characteristics.

Training Group	Participant ID	Gender		Age		
		Male	Female	Range	Mean	Std. Dev.
Previous	101, 106, 108, 109,110, 111	3	3	20–39	24.0	7.43
New	122, 123, 124, 127, 128, 129	4	2	18–23	20.7	1.75
Combined Totals:		**7**	**5**	**18–39**	**22.3**	**5.43**

At the beginning of the first session, each participant was provided with an overview of the study and asked to read and sign an Informed Consent Form (Appendix A) and complete a survey to collect participant demographics (Appendix B). Having completed the first three lessons in the GRT Training sequence during the previous study, the previous participants (101, 106, 108, 109, 110, and 111) attended two sessions across a two-day period. Session 1 provided the participants with an overview of the study, a review of critical RMS concepts, and approximately 1.5 hours of hands-on practice using the new hand controllers. The practice session consisted of alternating fly-to and grapple exercises that had been developed for use during the previous study. During Session 2, participants completed two replicates of the test sequence separated by a one-hour rest period. The previous participants then completed a debriefing questionnaire (Appendix C) regarding their impressions of the study. Both sessions were conducted one-on-one with the researchers. The total time requirement for the previous participants was approximately five hours.

To ensure that the six new participants (122, 123, 124, 127, 128, and 129) received comparable training and practice, attendance was required at six sessions. Session 1 was a two-hour long group Orientation session that provided the participants with an overview of the study, acquired the necessary participant consent and information, and presented Lesson 1, which introduced basic robotics vocabulary and terminology and taught the fundamentals of robotic coordinate systems that define motions in space. The BORIS simulator was used in all but Orientation and Lesson 1. The remaining sessions were scheduled over five consecutive days. Session 2 began with Lesson 2A, which provided hands-on training in the translational aspects of maneuvering the BORIS arm, after which the participant completed a trial replicate of the test sequence. These data were collected to represent "untrained" performance for use in the overall RMS project, but the data were not examined for this dissertation. This test session was also included to achieve comparable BORIS experience for the new participants. Lesson 2B, covered in Session 3, built on the previous lesson by providing instruction and hands-on experience in commanding rotational arm motions. Session 4 completed training with Lesson 3, which taught fundamentals for navigating in 3-D space such as triangulation and camera selection, and provided practice in flying-to and grappling a payload. Session 5 was included to provide two additional hours of guided practice on the BORIS simulator. The practice session allowed the participant to apply all of the knowledge learned in the lessons, including camera selection and set-up, operations in various command modes, triangulation, and hands-on practice in achieving smooth, multi-axis movements using the hand controllers. Finally, Session 6 consisted of two test sessions and a debriefing period (i.e., it was identical to Session 2 for the previous participants). For the new participants, training was conducted in pairs to match the methodology used in the previous study. However, the practice session (Session 5) and all test sessions were conducted one-on-one with the researchers. The total time requirement for the new participants was approximately twelve hours. A summary of the participant schedule is given in Table 8.

Table 8. RMS Study Participant Training / Testing Session Schedule.

<table>
<tr><th colspan="3">Previous Participants</th><th colspan="3">New Participants</th></tr>
<tr><th>Session</th><th>Content</th><th>Time (hrs)</th><th>Session</th><th>Content</th><th>Time (hrs)</th></tr>
<tr><td rowspan="3">1</td><td rowspan="3">Orientation
Training: Review
Practice</td><td rowspan="3">½
½
1½</td><td>1</td><td>Orientation
Training: Lesson 1</td><td>½
1½</td></tr>
<tr><td>2</td><td>Training: Lesson 2A
Testing: Trial</td><td>1½
1</td></tr>
<tr><td>3</td><td>Training: Lesson 2B</td><td>1</td></tr>
<tr><td rowspan="3">2</td><td rowspan="3">Testing: Part 1
Testing: Part 2
Debriefing</td><td rowspan="3">1
1
½</td><td>4</td><td>Training: Lesson 3</td><td>2</td></tr>
<tr><td>5</td><td>Practice</td><td>2</td></tr>
<tr><td>6</td><td>Testing: Part 1
Testing: Part 2
Debriefing</td><td>1
1
½</td></tr>
<tr><td colspan="2">Total Time Requirements:</td><td>5 hrs</td><td colspan="2">Total Time Requirements:</td><td>12 hrs</td></tr>
</table>

The training protocol used in this study was adapted from that used by the NASA GRT instructors at Johnson Space Center in Houston. While the simple translational tasks developed for this dissertation did not necessarily require the extent of training provided, the training regimen was determined to ensure equity in experience and knowledge between the operators, and to create a viable participant base for use in future research efforts.

4.2.1.2 Equipment

The BORIS simulation was run on a PC equipped with dual 1.5 GHz Intel® XEON™ Processors (providing 512 MB of RAM), dual 40 GB hard drives, and a dual-head Elsa® Synergy III™ video graphics card. BORIS operated on the Linux Red Hat Version 7.1 platform. The simulator utilized two 18.1" (viewable area) SONY® SDM-S81R TFT LCD flat-screen color displays with a resolution of 1280 RGB × 1024. The monitors were linked such that the display spread across the two monitors. A standard keyboard and mouse were used to input test commands and make menu selections.

Movement of the BORIS arm was controlled with a set of hand controllers custom-made by Measurement Systems Incorporated and integrated by Lockheed at NASA Johnson Space Center. The RHC (model 544-G3161) controls rotational motion, while the THC (model 544-G1810) controls translations. The experimental tasks for this study utilized only the translational controller.

4.2.1.3 Test Facilities

The experimental sessions for this study were conducted in a well-appointed laboratory space in the basement of the Carson Engineering Center on the Norman campus. The room was equipped with its own central heat and air control that permitted the researchers to maintain the lab temperature at a constant 72° Fahrenheit. The room contained two computer workstations: one for the experimenter/technician and another for the operator. Each workstation held two 18.1" flat-screen LCD monitors. The monitors were positioned side-by-side, approximately 46 cm (18") from the front edge of the workstation. The computer keyboard, mouse, and rotational hand controller alternated between the two stations, depending upon the tasks being performed. For training and practice sessions, the RHC and the THC were positioned at the operator workstation. However, the RHC was moved to the experimenter's workstation for the test sessions, in which only translational movements were made. The translational hand controller was fixed to the left side of the operators' workstation. The workstation dimensions were approximately 152 cm (60") wide by 91 cm (36") deep. The height of the table surface was approximately 74 cm (29"). Each station was equipped with an adjustable-height computer chair. An additional worktable (90 cm wide × 90 cm deep × 74 cm high) and two additional computer chairs were available for use during training and testing. A simple diagram of the room arrangement is shown in Figure 24.

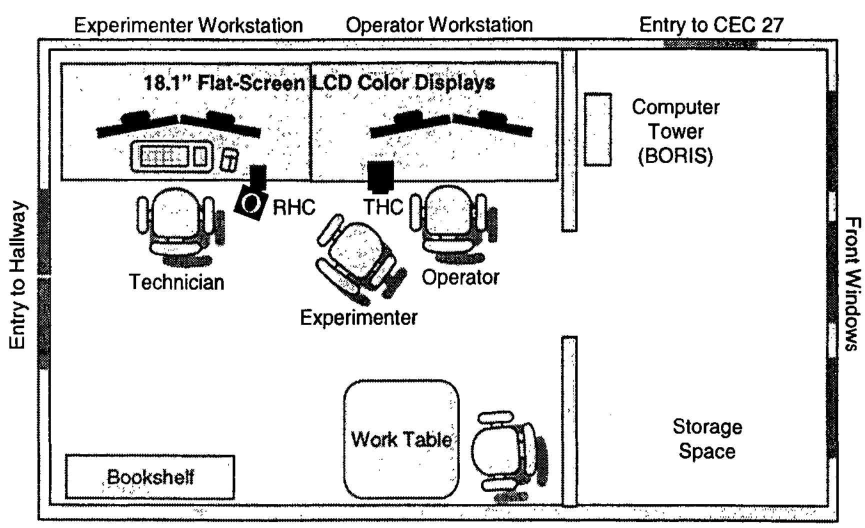

Figure 24. Floor Plan Diagram of the Test Facility.

4.2.1.4 Test Procedure

Once participants had completed the assigned training and practice, they were ready to complete two replicates of the test sequence. The participant took a seat at the workstation, and made any necessary adjustments to the chair to provide a comfortable posture during testing. To reduce distractions during testing, all cell phones were turned off and a "DO NOT DISTURB" sign was placed on the outside of the door. No entry was permitted to the test room after testing began.

Two researchers were present during testing. The first served as the "experimenter" and handled all interactions with the participant, while the second served as a "technician" to manage the operation of the BORIS simulation. The technician was responsible for entering the appropriate commands to run the simulation script, making sure that the appropriate task sequence was run, making the necessary adjustments to the display of the BORIS environment at the start of each run, watching for cross-coupling and other errors during the run, verifying task completion, and making any needed rotational adjustments between tasks. Due to the proximity to the THC, translational adjustments were made by the experimenter when necessary.

Before testing began, the experimenter reviewed the Participant Test Instructions (Appendix D) and the RMS Study Directions (Appendix E) with the participant, emphasizing the task objectives (speed, smoothness, multi-axis, no cross-coupling) and the task completion criteria for the 1-D, 2-D, and 3-D tasks. The experimenter reminded the participant that the gridlines in the VEGA are one meter apart, and that the target location would always be given with respect to the hand controller frame. A diagram of the control-display mappings was located at the workstation for reference purposes. The experimenter explained that the control-display mappings depicted the motion that would be seen on the display in response to the hand controller input. The participant was instructed to plan the motion in order to stop when the crosshairs were located within the target boundaries, and to remove his/her hand from the controls to indicate when the task was completed. The participant was encouraged to verbalize relevant thoughts and plans during testing. If the participant had no questions, the test sequence was initiated.

To minimize visual distraction during testing, the operator's left-hand display was turned off. Three different monitor views were presented in the right-hand display during testing, as shown in Figure 25. At the start of each simulation run, the technician manually adjusted the camera views on this display. The largest monitor (located to the right) provided the standard EE camera view. The top left monitor presented a view from Camera 2, and the bottom left monitor displayed the view from the window in the forward wall. The Camera 2 crosshairs were turned off for 1-D and 2-D tasks, while the position of the crosshairs was verified for 3-D tasks to provide the proper Z-elevation cue. The monitor views were selected to provide the operator with sufficient visual cues to verify the final target position. In addition, a script box was generated in the lower right-hand corner of the display to provide the operator with the control-display mapping and target locations for each run. The technician turned on all camera lights except the boom lights. Finally, the technician verified that the rate mode was set on "coarse" and turned the brakes off to allow the operator to initiate motion.

While the technician was configuring the simulator, the experimenter described the upcoming task(s), reviewed the instructions for performing and completing the task, indicated which mapping was being used, and specified the location of the target

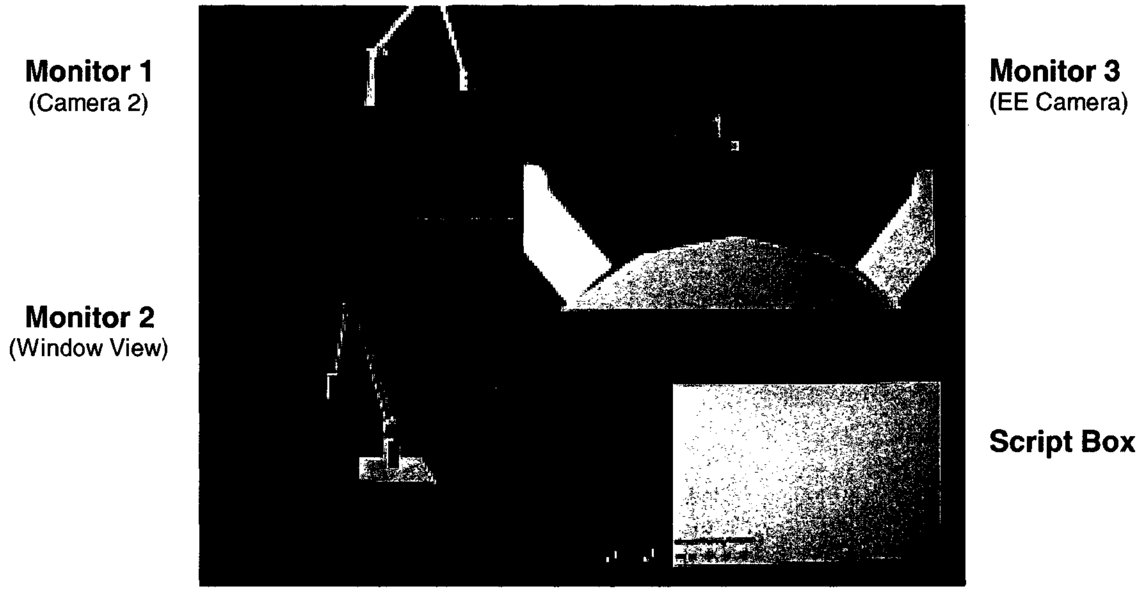

Figure 25. Standard Display Setup Used During Testing.

(intersection of gridlines) by giving the target number, distance, and the axis and direction of motion. All directions were given with respect to the hand controller frame. Before each task, the experimenter asked the operator to point to the designated target location on (or slightly off) the display, and to state the control inputs that would be used to move to the target, such as "I will move the controller forward and to the left." To ensure consistency throughout the experiment, separate dialogues were created and followed for each of the 1-D, 2-D, and 3-D task runs. The experimenter dialogues are given in Appendix F.

At the start of each task, the EE camera crosshairs were located at the intersection of a set of gridlines. The operator's assigned task was to move the crosshairs to the target as quickly as possible using smooth hand controller inputs and multi-axis control (when appropriate) while minimizing cross-coupling (control movement in unwanted directions). The task was completed only when the crosshairs were completely within the target boundaries. If the crosshairs were outside of the target boundaries, the operator was required to adjust the position until the crosshairs were within the boundaries. After completion of each task, the technician engaged the trigger to flag the end of the task data. When necessary, adjustments were made to clean up the starting position before beginning the next task in the run. After all adjustments were made, the trigger was again engaged. This methodology was employed to ensure usable data that would allow the evaluation of metrics that measured ramping and multi-axis performance. Erroneous movements would introduce excessive variation in the data that would reduce the ability to detect small differences in performance. Therefore, the tasks needed to be performed correctly. If the criteria for completion of the task were not met, the technician immediately instructed the operator to continue until the error was corrected.

During the task, both the experimenter and the technician noted any observed or suspected problems, disturbances, movement strategies, and operator comments. If errors occurred, the task was rerun (e.g., when the operator moved in the wrong direction or lost track of the target). If cross-coupling was observed, the technician alerted the operator and counseled them to be more careful of unwanted inputs.

The operator completed two one-hour test sessions on the same day. A one-hour break was provided between the sessions to reduce any effects of fatigue. During each test session, the operator completed 37 tasks in 15 runs: two runs of six (a total of 12) 1-D tasks, six runs of three (a total of 18) 2-D tasks, and seven runs of single (a total of 7) 3-D tasks. After both test sessions were completed, the participant was debriefed. The tasks used in the testing are detailed in the following sections.

4.2.2 Design of Tasks to Evaluate Ramping Performance

The ramping tasks employed in this research were designed to evaluate several critical aspects of ramping performance, including smoothness and consistency of hand controller inputs, the ability to plan and control motion, and overall task efficiency. Preliminary research and pilot studies conducted for this dissertation helped to identify several factors that were believed to affect the critical aspects of ramping performance, including operator experience and ability, target distance, target size, and direction and axis of motion. These factors were varied or controlled in the study to evaluate ramping performance.

4.2.2.1 Independent Variables for the 1-D Tasks

The independent variables used in the experimental design of the 1-D tasks to evaluate the potential metrics for ramping performance are listed in Table 9.

Table 9. Independent Variables Used to Evaluate Ramping Performance.

Independent Variable	Number of Levels	Levels
Direction of Motion	2	Positive (+) , Negative (–)
Target Distance	2	1m , 3m
Axis of Motion	3	X , Y , Z
Replicate	2	A , B
Operator	12	101 , 106 , 108 , 109 , 110 , 111 , 122 , 123 , 124 , 127 , 128 , 129

In order to evaluate whether differences existed due to the direction of motion (+ and –) and axis of motion (X, Y, and Z), all available 1-D translation combinations were included in the design of the ramping tasks. Based on the results of pilot tests, two target distances (1 m and 3 m) were selected to evaluate differences in ramping performance due to distance. The shorter (1 m) distance was designed to constrain the operator by providing little time between ramp-in and ramp-out, while the longer (3 m) distance was chosen to allow more travel time and, hence, more time to plan the ramp-out. These three variables were combined factorially to create twelve individual 1-D tasks. The twelve 1-D tasks are presented in Table 10. Two replicates of each of the twelve 1-D tasks were performed by each of the twelve operators to allow assessment of changes in performance over time (skill acquisition) and to provide a measure of random error.

Table 10. Task Codes and Variable Combinations for the 1-D Tasks.

Task Code	1a	1b	1c	1d	1e	1f	1g	1h	1i	1j	1k	1l
Task Variable Combination	+1X	+1Y	+1Z	-1X	-1Y	-1Z	+3X	+3Y	+3Z	-3X	-3Y	-3Z

4.2.2.2 Dependent Variables for the 1-D Tasks

BORIS recorded the system variables listed in Table 6 at increments of 0.08 s throughout the performance of each of the 1-D tasks. These data were treated as described in Section 4.1.3 to produce the set of 23 potential metrics to evaluate ramping performance. The list of the potential ramping metrics was given previously in Table 3. Each of the metrics was evaluated for its sensitivity in detecting differences among operators and changes in performance over time, and its sensitivity to the effects of task factors such as direction of motion, axis of motion, and movement distance.

4.2.2.3 Experimental Controls for the 1-D Tasks

As mentioned, target distance can affect the ability of the operator to plan and control ramping. For shorter target distances, cognitive workload may be higher, since the operator must very quickly locate the point at which ramp-out should begin and adjust the inputs appropriately. Ramping accelerations might also vary based on target distance. For targets that are closer, the operator may proceed more cautiously, commanding slower velocities to allow more time to plan and verify the progress of the movement. These ideas find support in a well-studied theorem, Fitts' Law, which describes movement time as a function of target size and distance. Fitts' Law is expressed mathematically by the equation

$$\text{Motion Time (MT)} = a + b\ log_2(2D/W)$$

where a and b are situational constants, D is target distance and W is target width. The term $log_2(2D/W)$ is referred to as the "index of difficulty." Clearly, this suggests that task difficulty increases for longer distances and smaller target sizes [Kroemer, Kroemer, & Kroemer-Elbert, 1994]. Fitts' Law applies to a class of movements called targeted movements, in which movement is made from a start position to a target of a set size at a set distance. Based on the similarities to the theoretical model of ramping and appropriateness to the objectives of this study, a targeted movement task was selected to evaluate the critical factors involved in ramping.

In the VEGA, a targeted movement task equates to moving the POR until the crosshairs of the EE camera reside within the boundaries of a specified target. In the case of the ramping (1-D) tasks, the operator was instructed to move the camera crosshairs to a target (gridline) a specified distance from the start position as quickly as possible using smooth, pure X, Y, or Z hand-controller inputs. To control for individual differences in the ability to estimate distance, it was necessary to provide the operator with a clear and unambiguous visual target. The existing grid system within the VEGA provided the most plausible target option, although it limited the target distances to multiples of 100 cm, the established distance between gridlines. To eliminate the need to count gridlines when the target was located off-monitor, a small (6 mm x 6 mm) white square was programmed to mark the location of the target gridline. Additionally, a white numeral beside the marker was included to distinguish between multiple targets during an experimental run. Figure 26 is a diagram depicting a sample 1-D task.

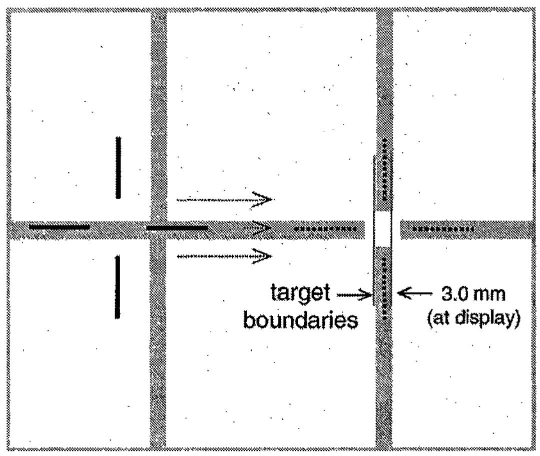

Figure 26. Sample 1-D (Ramping) Task Requiring Movement in the +Y Direction.

The size of the target was important to the overall efficiency of the task since it determined the allowable tolerance in the precision of the movement. Smaller targets require greater precision and are more difficult to acquire, as described by Fitts' Law. As target size decreases, the incidence of overshoots and undershoots increases. The need to make additional adjustments to achieve the final position increases task completion time and decreases task efficiency. However, the main objective of the task was to evaluate ramping performance. The primary aspect of ramping performance was related to the smoothness and consistency with which the inputs were made. Precision was a secondary component of ramping performance, but one that can indicate the operator's skill in planning and controlling the movements. If the target size was too small, the operator might place too much emphasis on precision and lose focus on the need to exert smoothly ramped commands. However, too large a target would increase the ambiguity of the task, and would introduce undesirable variation in measures of task precision.

Target size in the VEGA was determined by the camera zoom factor and the perpendicular distance of the target from the EE camera. Based on the results of pilot tests, a constant target size of 3.0 mm (gridline width measured at the display) was selected for use in the study to measure both ramping and multi-axis performance. This provided a target that was six times the width of the cursor (crosshair width = 0.5 mm). A constant target size of 3.0 mm was achieved by holding the EE at a perpendicular distance of 500 cm from the specified target and by setting the EE camera zoom to 1.00 (i.e., no zoom factor). To eliminate the "fat" gridlines that designate five-meter distances in the VEGA, the graphics were reprogrammed to provide consistent gridline widths throughout the room. In the ramping tasks, the EE orientation was held at [-90, 0, 0] at a Z-elevation of 0 cm (zero), such that the EE was pointing downward and the camera line-of-sight was perpendicular to the VEGA floor surface. This elevation provided a more stable orientation while also minimizing target size. At higher elevations, unacceptable drift was observed in pitch, yaw, and roll values. Failure to maintain a perpendicular EE orientation during the trial would result in a distorted view that could greatly affect the operator's precision.

Using the designated EE orientation, tasks in the X direction were performed using the external command frame. Positive X commands (pushing in on the THC knob) produced upward motion in the display, while negative X commands (pulling out on the THC) caused the crosshairs to move downward on the screen. Switching to an internal command frame kept the Z-axis tasks in the same plane and allowed all tasks to be performed in the same general area in the VEGA. This area was chosen based on the results of preliminary tests to provide minimum variability in the translational velocities. To reduce disruptions and enhance the natural flow between tasks, an attempt was made to minimize the number of simulation resets (runs) and the need to adjust the arm location or command frame between tasks. To help the operator mentally adjust between command frames, a visual aid was constructed to illustrate the hand-controller frame and the various control-display mappings that were used for each run (Figure 27). At the start of each run, the researcher told the operator which control-display mapping would be used. This was done to minimize any confusion due to the differences in the mapping of the hand-controller inputs and the resulting motion seen on the display.

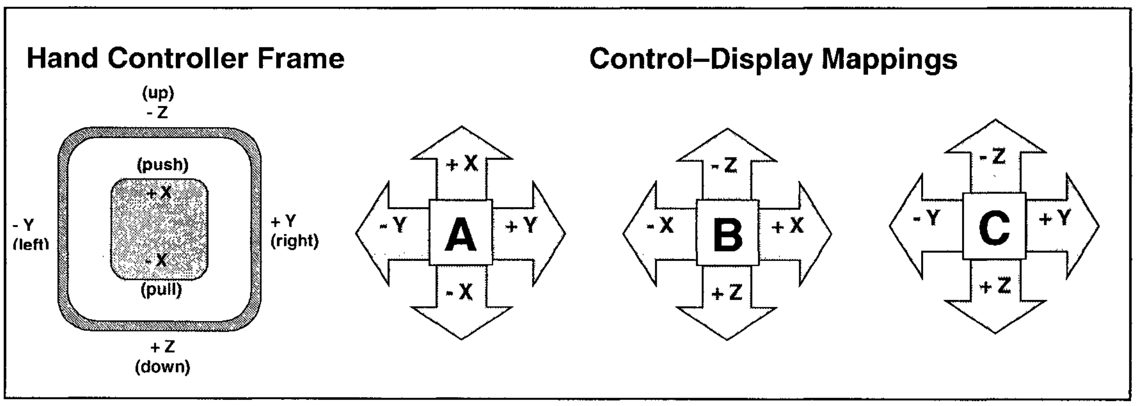

Figure 27. Visual Aid Illustrating Control Inputs and System Responses.

As seen in mappings A and B, +Y commands (moving the THC to the right) were always displayed as motion to the right, and –Y commands (moving the THC knob to the left) were seen as motion to the left on the display. Therefore, two of the Y-axis tasks were randomly grouped with the four X-axis tasks, and the other two were grouped with the Z-axis tasks. Then, the order of tasks in the X-Y task set was randomly assigned and counterbalanced separately from the tasks in the Y-Z set. This means that in each of the two 1-D task runs, the operator performed a counterbalanced set of six tasks along the X- and Y- axes or a counterbalanced set of six tasks along the Y- and Z- axes. The order of the sets was further counterbalanced so that the X-Y tasks were performed first in half of the trials, and the Y-Z tasks were performed first in the other half of the trials for each participant. Grouping the tasks in this manner allowed fewer simulation runs and reduced any effects that might occur due to switching between external and internal command frames.

Orientations and starting positions were selected to maximize stability in the arm. Plots of the movement patterns corresponding to the task sequence for each run facilitated the selection of appropriate start positions within the VEGA based on the information obtained in the pilot study. Each task sequence was tested, and the joint angles for the starting points were noted. These joint angles were programmed into the scripts that designated the contents of the simulation displays and the location and orientation of the BORIS arm at the start of the run. Appendix G contains the movement pattern plots, individual task orders, starting points, and display variables for all task sets used in this dissertation.

Results of the 1-D tests provided valuable information related to the way operators manage inputs requiring short distance movements. The short distance ramping task is very applicable to adjustment tasks at the end of a fly-to, and adjustments made prior to grappling. The need to make smooth, controlled inputs is very important, especially when distance is short. Clearly, proper ramping is essential in these situations, where the tendency to pulse the controls is especially high.

4.2.3 Design of Tasks to Evaluate Multi-Axis Performance

Commanding and monitoring motion in two- or three-dimensional space is more difficult than in one dimension. Simultaneous movement along two or more axis dimensions increases both cognitive and psychomotor workload. The operator must choose the sequence and magnitude of input along each axis to arrive at the desired target coordinate. There may be numerous ways in which an operator can accomplish a particular task while achieving the same level of efficiency. The particular "control strategy" employed by an operator, or the manner in which the operator chooses to command the movement, may be an indicator of skill. The 2-D and 3-D tasks employed in this research were designed to evaluate several critical aspects of multi-axis performance, including differences in control strategy, operator experience and ability, number of axes to be commanded, the distance of movement along each axis, and the direction in which the motion is made.

4.2.3.1 Independent Variables for the Multi-Axis Tasks

In order to evaluate whether differences exist in the ability of operators to simultaneously control multiple axes, tasks were created that required different minimum amounts of multi-axis control in order to be completed efficiently. As discussed previously, the minimal task completion time for a particular task can be defined as the time needed to complete the movement along the limiting axis, or the axis with the longest distance to be traveled (since the maximum travel velocities are the same along all three axes). Therefore, the ratio of the distances to be traveled along the various axes represents the minimal percentage of multi-axis control required to complete the task efficiently. The multi-axis tasks were selected to require one of three minimum percentages of multi-axis control: 33.3%, 66.7%, and 100%. These ratios were achieved by combining three distances (1 m, 2 m, and 3 m) with the three translational axes (X, Y, and Z). Because the direction of motion could also affect performance, both positive and negative directions were considered in the design of the multi-axis tasks.

Due to the large number of possible combinations, a full factorial combination of the task variables was not feasible. However, an attempt was made to select a balanced subset of all possible combinations that would provide a sufficient range to test the hypotheses. Additionally, combinations were selected that allowed comparisons across 2-D and 3-D tasks to investigate changes in performance related to the number of axes. Figure 28 shows the matrix of all possible 2-D task combinations (unshaded cells).

		Task Set 1: 100% Multi-Axis						Task Set 2: 66.7% Multi-Axis						Task Set 3: 33.3% Multi-Axis					
		Limiting Axis						Non-Limiting Axis						Non-Limiting Axis					
		3X	-3X	3Y	-3Y	3Z	-3Z	2X	-2X	2Y	-2Y	2Z	-2Z	X	-X	Y	-Y	Z	-Z
Limiting Axis	3X			●	●		●						●			●			
	-3X					●				●								●	
	3Y					●		●										●	
	-3Y						●						●	●					
	3Z														●				
	-3Z							●			●						●		

Figure 28. Variable Combination Matrix Used to Select the 2-D Tasks.

Six tasks were chosen to represent each level of percent of multi-axis control, resulting in the selection of eighteen 2-D tasks. This included half of the possible task combinations in the 100% multi-axis task set, and one-quarter of the 66.7% and 33.3% task sets. The 2-D task set achieved an equal inclusion of each axis (12 tasks each), an equal number of tasks where X, Y, and Z was the limiting axis (4 each), and an equal number of axis combinations (XY, XZ, YZ) represented in each level of percent of multi-axis control (2 each). Additionally, the selected tasks provided a range of movements in a radial pattern, as shown in the plot of 2-D task movement patterns (Figure 29). This ensured that movements were performed in a variety of directions.

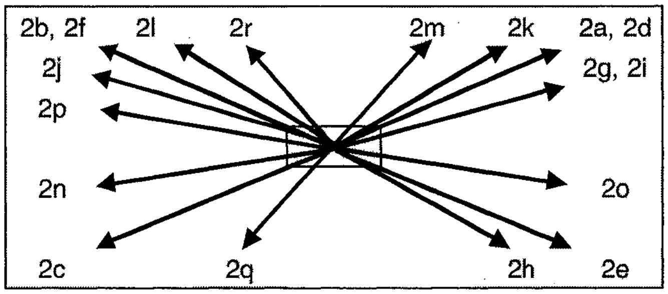

Figure 29. Pattern of Movement Direction Achieved by the 2-D Tasks.

The 3-D tasks were chosen to provide complementary tasks to allow comparisons between the performance on corresponding 2-D and 3-D tasks. Consideration of the demands on the study participants led to the decision to limit the number of 3-D tasks. Hence, only seven 3-D tasks were included in the testing. It was believed that the selected tasks would provide sufficient data to analyze the operator's ability to control three axes simultaneously and allow for comparisons with performance on the 2-D tasks. Three tasks required 33.3% multi-axis control, three tasks required 66.7% multi-axis control, and one task required simultaneous control of all three axes 100% of the time in order to complete the task with maximum efficiency. The tasks in the 33.3% control group were designed so that each of the three axes was the limiting axis in one task. Similarly, the tasks in the 66.7% control group were selected so that each axis was represented in the three tasks once as the limiting axis, once as the axis with a distance of 1 m, and once as the axis with a distance of 2 m. The task codes and variable combinations for the entire set of multi-axis tasks are presented in Table 11.

Table 11. Task Codes and Variable Combinations for the 2-D and 3-D Tasks.

	100% Multi-Axis								
Task Code	2a	2b	2c	2d	2e	2f	3g		
Task Variable Combination	3X 3Y	3X -3Y	-3X 3Z	3X -3Z	3Y 3Z	-3Y -3Z	3X 3Y 3Z		
	66.7% Multi-Axis								
Task Code	2g	2h	2i	2j	2k	2l	3d	3e	3f
Task Variable Combination	3X -2Z	-3X 2Y	2X 3Y	-3Y -2Z	2X -3Z	-2Y -3Z	3X -Y -2Z	2X 3Y Z	X -2Y -3Z
	33.3% Multi-Axis								
Task Code	2m	2n	2o	2p	2q	2r	3a	3b	3c
Task Variable Combination	3X Y	-3X Z	3Y Z	X -3Y	-X 3Z	-Y -3Z	3X Y -Z	X -3Y -Z	-X Y 3Z

The independent variables used in the analysis of the 2-D and 3-D tasks were included to investigate the effects of the task variables (representing the characteristics of the tasks) and participants (representing differences in skill). Two replicates of each of the tasks were included to examine changes in performance over time (skill acquisition) and to provide a measure of random error. The 2-D tasks were evaluated separately from the 3-D tasks in univariate analyses to examine differences in performance due to axis combinations. The independent variables for the 2-D analysis are listed in Table 12.

Table 12. Independent Variables Used to Evaluate the 2-D Metrics.

Independent Variable	Number of Levels	Levels
Multi-Axis Percent	3	33%, 66%, 100%
Axis Combination	3	XY, XZ, YZ
Replicate	2	A , B
Operator	12	101 , 106 , 108 , 109 , 110 , 111 , 122 , 123 , 124 , 127 , 128 , 129

The 2-D and 3-D data were combined in the multivariate analysis of a reduced set of multi-axis performance metrics. The univariate analysis of the 3-D task metrics and the multivariate analysis of the combined metrics used the independent variables shown in Table 13.

Table 13. Independent Variables Used to Evaluate the 3-D and Multi-Axis Metrics.

Independent Variable	Number of Levels	Levels
Multi-Axis Percent	3	33%, 66%, 100%
Limiting Axis	4	X , Y , Z, ALL
Replicate	2	A , B
Operator	12	101 , 106 , 108 , 109 , 110 , 111 , 122 , 123 , 124 , 127 , 128 , 129

4.2.3.2 Dependent Variables for the 2-D and 3-D Tasks

The list of potential metrics to assess multi-axis performance was presented in Table 5. Performance on the 3-D tasks can be represented by all 23 of the potential metrics. However, the metric representing percent of triple-axis control (P3A) was infeasible for the 2-D tasks, and the percent of dual-axis control metric (P2A) was identical to the percent of multi-axis control (PMA) metric. Therefore, the P3A and P2A metrics were eliminated, and the remaining 21 metrics formed the basis for assessing 2-D multi-axis performance. Each of the metrics was evaluated for the ability to detect differences among operators and changes in performance over time, and for sensitivity to the effects of task factors such as percentage of multi-axis control and axis combination.

Experimental Controls for the 2-D and 3-D Tasks

The 2-D tasks were designed to require movements along two axes: X and Y, or X and Z, or Y and Z. For XY and YZ task combinations, a constant target size of 3.0 mm was achieved using the same orientation and elevation restrictions as those employed in the 1-D tasks; the EE orientation was held at [-90, 0, 0] at a Z-elevation of 0 cm (zero), such that the EE was pointing straight down toward the VEGA floor surface. Using the designated EE orientation, the XY tasks were performed using an external command frame. Switching to an internal command frame allowed the YZ tasks to be performed using the same arm orientation. The control-display responses for the XY and YZ tasks are illustrated in Figure 27 as mappings A and C, respectively.

Based on the coordinate system that defines movements in the VEGA, XZ task movements were performed using an external command frame and an EE orientation of [0, -90, 0], such that the EE was pointed straight toward the Starboard wall. For the XZ task combinations, a constant target size of 3.0 mm was achieved by maintaining a perpendicular distance of 500 cm (i.e., holding Y at -1000 cm). The control-display responses for the XZ tasks are given by mapping B in Figure 27, where X commands produce horizontal motions and Z commands produce vertical motions. The use of the Starboard wall required reprogramming of the VEGA graphics to remove the "meteor hole." All tasks except the 2-D XZ tasks were performed using the [-90, 0, 0] arm orientation to allow for consistency in comparisons of performance across tasks. This also helped achieve a natural flow between tasks and reduced the number of simulation runs required. Figure 30 is a diagram depicting a sample 2-D task.

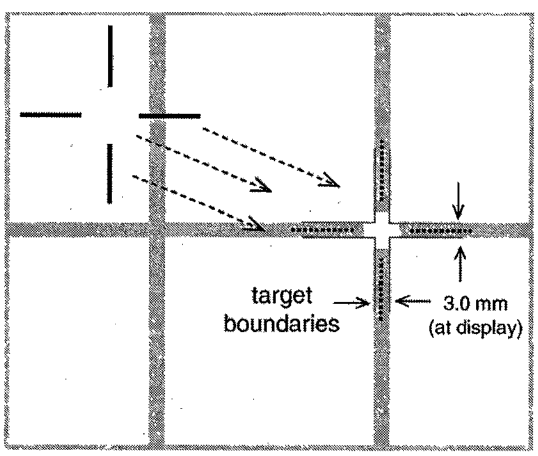

Figure 30. Sample 2-D (Multi-Axis) Task in the –X+Y (or +X+Z) Direction.

The order of the six tasks in each of the XY, XZ, and YZ task sets was counterbalanced separately due to the different command frame and arm orientation requirements of the tasks. Then, the counterbalanced sets were arranged so that an equal number of participants performed the XY, XZ, and YZ tasks at the beginning, middle, and end of testing. In each test session, the operator performed two counterbalanced sets of three tasks for each of the 2-D task axis combinations, or a total of six 2-D task runs. Grouping the tasks in this way required fewer simulations runs and reduced the need to manually switch between external and internal command frames.

Appropriate start positions were determined by arranging plots of the movement patterns corresponding to the task order sequence within the reach envelope determined in the pilot study. After testing each task sequence, the joint angles for the starting points were determined. Appendix G contains the individual task orders, movement pattern plots, starting points, and display variables for the 2-D tasks used in this dissertation.

The 3-D tasks involved moving from the starting position to a designated position in 3-D space. In order to provide sufficient visual cues to identify the target location, the XY target coordinates were displayed in Monitor 3 (as in the 2-D tasks) and the Z-elevation of the target was designated by the horizontal bars of the crosshairs displayed in Monitor 1. The task was successfully completed when the crosshairs in Monitor 3 were within the target boundaries and the tip of the EE was level with the horizontal bars of the crosshairs in Monitor 1. The correct positioning for 3-D task completion is seen in Figure 25. Using the EE orientation of [-90, 0, 0], the XYZ tasks were performed using an external command frame with control mapping C.

All of the 3-D tasks moved to the same target coordinates: [769, -400, 0]. Ending all of the 3-D tasks at these coordinates ensured a consistent target size of 3.0 mm at the completion of the tasks. Additionally, this allowed the camera views for all tasks to be held constant. The starting points of the 3-D tasks were determined by subtracting the task distances from the end coordinates. To eliminate the need to reposition the arm to a new start point, only one 3-D task was completed per run. Therefore, the operator completed seven 3-D task runs during each test replicate.

A standard counterbalancing scheme was applied to the seven 3-D tasks to produce seven unique task order sequences. One was dropped and the remaining six sequences were duplicated to create 12 task order sequences. The starting points, task order, and joint angles for the 3-D tasks are included in Appendix G.

To vary the presentation of the two 1-D runs, six 2-D runs, and seven 3-D runs, the original task orders were systematically integrated into unique run sequences for the 12 participants. The 15 test runs were ordered within the sequences to preserve the characteristics of the original orderings for the 1-D, 2-D, and 3-D tasks, as shown in Figure 31.

Original Task Orderings

Run Sets

Sequence	1-D		2-D						3-D						
1	O	N	H	I	L	M	J	K	C	G	D	B	A	E	F
2	O	N	H	I	L	M	J	K	G	D	B	A	E	F	C
3	O	N	H	I	L	M	K	J	D	B	A	E	F	C	G
4	O	N	I	H	M	L	K	J	B	A	E	F	C	G	D
5	O	N	M	L	J	K	I	H	A	E	F	C	G	D	B
6	O	N	M	L	J	K	I	H	E	F	C	G	D	B	A
7	N	O	M	L	[illegible]	[illegible]	H	I	C	G	D	B	A	E	F
8	N	O	M	L	K	[illegible]	H	I	G	D	B	A	E	F	C
9	N	O	[illegible]	K	H	I	M	L	D	B	A	E	F	C	G
10	N	O	[illegible]	K	I	H	L	M	B	A	E	F	C	G	D
11	N	O	K	[illegible]	I	H	L	M	A	E	F	C	G	D	B
12	N	O	K	[illegible]	I	H	L	M	E	F	C	G	D	B	A

Counterbalanced Run Sequence

Run Number

Sequence	1	2	3	4	5	6	7	8	9	10	11	12	13	14	15
1	O	C	G	H	D	I	L	M	B	N	J	A	K	E	F
2	O	H	G	I	N	D	B	A	L	M	E	F	[illegible]	K	C
3	D	O	H	B	I	A	E	N	F	C	L	G	M	K	[illegible]
4	B	I	O	A	E	F	H	M	C	G	L	K	D	N	[illegible]
5	M	A	L	O	E	F	C	[illegible]	K	G	D	I	H	B	N
6	M	E	L	F	C	O	G	D	[illegible]	B	[illegible]	I	H	A	N
7	C	G	M	D	L	[illegible]	[illegible]	B	N	H	A	I	E	F	O
8	G	D	B	M	L	A	E	[illegible]	[illegible]	F	N	H	C	I	O
9	[illegible]	D	N	[illegible]	B	H	A	E	O	F	C	I	G	M	L
10	[illegible]	N	B	A	E	K	I	F	C	H	L	G	O	M	D
11	N	K	A	[illegible]	E	F	O	C	G	I	D	H	L	M	B
12	N	E	F	C	K	[illegible]	G	D	I	H	B	O	L	A	M

Figure 31. Integration of Original Task Orders into Unique Run Sequences.

Table 14 contains the assignment of the individual task sequences to the participants. Details of the run sequences are found in Appendix H. Ultimately, a program was written to automatically generate and present the appropriate task sequence for each participant during testing.

Table 14. Run Sequence Assignments.

	Participant ID											
	101	106	108	109	110	111	122	123	124	127	128	129
Trial	---	---	---	---	---	---	4	2	8	10	6	12
Test 1	5	1	9	7	11	3	8	6	12	2	10	4
Test 2	9	5	1	11	3	7	12	10	4	6	2	8

4.2.4 Statistical Models

A three-step approach was employed in the statistical analyses to isolate the performance metrics that were the best indicators of differences in skill. Initially, the data collected on the 1-D, 2-D, and 3-D tasks were divided into three individual sets. Separate ANOVAs were performed using the three data sets where the potential metrics associated with each task set served as the dependent measures in the univariate models. Then, correlation analyses were run using the performance metric data sets. The results of the ANOVAs and correlation analyses were used to eliminate metrics that were less sensitive and to reduce the number of potential metrics to be included in subsequent multivariate analyses. The 1-D ANOVA and correlation analysis results were used to produce a reduced set of metrics to evaluate ramping performance. The results of the separate 2-D and 3-D analyses were integrated to produce a single reduced set of metrics to evaluate multi-axis performance. Finally, separate MANOVAs were performed on these two reduced metric sets.

The experimental design used in the empirical study was a *mixed-effects factorial design with repeated measures.* Each participant in the study performed two replicates of 37 targeted movement tasks that were presented in a counterbalanced sequence of 15 simulation runs that included two runs of six 1-D tasks, six runs of three 2-D tasks, and seven runs of single 3-D tasks. The statistical analyses were performed using the SAS® System for Windows® (Version 8.01). The statistical models for the analyses are described below.

4.2.4.1 1-D ANOVA and Ramping MANOVA Model

The SAS GLM procedure was applied to each 1-D performance metric to determine the effects of the task variables (differences in direction of motion, movement distance, and axis of motion), the replicate, and the participant. Hence, a 2 × 2 × 3 × 2 × 12 mixed-effects factorial model was used to evaluate the 1-D performance metrics. The inclusion of replicate as a term in the model required elimination of the highest order interaction term to provide sufficient degrees of freedom for error. The statistical model used for the 1-D task analysis is given in Equation 1.

$$\begin{aligned} y_{ijklm} = {} & \mu + \mathbf{A}_i + \mathbf{B}_j + \mathbf{C}_k + \mathbf{D}_l + \mathbf{E}_m + \mathbf{AB}_{ij} + \mathbf{AC}_{ik} + \mathbf{AD}_{il} + \mathbf{AE}_{im} + \mathbf{BC}_{jk} + \mathbf{BD}_{jl} + \\ & \mathbf{BE}_{jm} + \mathbf{CD}_{kl} + \mathbf{CE}_{km} + \mathbf{DE}_{lm} + \mathbf{ABC}_{ijk} + \mathbf{ABD}_{ijl} + \mathbf{ABE}_{ijm} + \mathbf{ACD}_{ikl} + \\ & \mathbf{ACE}_{ikm} + \mathbf{ADE}_{ilm} + \mathbf{BCD}_{jkl} + \mathbf{BCE}_{jkm} + \mathbf{CDE}_{klm} + \mathbf{ABCD}_{ijkl} + \mathbf{ABCE}_{ijkm} + \\ & \mathbf{BCDE}_{jklm} + \varepsilon_{ijklm}, \qquad \text{(Equation 1)} \end{aligned}$$

where

y_{ijklm} = the 1-D performance metric(s),

μ = the grand mean,

$\mathbf{A}_i$ = the effect of the i^{th} level of ***direction of motion*** (i = 1 to 2),

$\mathbf{B}_j$ = the effect of the j^{th} level of ***movement distance*** (j = 1 to 2),

$\mathbf{C}_k$ = the effect of the k^{th} level of ***axis of motion*** (k = 1 to 3),

$\mathbf{D}_l$ = the effect of the l^{th} level of ***replicate*** (l = 1 to 2),

$\mathbf{E}_m$ = the effect of the m^{th} level of ***participant*** (m = 1 to 12), and

ε_{ijklm} = ***random error.***

Table 15 presents the Expected Mean Squares and correct F-ratios for the 1-D model.

Table 15. Expected Mean Squares and F-Tests for the 1-D Model.

Source	Degrees of Freedom	Expected Mean Square	F-ratio
A_i	a-1	σ^2 + AE + A	MS_A/MS_{AE}
B_j	b-1	σ^2 + BE + B	MS_B/MS_{BE}
C_k	c-1	σ^2 + CE + C	MS_C/MS_{CE}
D_l	d-1	σ^2 + DE + D	MS_D/MS_{DE}
E_m	e-1	σ^2 + E	MS_E/MS_{Error}
AB_{ij}	(a-1)(b-1)	σ^2 + ABE + AB	MS_{AB}/MS_{ABE}
AC_{ik}	(a-1)(c-1)	σ^2 + ACE + AC	MS_{AC}/MS_{ACE}
AD_{il}	(a-1)(d-1)	σ^2 + ADE + AD	MS_{AD}/MS_{ADE}
AE_{im}	(a-1)(e-1)	σ^2 + AE	MS_{AE}/MS_{Error}
BC_{jk}	(b-1)(c-1)	σ^2 + BCE + BC	MS_{BC}/MS_{BCE}
BD_{jl}	(b-1)(d-1)	σ^2 + BDE + BD	MS_{BD}/MS_{BDE}
CD_{kl}	(c-1)(d-1)	σ^2 + CDE + CD	MS_{CD}/MS_{CDE}
CE_{km}	(c-1)(e-1)	σ^2 + CE	MS_{CE}/MS_{Error}
DE_{lm}	(d-1)(e-1)	σ^2 + DE	MS_{DE}/MS_{Error}
ABC_{ijk}	(a-1)(b-1)(c-1)	σ^2 + ABCE + ABC	MS_{ABC}/MS_{ABCE}
ABD_{ijl}	(a-1)(b-1)(d-1)	σ^2 + ABDE + ABD	MS_{ABD}/MS_{ABDE}
ABE_{ijm}	(a-1)(b-1)(e-1)	σ^2 + ABE	MS_{ABE}/MS_{Error}
ACD_{ikl}	(a-1)(c-1)(d-1)	σ^2 + ACDE + ACD	MS_{ACD}/MS_{ACDE}
ACE_{ikm}	(a-1)(c-1)(e-1)	σ^2 + ACE	MS_{ACE}/MS_{Error}
ADE_{ilm}	(a-1)(d-1)(e-1)	σ^2 + ADE	MS_{ADE}/MS_{Error}
BCD_{jkl}	(b-1)(c-1)(d-1)	σ^2 + BCDE + BCD	MS_{BCD}/MS_{BCDE}
BCE_{jkm}	(b-1)(c-1)(e-1)	σ^2 + BCE	MS_{BCE}/MS_{Error}
BDE_{jlm}	(b-1)(d-1)(e-1)	σ^2 + BDE	MS_{BDE}/MS_{Error}
CDE_{klm}	(c-1)(d-1)(e-1)	σ^2 + CDE	MS_{CDE}/MS_{Error}
$ABCD_{ijkl}$	(a-1)(b-1)(c-1)(d-1)	σ^2 + ABCDE + ABCD	MS_{ABCD}/MS_{Error}
$ABCE_{ijkm}$	(a-1)(b-1)(c-1)(e-1)	σ^2 + ABCE	MS_{ABCE}/MS_{Error}
$ABDE_{ijlm}$	(a-1)(b-1)(d-1)(e-1)	σ^2 + ABDE	MS_{ABDE}/MS_{Error}
$ACDE_{iklm}$	(a-1)(c-1)(d-1)(e-1)	σ^2 + ACDE	MS_{ACDE}/MS_{Error}
$BCDE_{jklm}$	(b-1)(c-1)(d-1)(e-1)	σ^2 + BCDE	MS_{BCDE}/MS_{Error}
$Error_{ijklm}$	(a-1)(b-1)(c-1)(d-1)(e-1)	σ^2	

4.2.4.2 2-D ANOVA Model

The 2-D analyses tested each 2-D performance metric to determine the effects of the task variables (required percent of multi-axis control and axis combination), the replicate, and the participant. The 3 × 3 × 2 × 12 mixed-effects factorial model used in the 2-D analyses is given in Equation 2.

$$y_{ijklm} = \mu + \mathbf{A}_i + \mathbf{B}_j + \mathbf{C}_k + \mathbf{D}_l + \mathbf{AB}_{ij} + \mathbf{AC}_{ik} + \mathbf{AD}_{il} + \mathbf{BC}_{jk} + \mathbf{BD}_{jl} + \mathbf{CD}_{kl} + \mathbf{ABC}_{ijk} + \mathbf{ABD}_{ijl} + \mathbf{ACD}_{ikl} + \mathbf{BCD}_{jkl} + \mathbf{ABCD}_{ijkl} + \varepsilon_{ijklm}, \qquad \text{(Equation 2)}$$

where

y_{ijkl} = the 2-D performance metric,

μ = the grand mean,

$\mathbf{A}_i$ = the effect of the i^{th} level of ***percent of multi-axis control*** (i = 1 to 3),

$\mathbf{B}_j$ = the effect of the j^{th} level of ***axis combination*** (j = 1 to 3),

$\mathbf{C}_k$ = the effect of the k^{th} level of ***replicate*** (k = 1 to 2),

$\mathbf{D}_l$ = the effect of the l^{th} level of ***participant*** (l = 1 to 12), and

ε_{ijklm} = ***random error.***

The Expected Mean Squares and appropriate F-ratios for the 2-D model are presented in Table 16.

4.2.4.3 3-D ANOVA and Multi-Axis MANOVA Model

The 3-D performance metrics were tested to determine the effects due to the task variables (required percent of multi-axis control and limiting axis), the replicate, and the participant. Due to overspecification of the model, the highest order interaction term was eliminated to provide sufficient error degrees of freedom. The 3 × 4 × 2 × 12 mixed-effects factorial model used in the 3-D analyses is given in Equation 3.

Table 16. Expected Mean Squares and F-Tests for the 2-D Model.

Source	Degrees of Freedom	Expected Mean Square	F-ratio
A_i	a-1	σ^2 + AD + A	MS_A/MS_{AD}
B_j	b-1	σ^2 + BD + B	MS_B/MS_{BD}
C_k	c-1	σ^2 + CD + C	MS_C/MS_{CD}
D_l	d-1	σ^2 + D	MS_D/MS_{Error}
AB_{ij}	(a-1)(b-1)	σ^2 + ABD + AB	MS_{AB}/MS_{ABD}
AC_{ik}	(a-1)(c-1)	σ^2 + ACD + AC	MS_{AC}/MS_{ACD}
AD_{il}	(a-1)(d-1)	σ^2 + AD	MS_{AD}/MS_{Error}
BC_{jk}	(b-1)(c-1)	σ^2 + BCD + BC	MS_{BC}/MS_{BCD}
BD_{jl}	(b-1)(d-1)	σ^2 + BD	MS_{BD}/MS_{Error}
CD_{kl}	(c-1)(d-1)	σ^2 + CD	MS_{CD}/MS_{Error}
ABC_{ijk}	(a-1)(b-1)(c-1)	σ^2 + ABCD + ABC	MS_{ABC}/MS_{ABCD}
ABD_{ijl}	(a-1)(b-1)(d-1)	σ^2 + ABD	MS_{ABD}/MS_{Error}
ACD_{ikl}	(a-1)(c-1)(d-1)	σ^2 + ACD	MS_{ACD}/MS_{Error}
BCD_{jkl}	(b-1)(c-1)(d-1)	σ^2 + BCD	MS_{BCD}/MS_{Error}
$ABCD_{ijkl}$	(a-1)(b-1)(c-1)(d-1)	σ^2 + ABCD	MS_{ABCD}/MS_{Error}
$Error_{ijkl}$	abcd(n-1)	σ^2	

$$y_{ijkl} = \mu + \mathbf{A}_i + \mathbf{B}_j + \mathbf{C}_k + \mathbf{D}_l + \mathbf{AB}_{ij} + \mathbf{AC}_{ik} + \mathbf{AD}_{il} + \mathbf{BC}_{jk} + \mathbf{BD}_{jl} + \mathbf{CD}_{kl} + \mathbf{ABC}_{ijk} + \mathbf{ABD}_{ijl} + \mathbf{ACD}_{ikl} + \mathbf{BCD}_{jk}l + \varepsilon_{ijkl}, \qquad \text{(Equation 3)}$$

where

y_{ijkl} = the 3-D or multi-axis performance metric(s),

μ = the grand mean,

$\mathbf{A}_i$ = the effect of the i^{th} level of ***percent of multi-axis control*** (i = 1 to 3),

$\mathbf{B}_j$ = the effect of the j^{th} level of ***limiting axis*** (j = 1 to 4),

$\mathbf{C}_k$ = the effect of the k^{th} level of ***replicate*** (k = 1 to 2),

$\mathbf{D}_l$ = the effect of the l^{th} level of ***participant*** (l = 1 to 12), and

ε_{ijkl} = ***random error.***

The Expected Mean Squares and appropriate F-ratios for the 3-D model are presented in Table 17.

Table 17. Expected Mean Squares and F-Tests for the 3-D Model.

Source	Degrees of Freedom	Expected Mean Square	F-ratio
A_i	a-1	σ^2 + AD + A	MS_A/MS_{AD}
B_j	b-1	σ^2 + BD + B	MS_B/MS_{BD}
C_k	c-1	σ^2 + CD + C	MS_C/MS_{CD}
D_l	d-1	σ^2 + D	MS_D/MS_{Error}
AB_{ij}	(a-1)(b-1)	σ^2 + ABD + AB	MS_{AB}/MS_{ABD}
AC_{ik}	(a-1)(c-1)	σ^2 + ACD + AC	MS_{AC}/MS_{ACD}
AD_{il}	(a-1)(d-1)	σ^2 + AD	MS_{AD}/MS_{Error}
BC_{jk}	(b-1)(c-1)	σ^2 + BCD + BC	MS_{BC}/MS_{BCD}
BD_{jl}	(b-1)(d-1)	σ^2 + BD	MS_{BD}/MS_{Error}
CD_{kl}	(c-1)(d-1)	σ^2 + CD	MS_{CD}/MS_{Error}
ABC_{ijk}	(a-1)(b-1)(c-1)	σ^2 + ABCD + ABC	MS_{ABC}/MS_{ABCD}
ABD_{ijl}	(a-1)(b-1)(d-1)	σ^2 + ABD	MS_{ABD}/MS_{Error}
ACD_{ikl}	(a-1)(c-1)(d-1)	σ^2 + ACD	MS_{ACD}/MS_{Error}
BCD_{jkl}	(b-1)(c-1)(d-1)	σ^2 + BCD	MS_{BCD}/MS_{Error}
$Error_{ijkl}$	(a-1)(b-1)(c-1)(d-1)	σ^2	

CHAPTER 5

RESULTS AND ANALYSES

5.1 Graphical Analysis Results

Graphical analysis of the performance data was employed to identify performance input patterns and to provide the acceleration and smoothness metrics for the ramping tasks. Plots of commanded velocity over time were examined to help identify differences in the input patterns that suggested critical aspects of performance. Comparisons were made between the participants and with the rational models. Metrics to evaluate ramping and multi-axis performance were selected that quantified the differences observed in performance patterns. The data collected in the empirical study were used to determine the metric values. Summary statistics were calculated for each metric set, including the mean, standard deviation, minimum and maximum values, and percent standard error, where

$$\text{Percent Standard Error} = \frac{s/\sqrt{n}}{\bar{x}} \times 100\% .$$

Metrics with higher variation were thought to be more representative of performance aspects that are more difficult to learn or require greater skill. This assumption played a key role in the selection of the reduced set of metrics used in the multivariate analyses. Table 18 contains the summary statistics for the 1-D performance metrics. Table 19 summarizes the performance metric statistics for the 2-D and 3-D tasks.

Table 18. Summary Statistics for the 1-D Performance Metrics.

Metric	1-D Tasks				
	Mean	StDev	%StdErr	Min	Max
A_In	15.8	24.7	9.2	0.2	187.5
R_In	0.8	0.2	1.5	0.1	1.0
A_Out_1	6.6	20.1	18.0	0.0	234.7
R_Out_1	0.7	0.2	2.0	0.0	1.0
A_Out_2	3.9	7.2	10.8	0.0	96.4
R_Out_2	0.7	0.2	2.0	0.0	1.0
V_Max	22.0	7.0	1.9	8.1	30.1
PRIT	23.9	16.9	4.2	0.7	77.2
PRID	24.1	18.8	4.6	0.0	80.4
PTT	26.3	18.0	4.0	1.1	85.2
PTD	41.0	23.1	3.3	1.9	101.5
PRO1T	37.2	19.6	3.1	0.8	91.7
PRO1D	34.1	19.2	3.3	1.3	93.7
PCT	12.6	16.5	7.7	0.0	71.9
RIT	3.7	3.3	5.3	0.2	20.3
RID	44.5	45.1	6.0	0.0	231.0
TT	3.8	2.9	4.4	0.1	19.4
TD	83.8	68.6	4.8	1.9	253.5
RO1T	5.6	3.7	3.9	0.1	21.9
RO1D	66.3	50.0	4.4	1.3	278.9
CT	2.1	3.1	8.6	0.0	21.6
CD	1.2	8.2	40.9	-13.2	97.4
TCT	15.2	6.0	2.3	4.6	31.8

Table 19. Summary Statistics for the 2-D and 3-D Performance Metrics.

Metric	2-D Tasks					3-D Tasks				
	Mean	StDev	%StdErr	Min	Max	Mean	StDev	%StdErr	Min	Max
P1A	27.5	13.9	2.4	0.7	88.4	39.5	13.1	2.6	5.3	81.3
P2A	59.1	19.1	1.6	0.0	98.8	20.7	12.5	4.7	0.0	63.2
P3A	-----	-----	-----	-----	-----	21.4	15.7	5.7	0.0	69.6
PMA	59.1	19.1	1.9	0.0	98.8	42.1	16.2	3.0	2.1	88.6
X1	0.4	1.9	32.0	0.0	31.1	0.7	1.9	22.6	0.0	17.1
Y1	0.6	1.0	8.1	0.0	7.4	1.6	2.4	11.5	0.0	23.0
Z1	1.3	1.8	8.3	0.0	12.3	5.4	9.8	14.1	0.0	63.4
TCT	27.8	10.2	2.2	11.1	114.3	42.8	15.2	2.7	19.0	100.5
XCT	11.7	11.1	5.6	0.0	95.5	20.3	16.3	6.2	0.0	95.1
YCT	7.6	7.8	6.1	0.0	37.8	16.1	14.5	6.9	0.0	71.2
ZCT	8.9	11.3	7.5	0.0	90.2	24.7	14.4	4.5	0.0	73.4
XPC	37.9	24.9	3.9	0.0	98.0	44.0	25.9	4.5	0.0	97.8
YPC	26.5	23.4	5.2	0.0	98.2	34.9	25.2	5.6	0.0	99.3
ZPC	27.7	23.5	5.0	0.0	98.1	57.3	25.0	3.4	0.0	99.1
XS	3.2	1.7	3.1	1	11	3.8	2.2	4.5	1	12
YS	2.7	1.4	3.2	1	9	3.4	1.7	3.9	1	8
ZS	2.8	1.6	3.4	1	10	3.9	1.9	3.8	1	11
XA>15	21.8	10.1	2.7	3	66	21.9	11.1	3.9	4	63
YA>15	21.5	9.3	2.6	4	53	22.3	10.3	3.6	4	51
ZA>15	20.2	10.7	3.1	2	57	20.6	12.2	4.6	2	73
XA>30	11.4	6.5	3.4	1	41	12.2	7.9	5.0	2	45
YA>30	8.9	5.6	3.7	0	30	9.8	6.1	4.8	1	29
ZA>30	8.8	5.7	3.8	0	33	9.0	7.3	6.2	0	45

Plots of the mean metric values were used to examine differences in performance between the 2-D tasks and the 3-D tasks. Figure 32 plots the mean percent of single-axis, dual-axis, triple-axis, and multi-axis control input for the 2-D and 3-D tasks. Increased use of multi-axis control could result in increased task efficiency and demonstrate operator skill. As shown, while simultaneous control of two axes was used more often in the 2-D tasks, more single-axis control usage was seen during performance of the 3-D tasks. Overall, participants used multi-axis commands more often in the 2-D tasks than in the 3-D tasks.

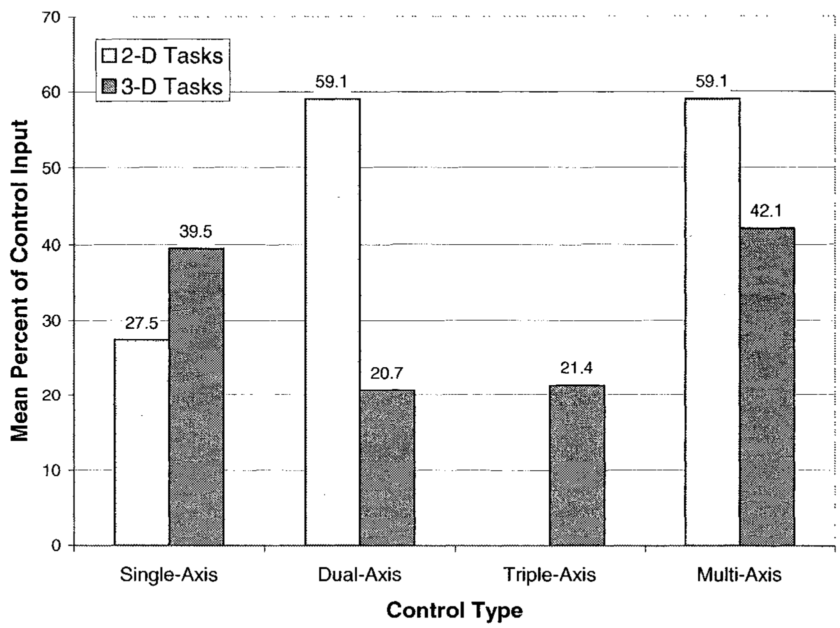

Figure 32. Comparison of Control Input Between 2-D and 3-D Tasks.

Mean lag times for each axis of motion are plotted in Figure 33. In general, lag times were longer for the 3-D tasks across all axes. Lag times for the X inputs were smallest, with an increase across the Y and Z inputs. Larger differences were indicated in the initial input time of the Y- and Z-axes between the 2-D and 3-D tasks. In particular, 3-D task lag time for the Z-axis input was four times greater than the Z-axis lag for the 2-D tasks.

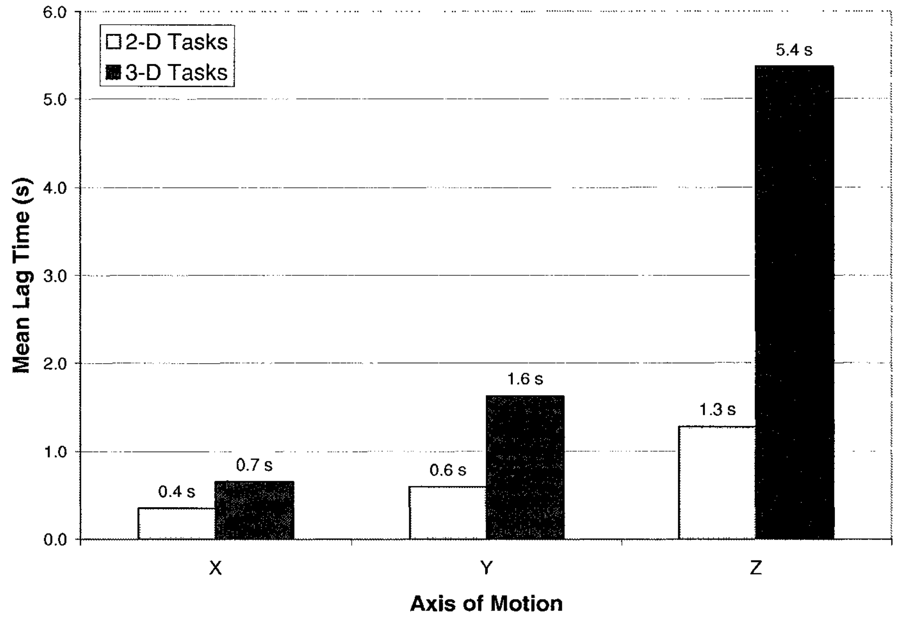

Figure 33. Lag Time Comparison Between 2-D and 3-D Tasks.

Task completion time can be used to indicate the efficiency of a task relative to some standard completion time. In a targeted movement task, completion time is a function of rate of travel, distance, and target size. When these factors are constant, greater task completion times may be attributed to a lack of operator skill. As seen in Figure 34, the mean task completion time was greater for the 3-D tasks.

An additional contributing factor in task completion time is the amount of time spent in making corrections. Increased correction time often results in increased task completion time. Therefore, correction time is a measure of the inefficiency in a task. Figure 35 shows the mean correction time and percentage of total time spent making corrections for the 2-D and 3-D tasks. In the 2-D tasks, X corrections required the

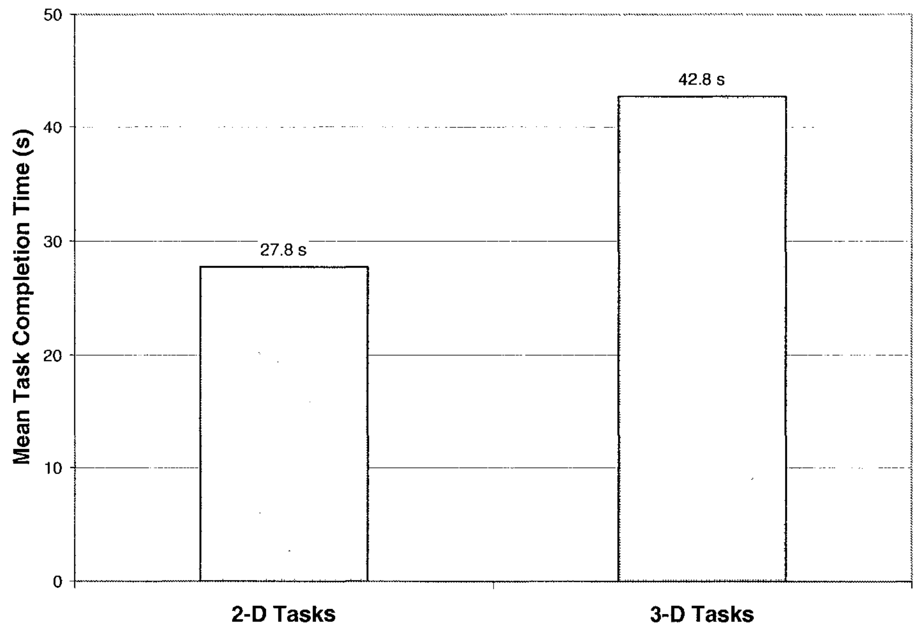

Figure 34. Mean Task Completion Time for 2-D and 3-D Tasks.

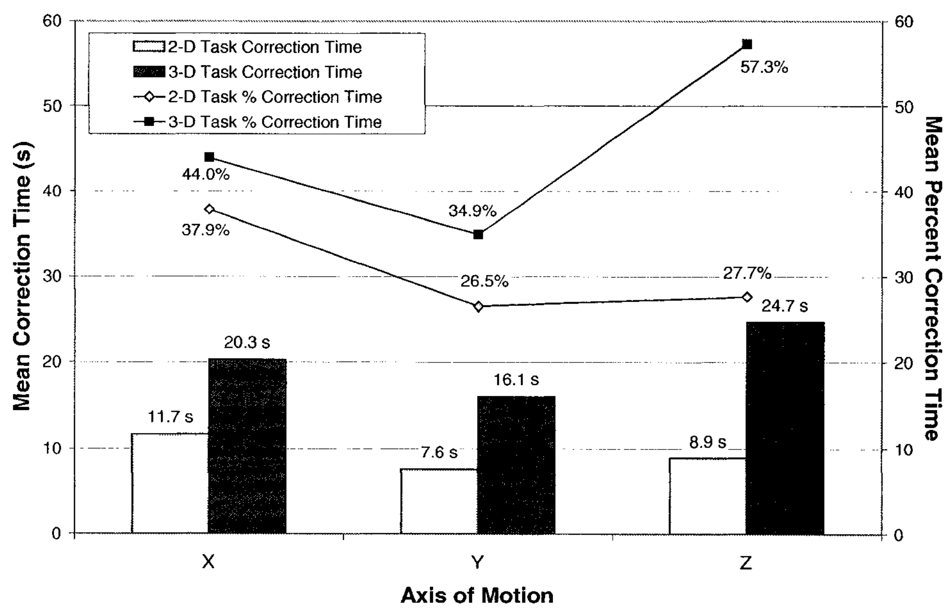

Figure 35. Comparison of Corrections for 2-D and 3-D Tasks.

greatest amount of time, followed by Z and Y, respectively. In the 3-D tasks, Z-axis correction time was highest. Across tasks, movements in the Y-axis were completed with the least correction time. Overall, more time was spent making corrections for the 3-D tasks, as indicated by the higher percentage of total time used to make corrections.

Similar trends were seen in the mean number of starts along each axis. A "start" is defined as the initiation of input from a zero velocity (i.e., beginning a new movement along a particular axis). If a movement is controlled accurately, it will stop at exactly the right location. If movement stops off-target, it must be "re-started." Hence, inefficiency is indicated by a higher number of starts. As shown in Figure 36, more starts were made in the 3-D tasks across all axes. In the 2-D tasks, more starts were made along the X-axis, followed by Z and Y, respectively. In the 3-D tasks, the Z-axis had the highest number of starts. Across tasks, movements in the Y-axis were completed with the fewest starts, which may imply greater control.

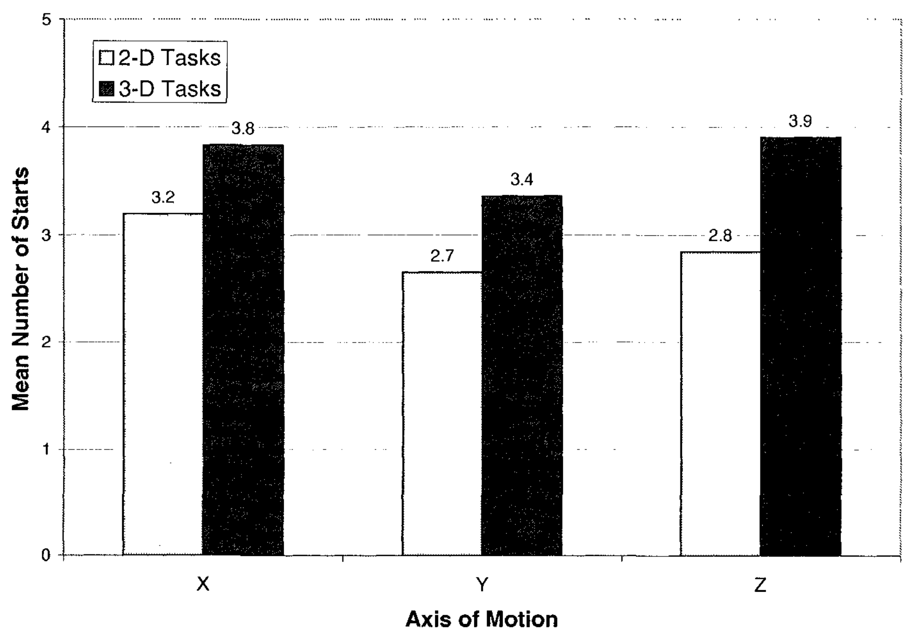

Figure 36. Mean Number of Starts by Axis for 2-D and 3-D Tasks.

Smooth (ramped) control inputs are characterized by steady, linear increases in velocity over time. Rapid accelerations may indicate unplanned or poorly controlled movements, and hence, lack of operator skill. A plot of the mean number of excessive accelerations (>15 cm/s^2 and > 30 cm/s^2) by axis for the 2-D and 3-D tasks is shown in Figure 37. In the 2-D tasks, the greatest number of rapid accelerations was made in the X-axis inputs, followed closely by those in the Y-axis and Z-axis, respectively. The trend was similar in the 3-D tasks, except that the greatest number of accelerations > 15 cm/s^2 was seen in the Y-axis inputs. Overall, more rapid accelerations were seen in the 3-D tasks across all axes.

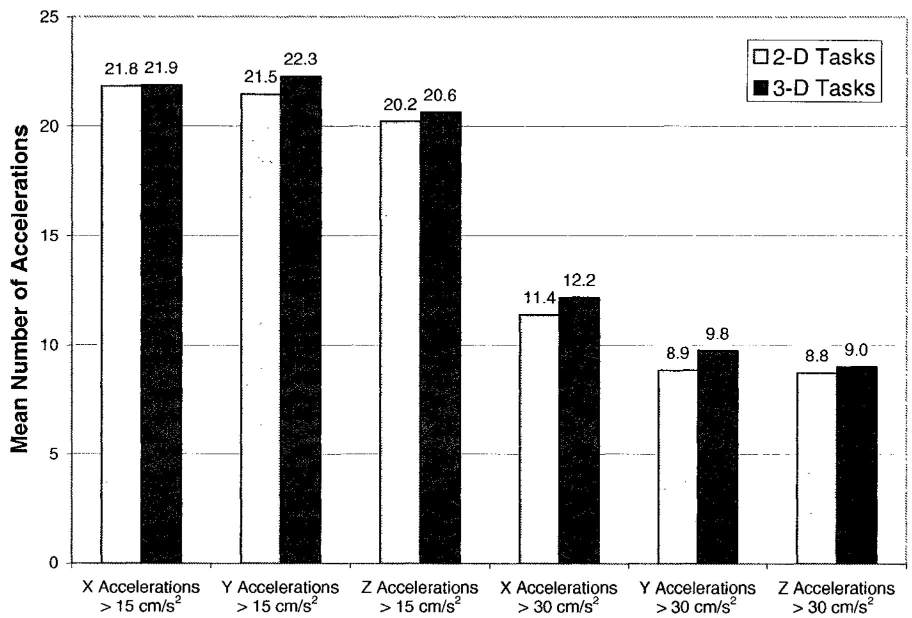

Figure 37. Accelerations by Axis for 2-D and 3-D Tasks.

5.2 ANOVA Results

Separate univariate analyses were performed on the performance metric data for the 1-D, 2-D, and 3-D tasks. The results of these analyses were used to examine differences in performance due to the task variables, replicates, and participants. Results are reported for all tests based on an alpha level of .05. However, to guard against inflated Type I error due to the large number of analyses, only effects that were highly significant ($p < .0001$) are discussed. When appropriate, Ryan's multiple comparison procedure was used to compare means of significant main effects. Specific results are discussed only briefly, as the main purpose of the univariate analyses was to identify a smaller set of metrics that were highly responsive to differences in operator performance. This reduced set of metrics served as the dependent variables in subsequent multivariate analyses.

5.2.1 1-D Task ANOVA Results

The statistical model presented in Equation 1 was used to test the effects of direction of motion, movement distance, axis of motion, replicate, and participant on each of the 23 performance metrics developed for the 1-D tasks to represent critical aspects of ramping performance. A summary of the ANOVA results for the 1-D metrics is given in Table 20, where highly significant effects are highlighted.

Direction of motion, axis of motion, and replicate did not produce any highly significant effects. However, ***movement distance*** significantly affected maximum velocity ($F_{1,11} = 167.44$), travel time ($F_{1,11} = 83.44$), travel distance ($F_{1,11} = 90.18$), initial ramp-out time ($F_{1,11} = 74.88$), initial ramp-out distance ($F_{1,11} = 139.32$), and task completion time ($F_{1,11} = 1295.19$). In all cases, the movement distance of 3 m produced significantly higher means than the 1 m movement distance. Highly significant differences were found among ***participants*** with respect to ramp-in acceleration ($F_{11,22} = 9.25$), ramp-in R^2 ($F_{11,22} = 8.76$), overall ramp-out R^2 ($F_{11,22} = 6.32$), maximum velocity

($F_{11,22}$ = 47.86), percent ramp-in time ($F_{11,22}$ = 11.50), percent ramp-in distance ($F_{11,22}$ = 13.51), percent initial ramp-out time ($F_{11,22}$ = 7.78), ramp-in time ($F_{11,22}$ = 21.98), ramp-in distance ($F_{11,22}$ = 8.49), initial ramp-out time ($F_{11,22}$ = 9.04), and task completion time ($F_{11,22}$ = 31.93).

Table 20. Summary of 1-D ANOVA Results.

	Model (df=265)	dir (A)	dis (B)	axs (C)	rep (D)	pid (E)	dir*dis AB	dir*axs AC	dir*rep AD	dir*pid AE	dis*axs BC	dis*rep BD	dis*pid BE	axs*rep CD	axs*pid CE	rep*pid DE
a_in			.018		.033	< .0001										
r_in						< .0001										
a_out1																
r_out1		.006				.004					.023					.005
a_out2						.003							.049			
r_out2			.010			< .0001						.034	.015			
vmax	< .0001		< .0001			< .0001							.002		.023	.006
prit	.047			.005		< .0001							.025	.018		
prid	.007		.045	.006		< .0001			.046				.023	.018	.030	
ptt						.000										
ptd						.001							.008			
pro1t						< .0001										
pro1d						.001										
pct	.017					.002							.010		.006	
rit	.013		.012	.003	.023	< .0001							.013	.027		
rid	.039		.001	.009		< .0001						.049	.001	.003		
tt			< .0001			.012										
td	.006		< .0001			.002							.006			
ro1t	.048		< .0001			< .0001		.033								
ro1d	.007		< .0001			.000										
ct	.018					.003							.006		.004	
cd	.018					.000				.017						.029
tct	< .0001		< .0001			< .0001									.020	.007

	ABC	ABD	ABE	ACD	ACE	ADE	BCD	BCE	BDE	CDE	ABCD	ABCE	ABDE	ACDE	BCDE	ABCDE (error)
a_in																
r_in																
a_out1																
r_out1														.018		
a_out2																
r_out2																
vmax					.020				.030	.026						
prit							.043									
prid														.008		
ptt														.027		
ptd														.048		
pro1t									.043							
pro1d																
pct									.006			.001				
rit					.025		.042									
rid							.012									
tt																
td																
ro1t																
ro1d																
ct			.046						.003	.042		.005				
cd		.039							.000			.017	.010			
tct																

5.2.2 2-D Task ANOVA Results

An ANOVA was run on each of the 21 metrics developed to evaluate critical aspects of multi-axis performance on the 2-D tasks. The statistical model given in Equation 2 was used to test the effects of levels of required percent of multi-axis control, axis combination, replicate, and participant. A summary of the ANOVA results on the 2-D metrics is given in Table 21, where highly significant effects are highlighted.

Table 21. Summary of 2-D ANOVA Results.

	Model	map (A)	axs (B)	rep (C)	pid (D)	map*axs AB	map*rep AC	map*pid AD	axs*rep BC	axs*pid BD	rep*pid CD	ABC	ABD	ACD	BCD	ABCD
p1a	< .0001	< .0001	< .0001	.033	< .0001					.000						
pma	< .0001	< .0001	< .0001	.019	< .0001	.040				.003						
x1																
y1	< .0001		.029		< .0001					< .0001						
z1	< .0001				< .0001			< .0001						.015	.019	
tct	< .0001	< .0001		.040	< .0001				.038	< .0001	.015					
xs					.002	.001				.038						
ys	.014				.001						.004				.040	
zs			.014	.004												
xct				.027	< .0001	.001										
yct		.046								.029						
zct	.003		.036	.030	< .0001					.000						
xpc						< .0001										
ypc		.000														
zpc		.010	.001	.018	.047											
xa15	.012	.001			< .0001	.005										
ya15	.000	.039			< .0001											
za15	< .0001	.019	.013		< .0001											
xa30	< .0001	.032			< .0001											
ya30	< .0001	.034			< .0001											
za30	< .0001	.006	.008		< .0001											

The levels of required ***percent multi-axis control*** in the 2-D tasks produced highly significant differences in the percent of single-axis control ($F_{2,22} = 52.64$), percent of multi-axis (i.e., dual-axis) control ($F_{2,22} = 36.94$), and task completion time ($F_{2,22} = 24.20$). Appropriately, as the multi-axis requirements of the task increased from 33.3% to 66.7% the use of single-axis control decreased and the use of multi-axis control increased, but no significant differences were found between the tasks requiring 66.7% and 100%. Further, task completion time increased significantly for each increase in the multi-axis requirements of the task. ***Axis combination*** significantly affected the percent of single-axis control ($F_{2,22}$ = 15.76) and the percent of multi-axis control ($F_{2,22}$ = 25.11). Single-axis control was used with much greater frequency during the XZ axis combination tasks, and multi-axis control increased significantly from the XZ to the XY to the YZ axis combinations. No highly significant differences were found between replicates. ***Participants*** differed significantly in use of single-axis control ($F_{11,216}$ = 16.00), use of multi-axis control ($F_{11,216}$ = 17.15), Y lag time ($F_{11,144}$ = 11.44), Z lag time ($F_{11,144}$ = 24.12), task completion time ($F_{11,216}$ = 20.26), X correction time ($F_{11,144}$ = 5.27), Z correction time ($F_{11,144}$ = 5.70), X accelerations > 15 cm/s^2 ($F_{11,144}$ = 8.32), Y accelerations > 15 cm/s^2 ($F_{11,144}$ = 12.25), Z accelerations > 15 cm/s^2 ($F_{11,144}$ = 14.97), X accelerations > 30 cm/s^2 ($F_{11,144}$ = 18.50), Y accelerations > 30 cm/s^2 ($F_{11,144}$ = 14.56), and Z accelerations > 30 cm/s^2 ($F_{11,144}$ = 15.79). The ***participant*** × ***percent multi-axis control*** interaction produced highly significant differences in the Z lag time ($F_{22,216}$ = 3.84). As shown in Figure 38, the Z lag times of Participant 101 on the tasks requiring 66.7% and 100% multi-axis control were much longer than for the other participants.

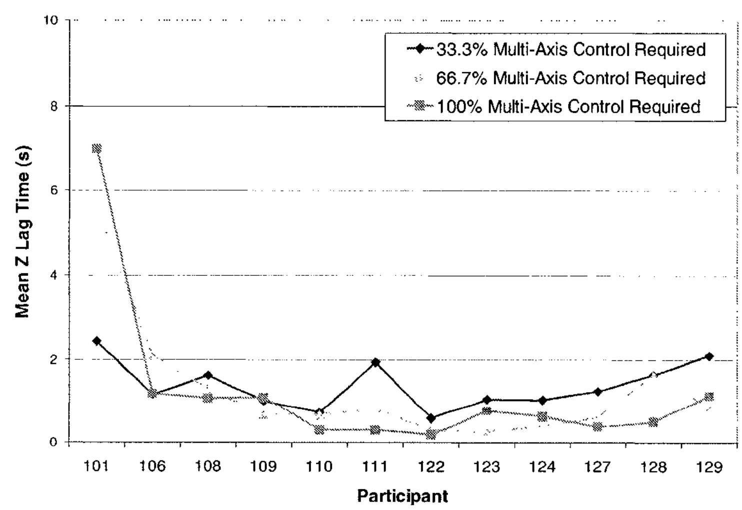

Figure 38. Mean Z Lag Time by Required Percent Multi-Axis and Participant.

The ***axis combination*** × ***participant*** interaction resulted in highly significant differences in Y lag time ($F_{22,144} = 14.92$) and task completion time ($F_{22,216} = 2.82$). The plot of the interaction in Figure 39 shows that the difference in the mean Y lag time between the XY and YZ tasks was much greater for participants 101, 106, and 108 than for the other participants. The significant interaction in Figure 40 seems to be a result of the high task completion times of Participant 101 on the XZ axis combination tasks.

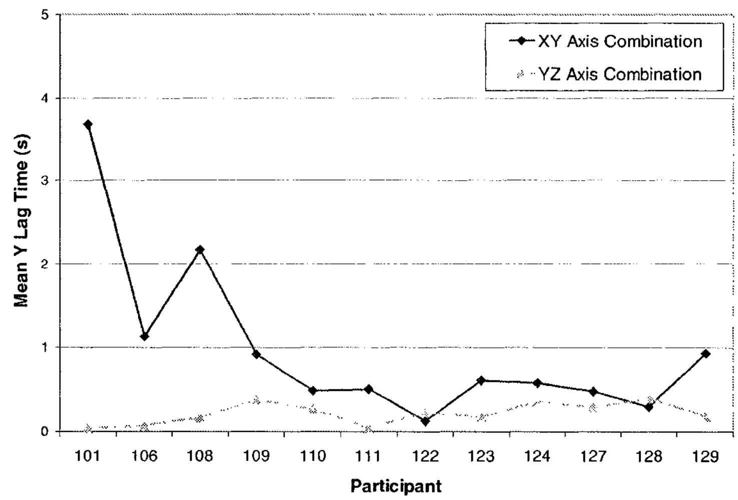

Figure 39. Mean Y Lag Time by Axis Combination and Participant.

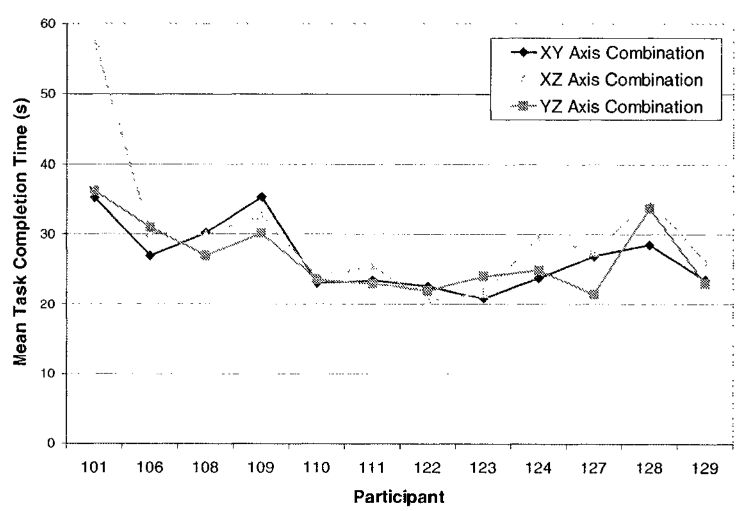

Figure 40. Mean Task Completion Time by Axis Combination and Participant.

Finally, a highly significant ***percent multi-axis control*** × ***axis combination*** interaction was found for the percent of time spent making X corrections ($F_{2,22} = 15.56$). As seen in Figure 41, when the task required 33.3% multi-axis control, X corrections took a greater percentage of time in the XY tasks than in the XZ tasks. However, the opposite trend was seen when the task required 66.7% or 100% multi-axis control: X corrections took a greater percentage of time in the XZ tasks than in the XY tasks.

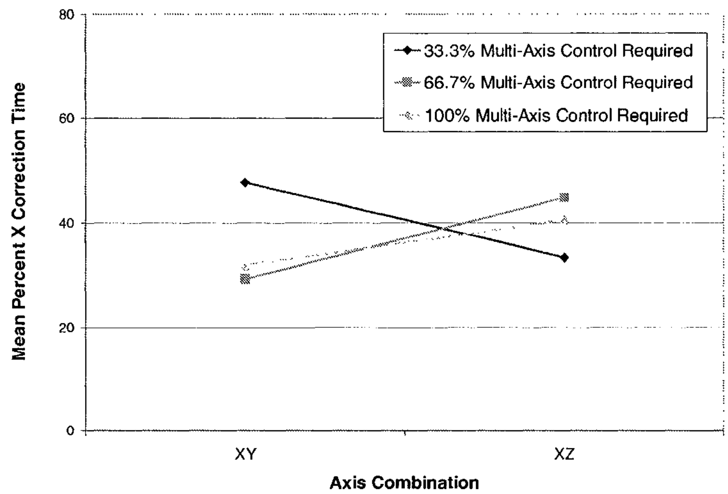

Figure 41. Mean Percent X Correction Time by Required Percent Multi-Axis and Axis Combination.

5.2.3 3-D Task ANOVA Results

The 23 performance metrics developed to represent critical aspects of multi-axis performance for the 3-D tasks were analyzed separately. Each ANOVA used the statistical model given in Equation 3 to test the effects of levels of the task variables (required percent of multi-axis control and limiting axis), replicate, and participant. A summary of the ANOVA results on the 3-D metrics is given in Table 22, where highly significant effects are highlighted.

Table 22. Summary of 3-D ANOVA Results.

	Model	map (A)	axs (B)	rep (C)	pid (D)	map*axs AB	map*rep AC	map*pid AD	axs*rep BC	axs*pid BD	rep*pid CD	ABC	ABD	ACD	BCD
p1a	.041		.036		< .0001		.038								
p2a	.001				.002	.028		.009		< .0001	.036		.041	.006	.017
p3a	< .0001			.036	< .0001					.006	.009				.038
pma	.000			.001	< .0001			.003		.035					.032
x1			.014	.050											
y1	.010				< .0001			.050		.005					.037
z1	.001				< .0001			.002							
tct	< .0001	.007		< .0001	< .0001			.001	.025				.006	.122	
xs				.005		.006		.018							
ys		.016		.001	.036		.021								
zs				.007											
xct	.006	.025	.022	.001	.004	.022		.002					.011		
yct	.034	.015		.000	.007			.018					.017		
zct			.034	.001											
xpc		.036	.007	.031	.034	.002									
ypc		.015			.049										
zpc			.005												
xa15	.005	.008	.024		< .0001	.036		.012							
ya15		.020	.002		.000	.008									
za15	.004		.003		< .0001										
xa30	.000	.023		.025	< .0001			.001		.049					
ya30	.002		.002		< .0001					.038					
za30	< .0001		.013		.000	.002				.006	.011				

The task variables (required percent multi-axis and limiting axis) failed to produce any highly significant effects. However, the levels of ***replicate*** produced significantly different task completion times ($F_{1,11}$ = 56.62). Specifically, the participants completed the second replicate significantly faster than the first. ***Participants*** differed significantly in use of single-axis control ($F_{11,22}$ = 9.36), use of triple-axis control ($F_{11,22}$ = 16.85), use of multi-axis control ($F_{11,22}$ = 19.70), Y lag time ($F_{11,22}$ = 6.62), Z lag time ($F_{11,22}$ = 24.72), task completion time ($F_{11,22}$ = 23.11), X accelerations > 15 cm/s^2 ($F_{11,22}$ = 9.79), Z accelerations > 15 cm/s^2 ($F_{11,22}$ = 15.98), X accelerations > 30 cm/s^2 ($F_{11,22}$ = 17.75), and Y accelerations > 30 cm/s^2 ($F_{11,22}$ = 14.56). The ***limiting axis*** × ***participant*** interaction significantly affected the percent of dual-axis control ($F_{22,22}$ = 5.61). As shown in Figure 42, the use of dual-axis control generally decreased as multi-axis requirements increased. However, the percent of dual-axis control increased in the tasks requiring 66.7% multi-axis control for participants 106, 111, 127, 128, and 129.

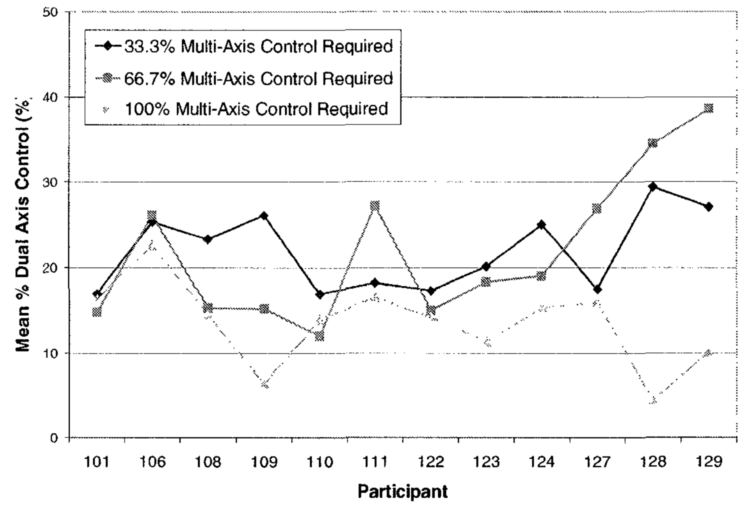

Figure 42. Mean Percent Dual-Axis Control by Required Percent Multi-Axis and Participant.

5.3 Metric Reduction

The results of the ANOVA analyses were combined with correlation analyses of the 1-D, 2-D, and 3-D performance metrics to reduce the number of metrics for the multivariate analyses. The methodology and results of this process are detailed in this section and illustrated using the reduction of the 1-D metric set as an example.

The first step in the reduction process was to eliminate all metrics that did not demonstrate highly significant differences among participants in the ANOVA results. Each of the remaining metrics was assigned a two-digit rank code in which the first digit represented the number of highly significant effects ($p < .0001$) and the second digit represented the number of effects that were significant at a Bonferroni alpha of .002. The Bonferroni method is used to adjust the original alpha level to control for Type I error [Hair, Anderson, Tatham, & Black, 1998]. The value is calculated by dividing the original alpha level by the total number of statistical tests being performed (in this case, .05/23 = .002). Hence, the rank was weighted to identify the metrics that were most responsive to differences between participants. The metrics were then sorted in descending order based on the rank code, as shown in Figure 43. When ranks were tied, the ranking of the best metric was based on the one with the highest percent standard error. This measure was chosen because it indicated large differences that might represent sensitivity to critical aspects of performance, and was acceptable since the metrics had already demonstrated sufficient power to discriminate among the variable levels.

1-D Metric	Rank	% StdError
V_Max	31	1.87
TCT	30	2.34
RO1T	20	3.95
RID	12	5.98
A_In	10	9.19
RIT	10	5.35
PRID	10	4.60
PRIT	10	4.17
PRO1T	10	3.10
R_Out_2	10	1.98
R_In	10	1.49

Matrix of 1D Correlations $\geq$ .60

	PRIT	PRID	PRO1T	RIT	RID	RO1T
PRIT		.94		.83	.73	
PRID	.94			.82	.75	
PRO1T						.76
RIT	.83	.82			.88	
RID	.73	.75		.88		
RO1T			.76			

KEY

Retained

Eliminated due to correlations

Figure 43. Illustration of the Reduction Process for the 1-D Metrics.

The reduction process began by retaining the highest ranked metric in the list. Hence, the 1-D metric V_Max was retained. Then, all metrics that were highly correlated ($r \geq .60$) with the retained metric were eliminated. In the 1-D example, retention of RO1T led to the elimination of PRO1T, and the retention of RID eliminated RIT, PRID, and PRIT. The reduction process continued in this manner until all metrics were retained or eliminated. The process resulted in the retention of seven 1–D metrics (V_Max, TCT, RO1T, RID, A_In, R_Out_2, and R_In), seven 2-D metrics (P1A, TCT, Z1, Y1, ZA>30, XA>30, and YA>15), and six 3-D metrics (TCT, P3A, XA>30, YA>30, Y1, and ZA>15).

As the 2-D and 3-D tasks were designed to measure multi-axis performance collectively, the data collected on these tasks were combined for the multivariate analysis. To achieve a reduced set of metrics that would best represent the combined set of multi-axis tasks, the highly significant 2-D and 3-D metrics were compared. As shown in Figure 44, TCT was retained for both 2-D and 3-D tasks, so it was included in the set of combined multi-axis metrics. Of the originally retained variables representing the use of multi-axis control, P1A was selected since it was highly significant in both 2-D and 3-D tasks (although it was eliminated from the 3-D metric set for being highly correlated with P3A). Due to the inability of multivariate procedures to account for missing or unbalanced data, metrics that measured aspects of performance along individual axes were combined to represent the measured aspect across all axes. For example, X, Y, and Z lag times were summed to create an overall lag time metric. Similarly, a combined metric was created to represent the overall number of accelerations greater than 30 cm/s^2. Therefore, TCT, P1A, LAG, and A>30 were selected as the dependent variables in the multivariate analysis to evaluate multi-axis performance.

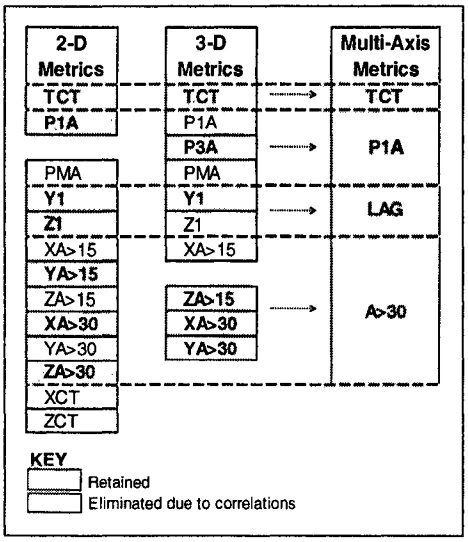

Figure 44. Combination of 2-D and 3-D Metrics to Form a Multi-Axis Metric Set.

5.4 MANOVA Results

The multivariate analyses were performed to evaluate the ability of the selected metrics to indicate differences in ramping performance and multi-axis performance. Seven metrics extracted from the 1-D tasks were included as the dependent variables in the model to assess ramping performance: V_Max, TCT, RO1T, RID, A_In, R_Out_2, and R_In. Four metrics from the 2-D and 3-D tasks were used to assess multi-axis performance: TCT, P1A, LAG, and A>30. The results of these analyses were used to examine differences in performance across all measures due to the task variables, replicates, and participants. Results are reported for all tests based on an alpha level of .05. To investigate any significant differences that were found by the MANOVA, the results of the univariate means comparisons were consulted. Canonical Variates Analysis (CVA) was also employed in an attempt to assess participant differences due to the simultaneous influence of all of the measures. This procedure creates new variables (i.e. canonical variates) from linear combinations of the metrics. The magnitude of the standardized canonical coefficient associated with each metric in a canonical variate equation represents the relative contribution of the metric to the variate [Johnson, 1998]. Additionally, mean comparison procedures were run on the canonical variates to investigate statistically significant group differences.

5.4.1 Results of the MANOVA on the Ramping Metrics

The statistical model given in Equation 1 was used to test the effects of the task variables (direction of motion, movement distance, and axis of motion), replicate, and participant on the selected set of seven ramping performance metrics. A summary of the

MANOVA results for the ramping metrics is given in Table 23, where significant effects are highlighted.

Table 23. Summary of MANOVA Results for the Ramping Metrics.

Metrics: **A_In, R_In, R_Out_2, V_Max, RID, RO1T, and TCT**

Factor	dir (A)	dis (B)	axs (C)	rep (D)	pid (E)	dir*dis AB	dir*axs AC	dir*rep AD	dir*pid AE	dis*axs BC
Wilks' Lambda *p*-value	.152	**<.0001**	.388	.548	**<.0001**	.651	.237	.794	.122	.214

Factor	dis*rep BD	dis*pid BE	axs*rep CD	axs*pid CE	rep*pid DE	ABC	ABD	ABE	ACD	ACE
Wilks' Lambda *p*-value	.106	**.001**	.122	**.041**	.056	.803	.563	.405	.562	.187

Factor	ADE	BCD	BCE	BDE	CDE	ABCD	ABCE	ABDE	ACDE	BCDE
Wilks' Lambda *p*-value	.674	.602	.773	.122	.411	.916	.125	.797	.206	.361

Direction of motion, axis of motion, and replicate did not significantly affect the ramping measures. However, significant main effects were found due to the levels of ***movement distance*** ($F_{7,5} = 333.02$) and ***participant*** ($F_{77,103.32} = 6.86$). Canonical variates analysis (CVA) was used to help investigate the significant group differences. The CVA produced a single canonical variate (CV1) for the test on the means of movement distance, indicating that the means were significantly different and resided in a one-dimensional subspace (i.e., the sample means fell along a line). The first canonical variate represents the linear combination of the metrics that provide the largest F statistic in an analysis of variance [Johnson, 1998]. The first canonical variate for the test of movement distance was given by

$$CV1_{distance} = -0.013\, A\_In - 7.625\, R\_In + 9.095\, R\_Out\_2 + 0.194\ \mathrm{V\_Max}$$
$$- 0.015\, RID - 0.717\, RO1T + 1.190\, TCT.$$

Interpretation of the variate is aided by examining the standardized canonical coefficients for the variate. The relative contribution (weight) of each metric to the canonical variate is given by the ratio of the magnitude of the standardized canonical coefficient for that metric to the sum of the coefficient magnitudes for all of the metrics. The weights of each metric in the first canonical variate for the distance means are given in Table 24. As shown, three metrics (TCT, RO1T, and R_Out_2) account for more than 75% of the variate value. Hence, $CV1_{distance}$ places heavier importance on task completion time, initial ramp-out time, and the R^2 value of the overall ramp-out when assessing differences in performance due to the levels of distance.

Table 24. Contribution of Ramping Metrics to the Distance Variate.

Metric	TCT	RO1T	R_Out_2	R_In	V_Max	RID	A_In
Contribution to $CV1_{distance}$	45.32%	17.13%	13.42%	9.35%	8.54%	4.18%	2.05%
Cumulative	**45.32%**	**62.45%**	**75.87%**	**85.22%**	**93.76%**	**97.95%**	**100%**

An examination of the results of the univariate means comparisons was performed to further clarify the differences between the levels of movement distance. Figure 45 shows a plot of the individual means at the 1m and 3m distances for the first canonical variate (CV1) and each of the seven metrics along with the 95% significance range for each item. Significant differences between the levels of movement distance are indicated when the significance ranges of the metric do not overlap. As shown, the means of the ramping metrics for the 3 m tasks were always larger than for the 1 m tasks. This difference was significant for all metrics except for the mean R^2 for ramp-in (R_In).

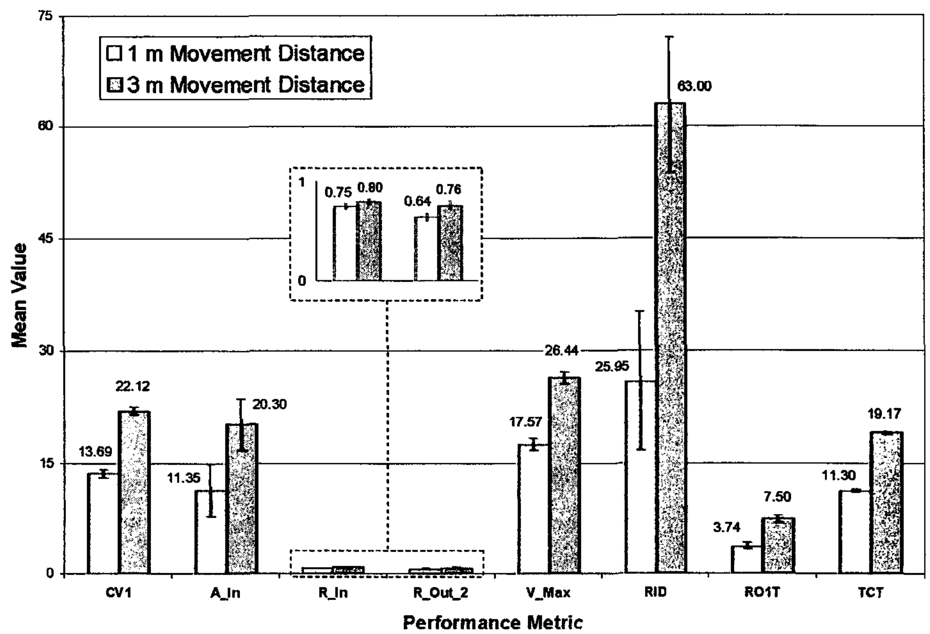

Figure 45. Mean Values of Ramping Performance Metrics by Movement Distance.

The CVA for the test on the participant means produced four canonical variates, indicating that the means for participants were significantly different and resided in a four-dimensional subspace. The first canonical variate, given by the equation

$$CV1_{participant} = -0.002\,A\_In - 2.586\,R\_In + 0.123\,R\_Out\_2 + 0.372\ \mathrm{V\_Max}$$
$$-\,0.006\,RID - 0.142\,RO1T - 0.107\,TCT,$$

accounted for 67% of the total variation among participants. The second, third, and fourth canonical variates accounted for an additional 14%, 9%, and 4% of the variation, respectively. While the canonical variates provide a measure of participant performance across all metrics, interpretation is much more complex in the four-dimensional case. Each variate provides a unique weighting of the metrics that accounts for an increasingly smaller proportion of the total variation between the participants. Unfortunately, it is very difficult to determine the values of the variates that represent desirable vs.

undesirable performance. Hence, in order to derive a meaningful classification of the performance of the participants across all metrics, a methodology was devised to combine the results of the univariate means comparison tests with the CVA results. The application of the participant classification methodology is demonstrated below with respect to ramping performance.

Initially, the univariate means for each participant on each of the metrics were sorted from "best" to "worst" based on an assumption of desirable performance for the measure. The assumption of optimal performance and the corresponding sorting scheme for each of the ramping metrics are shown in Table 25.

Table 25. Optimality Criteria for Sorting the Univariate Ramping Metric Means.

Metric	Assumed Optimal	Sorting Scheme
TCT	Low	Low to High
R_Out_2	High	High to Low
R_In	High	High to Low
V_Max	Average	Smallest to largest difference from the mean
RO1T	Average	Smallest to largest difference from the mean
A_In	Average	Smallest to largest difference from the mean
RID	Average	Smallest to largest difference from the mean

Each of the means was then standardized to account for unit and magnitude differences. The participants' performance on the individual metrics was classified (from very poor to very good) with guidance from the results of the Ryan's univariate means comparison test. This initial classification was made to obtain a more comprehensive understanding of individual differences in performance. To arrive at a classification of the participant's performance across all metrics, the weights of the four canonical variates and the average weight across the variates (shown in Table 26) were applied to the standardized mean scores. For the ramping data, this step resulted in five sets (7 metrics

$\times$ 12 participants) of weighted scores obtained with CV1, CV2, CV3, and CV4 weights, and AVG (the average of the weights).

Table 26. Canonical Weights Applied to Participant Ramping Means.

	Ramping Metrics						
Weights	**V_Max**	**TCT**	**RO1T**	**A_In**	**R_In**	**R_Out_2**	**RID**
CV1	0.56	0.14	0.11	0.01	0.11	0.01	0.06
CV2	0.20	0.29	0.20	0.01	0.16	0.08	0.07
CV3	0.26	0.28	0.18	0.03	0.06	0.05	0.15
CV4	0.21	0.37	0.07	0.24	0.02	0.06	0.03
AVG	**0.31**	**0.27**	**0.14**	**0.07**	**0.08**	**0.05**	**0.07**

A single performance score for each participant was obtained through a linear combination of the weighted scores in each CV set across all seven metrics. To ensure that the most desirable performance would be indicated by lower values, R_In and R_Out_2 were subtracted from the sum of the other five metrics. For example, each participant's performance score based on the CV1 weights was given by

$$CV1\ Score = 0.56\ V\_Max + 0.14\ TCT + 0.11\ RO1T + 0.01\ A\_In - 0.11\ R\_In$$
$$- 0.01\ R\_Out\_2 + 0.06\ RID.$$

The participants were then sorted on each of the five sets of CV scores such that the lowest sum represented the best performer of the group. While the rankings for each of the five weighting schemes were considered, the weights of the first canonical variate provided the ranking that best matched the subjective evaluation of the participants' performance. A brief synopsis of the subjective evaluation made by the experimenters through real-time observation of the participants during testing and inspection of the performance plots is included in Appendix I. The final classification of the participants was based on the 95% confidence level of the CV1 scores. This level was given by the equation

$$95\%\ \text{Confidence Level (CL)} = t_{\alpha,n-1}\frac{s}{\sqrt{n}}.$$

The performance classifications fall within the ranges designated by ±1, ±2, and ±3 times the CL from the mean of the CV1 scores (which is zero due to standardization). Table 27 displays the participant classifications for the ramping performance based on the 95% confidence level of the CV1 scores.

Table 27. Classification of Participant Ramping Performance.

95% Confidence Level Boundaries	CL Range	CV1 Score	Participant	Classification
- 0.94	< - 2 (< - 0.94)	-1.15	128	Very Good
- 0.47	- 1 to - 2 (- 0.47 to - 0.94)	- 0.69 - 0.55 - 0.54	129 122 124	Good
0.47	+ 1 to - 1 (0.47 to - 0.47)	- 0.30 - 0.25 - 0.13 0.34	127 109 123 111	Fair
0.94	+ 1 to + 2 (0.47 to 0.94)	0.48 0.63 0.64	110 108 101	Poor
	> + 2 (> 0.94)	1.52	106	Very Poor

To investigate the soundness of the methodology, a comparison was made between the classifications obtained with the CV1 scores and the distribution of the participants based on the Ryan's comparison of the maximum velocity means, since maximum velocity accounted for 56% of the CV1 score. Figure 46 displays the mean maximum velocity for each participant on the 1 m and 3 m tasks, the difference of the 1 m and 3 m means, and the grand mean across all task distances. The results of the Ryan's means comparison procedure (MCP) on the grand mean are represented by the system of horizontal lines, such that the means above each horizontal line are not significantly different. For example, the Ryan's test found no significant difference in the means for participants 108, 101, and 106, but indicated that these three participants had significantly lower mean maximum velocities than all of the other participants. As mentioned previously, the criteria for optimal performance on the maximum velocity measure was assumed to be the average across all participants ($\mu = 21.99$). Participant 128 was closest to this optimal, and appropriately received a classification of "very good." Note that the performance classifications get progressively worse as the mean maximum velocity gets farther away from the optimal value. Hence, it appears that the classification methodology produced a reasonable assessment of the participants' ramping performance with respect to mean maximum velocity.

	Maximum Velocity Means											
3 m Distance	30.00	29.74	29.04	30.00	30.00	26.78	26.82	27.76	26.63	20.68	20.70	19.09
1 m Distance	24.81	23.11	20.63	19.11	18.95	20.21	17.06	15.35	14.48	13.67	13.06	10.37
Mean Difference	5.19	6.63	8.41	10.89	11.05	6.57	9.76	12.41	12.15	7.01	7.64	8.72
Grand Mean	27.41	26.42	24.84	24.56	24.47	23.49	21.84	21.56	20.56	17.17	16.88	14.73
Participant	110	111	123	127	122	124	128	129	109	108	101	106

Ryan's MCP Results

Classification	poor	fair	fair	fair	good	good	very good	good	fair	poor	poor	very poor

Figure 46. Comparison of Classifications with Respect to Maximum Velocities.

Significant differences in the ramping metrics were also indicated for the interactions of ***movement distance*** × ***participant*** ($F_{77,103.32} = 1.91$) and ***limiting axis*** ×

participant ($F_{154,118.34} = 1.36$). The significant distance × participant interaction was driven by differences in the means of the metrics R_Out_2 and V_Max. Specifically, four of the twelve participants showed a greatly increased R^2 on the overall ramp-out when performing the 3 m distance tasks, as shown in Figure 47. Similarly, the large differences between the means of maximum velocity of the 1 m and 3 m tasks for participants 109, 122, 127, 128 and 129 given in Figure 46 are also illustrated in Figure 47. These five participants showed a marked increase in maximum velocity on the 3 m tasks. The significant limiting axis × participant interaction was due to differences in the mean V_Max and TCT among participants (Figure 48).

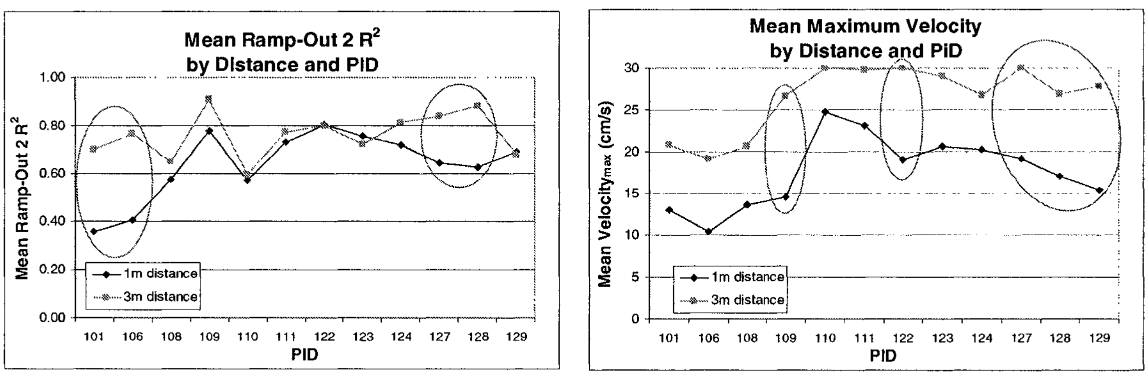

Figure 47. Significant Interactions of Movement Distance × Participant.

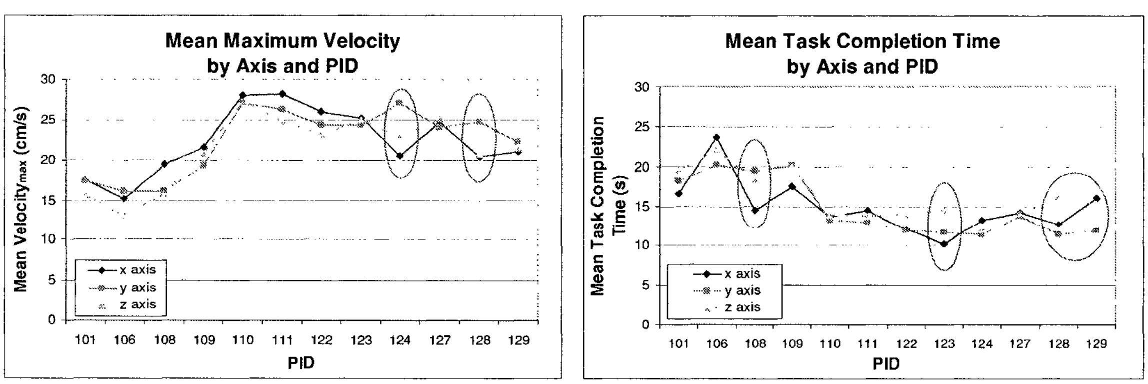

Figure 48. Significant Interactions of Limiting Axis × Participant.

5.4.2 Results of the MANOVA on the Multi-Axis Metrics

A multivariate analysis of variance was performed to test the effects of the task variables (required percent of multi-axis control and limiting axis), replicate, and participant on the four multi-axis performance metrics (percent of single-axis control, lag time, task completion time, and number of accelerations greater than 30 cm/s^2). The statistical model used in the multi-axis MANOVA was given in Equation 3. A summary of the MANOVA results on the multi-axis metrics is given in Table 28, where significant effects are highlighted.

Table 28. Summary of MANOVA Results for the Multi-Axis Metrics.

Metrics: **P1A, LAG, TCT, and A30**

Factor	map (A)	axs (B)	rep (C)	pid (D)	map*axs AB	map*rep AC	map*pid AD	axs*rep BC	axs*pid BD	rep*pid CD	ABC	ABD	ACD	BCD
Wilks' Lambda *p*-value	.000	.143	<.0001	<.0001	.097	.110	.463	.035	.290	.490	.782	.980	.997	.787

Significant main effects were found due to the levels of required ***percent of multi-axis control*** ($F_{4,8}$ = 22.63), ***replicate*** ($F_{4,8}$ = 35.87), and ***participant*** ($F_{44,1727.4}$ = 19.85). The multi-axis measures did not vary significantly due to the levels of limiting axis. The CVA produced a single canonical variate for the test on the means of required percent of multi-axis control, given by

$$CV1_{\%\ multi\text{-}axis} = 0.183\ P1A - 0.007\ LAG + 0.006\ TCT - 0.022\ A{>}30.$$

The weights of each metric in the first canonical variate are given in Table 29. As shown, P1A accounts for more than 86% of the variate value. Hence, $CV1_{\%\ \mathrm{multi\text{-}axis}}$ places heavier importance on the percent of single-axis control when assessing differences in performance due to the levels of required percent of multi-axis control.

Table 29. Contribution of Multi-Axis Metrics to the % Multi-Axis Variate.

Metric	P1A	A>30	TCT	LAG
Contribution to $CV1_{\% \text{ multi-axis}}$	86.46%	9.49%	2.80%	1.25%
Cumulative	**86.46%**	**95.95%**	**98.75%**	**100.00%**

The results of the univariate means comparisons were examined to investigate the significant differences found between the levels of required percent multi-axis control and replicate. Figure 49 shows a plot of the individual means for the tasks requiring 33.3%, 66.7%, and 100% multi-axis control for the first canonical variate (CV1) and for each of the four metrics along with the 95% significance range for each item.

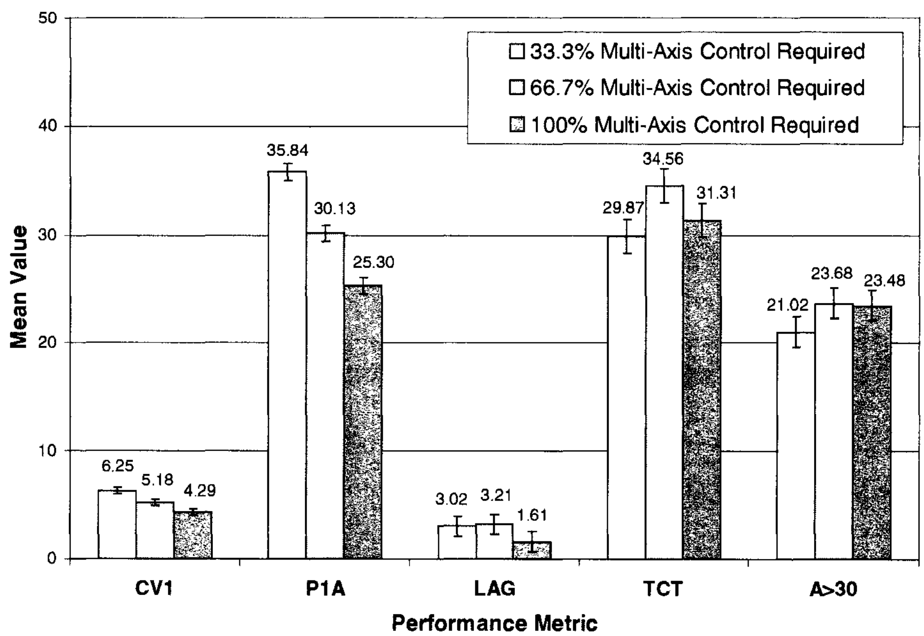

Figure 49. Mean Values of Multi-Axis Metrics by Required % Multi-Axis Control.

As expected, the trends in CV1 and P1A are similar. Appropriately, the use of single-axis control dropped significantly as the required percent of multi-axis control increased. However, the mean percent of single-axis control for the 100% multi-axis tasks is a direct indication of the inefficiency with which the participants performed those tasks. Lag times were longest in the tasks requiring 66.7% multi-axis control, and shortest in the tasks requiring 100% multi-axis control, although the differences in lag times were not significantly affected by the required percent of multi-axis control. Task completion times for the tasks requiring 66.7% multi-axis control were significantly longer than for all other tasks. While the task completion times for the 33.3% and 100% tasks were not significantly different, the 100% tasks took longer to complete. Theoretically, all tasks could be completed within the same amount of time. Therefore, it appears that as participants were required to use more multi-axis control, completion times suffered. The mean number of accelerations > 30 cm/s^2 did not vary significantly due to the required percent of multi-axis control.

The CVA produced a single canonical variate for the test on the replicate means, given by

$$CV1_{replicate} = -0.028\, P1A - 0.898\, LAG + 0.377\, TCT + 0.005\, A{>}30.$$

The weights of each metric in the first canonical variate are given in Table 30. As shown, LAG and TCT account for nearly 96% of the variate value. Hence, $CV1_{replicate}$ places heavier importance on the mean lag time and task completion time when assessing differences in performance due to the levels of replicate.

Table 30. Contribution of Multi-Axis Metrics to the Replicate Variate.

Metric	LAG	TCT	P1A	A>30
Contribution to $CV1_{replicate}$	48.33%	47.33%	3.78%	0.56%
Cumulative	**48.33%**	**95.66%**	**99.44%**	**100.00%**

Figure 50 shows a plot of the individual means of replicates A and B for CV1 and for each of the four metrics along with the 95% significance range for each item. Across all metrics, mean values were higher for replicate A, although these differences were not significant for LAG or A>30. Participants used significantly less single-axis control and managed to complete the task significantly faster during the second test session than during the first. This could be indicative of skill acquisition.

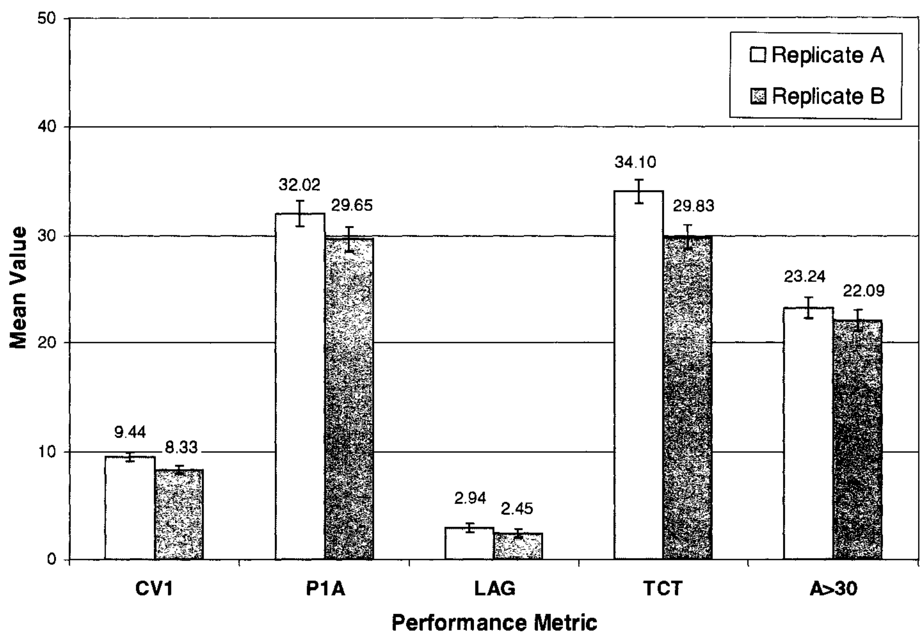

Figure 50. Mean Values of Multi-Axis Metrics by Replicate.

The CVA for the test on the participant means across all four multi-axis metrics produced four canonical variates, indicating that the means for participants were significantly different and resided in a four-dimensional subspace. The first canonical variate, given by

$$CV1_{participant} = 0.010\ P1A - 0.016\ LAG + 0.080\ TCT - 0.101\ A{>}30,$$

accounted for nearly 77% of the total variation between participants. The second, third, and fourth canonical variates accounted for an additional 18%, 3%, and 2% of the variation, respectively. The contributions of the metrics to each of the canonical variates and the average contribution across all variates are shown in Table 31.

Table 31. Canonical Weights Applied to Participant Multi-Axis Means.

	Multi-Axis Metrics			
Weights	**P1A**	**LAG**	**TCT**	**A>30**
CV1	0.06	0.03	0.40	0.51
CV2	0.34	0.36	0.19	0.11
CV3	0.32	0.01	0.42	0.25
CV4	0.32	0.43	0.20	0.04
AVG	**0.26**	**0.21**	**0.30**	**0.23**

As shown, two metrics (TCT and A>30) account for 91% of the CV1 value. Hence, $CV1_{participant}$ places heavier importance on task completion time and the number of accelerations exceeding 30 cm/s^2 when assessing differences in performance among participants.

The methodology described in the previous section was used to classify the participants with respect to multi-axis performance. Optimal performance was assumed to produce low values of P1A, LAG, TCT, and A>30. Therefore, the univariate participant means on all metrics were sorted from low to high, where low values represented better performance. Each of the means was then standardized and participants' performance on the individual metrics was classified (from very poor to very good) with guidance from the results of the Ryan's univariate means comparison test. The weights of the four canonical variates and the average weight across the variates (Table 33) were applied to the standardized mean scores of each metric. A single performance score for each participant was obtained by summing the weighted scores in each CV set across all four multi-axis metrics. The participants were then sorted on each of the five sets of CV scores such that the lowest sum represented the best performer of the group. As with the classification of participants on ramping performance, the weights of the first canonical variate provided the ranking that best matched the subjective evaluation of the participants' multi-axis performance (Appendix I). Therefore, the final classification of the participants was based on the 95% confidence level of the CV1 scores (Table 32).

Table 32. Classification of Participant Multi-Axis Performance.

95% Confidence Level Boundaries	CL Range	CV1 Score	Participant	Classification
- 0.64	< - 2 (< - 0.64)	-0.74 -0.64	122 109	Very Good
- 0.32	- 1 to - 2 (- 0.32 to - 0.64)	- 0.43	127	Good
0.32	+ 1 to - 1 (0.32 to - 0.32)	- 0.27 - 0.25 - 0.18 0.08 0.25	128 129 106 124 111	Fair
0.64	+ 1 to + 2 (0.32 to 0.64)	0.34 0.40 0.55	108 110 123	Poor
	> + 2 (> 0.64)	0.90	101	Very Poor

Significant differences in the multi-axis metrics were also indicated for the ***limiting axis*** × ***replicate*** interaction ($F_{8,38} = 2.38$). The significant axis × replicate interaction was driven by differences in the means of the metrics TCT and A>30. While task completion times were longer across all axes for replicate A, completion times improved much more during replicate B in tasks where X and Y were the limiting axes

(Figure 51). Differences in the mean number of accelerations > 30 cm/s^2 for replicates A and B are also shown in Figure 51. Specifically, during the first replicate the mean number of accelerations > 30 cm/s^2 was higher when X was the limiting axis and when the task required 100% multi-axis, while the number was fairly constant for all tasks during replicate B. This might also be seen as an improvement in the skill of the operators.

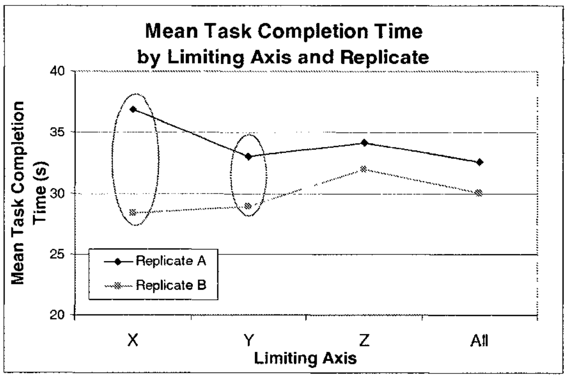

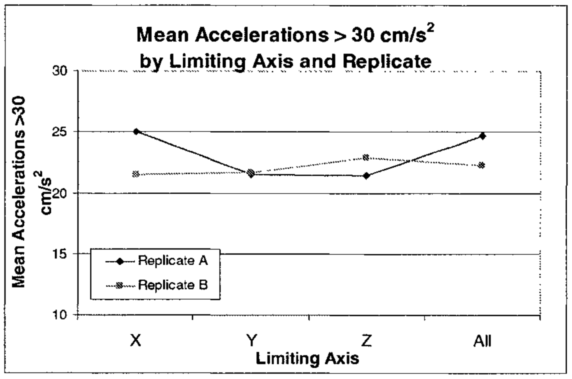

Figure 51. Significant Interactions of Limiting Axis × Replicate.

CHAPTER 6

CONCLUSIONS AND RECOMMENDATIONS

6.1 Summary

This dissertation served as the initial investigation into the development of objective metrics to assess the performance of NASA RMS operators. The overall objective of this research was to define the methodology for the development and validation of the metrics, to identify a select subset of measures that are highly sensitive to the factors that affect RMS performance, and to extract and validate the selected performance metrics from the BORIS simulation. The development and documentation of the methodology described herein constitutes a major contribution of the dissertation. In addition to achieving a successful validation of the methodology, the performance data collected during the empirical study were invaluable as they established the existing database of objective RMS performance measures.

This dissertation also succeeded in the development and validation of a set of performance metrics to evaluate smooth hand controller inputs, multi-axis commanding, and speed and accuracy associated with targeted movements of the BORIS robotic arm. The metric development was accomplished by investigating the critical aspects of performance on a typical RMS task. Two aspects of performance were selected that required several critical skills identified in the NASA GRT evaluation: smooth hand controller inputs (ramping) and multi-axis commanding. The input patterns of novice operators were examined to identify performance characteristics that might differentiate operator skill. In addition, comparisons were made between the observed control patterns and theoretical models that were developed to represent expert performance. Performance metrics were then selected that quantified the differences observed in the performance patterns. Each of the metrics was evaluated for its sensitivity to differences in participants and task characteristics in an empirical study. The metric reduction methodology succeeded in isolating a manageable subset of performance metrics that exhibited high variability yet were sensitive to differences among operators and task variables. The results of the study were presented in the previous chapter. This chapter discusses the implications of those results, and suggests recommendations for future study.

6.2 Evaluation of Ramping Performance

The reviewed literature identified visual/spatial perception, situation awareness, and psychomotor control as critical human factors abilities associated with good RMS control. Morphew et al. [2001] suggested that the most challenging aspect of RMS operation was the translation of environmental cues into hand controller inputs. Hence, the experiment sought to elicit these critical aspects in tasks designed to assess smooth hand controller inputs and multi-axis commanding. Smooth hand controller inputs were assessed by targeted movement tasks that additionally allowed assessment of speed, accuracy, and the effects of task characteristics such as target distance, direction of movement, and axis of movement. These ramping tasks required visual/spatial perception and psychomotor control. The need for situation awareness was generally controlled in the experimental tasks, however the ability of the operator to project the future system status was reflected in measures of accuracy. The target was often off-screen, so that the participant had to note the location mentally and update this information visually as the task progressed. This appeared to be problematic at times, as evidenced by hesitant arm movements and memory lapses regarding the target location, which increased task completion time.

One of the questions investigated in this research was the extent to which operators plan and control the ramp-out in advance of approaching the target. It was hypothesized that target distance would significantly affect the ability of the operator to plan and control the ramping task, and the tasks with 1 m target distances would be more cognitively demanding and would allow less time for information processing, planning, and implementation. Results of the ramping tasks confirmed that ramping performance varied significantly due to target distance and participant. Figure 52 is a graphic depiction of the average ramping performance observed for the1 m target distances, the 3 m target distances, and across both task distances. The shape of the plots was determined by the mean ramp-in and ramp-out accelerations, the mean maximum velocities, and the mean correction and task completion times. However, mean travel times are not accurately scaled on the graphs. The mean travel times were 2.44 s for the 1 m tasks, 5.20 s for the 3 m tasks, and 3.82 s across both task distances.

It was hypothesized that the ramp-out would be consistent with the ramp-in if it were accurately planned and controlled by the operator. However, the study participants generally exhibited inconsistent behavior between ramp-in and ramp-out. As shown, ramp-out decelerations were less than 50% the magnitude of the ramp-in accelerations for the 3 m task. Additionally, participants tended to ramp-in more quickly and ramp-out more slowly on the tasks with target distances of 3 m in comparison with the 1 m tasks. The differences in accelerations between the ramp-in and ramp-out may indicate a lack of

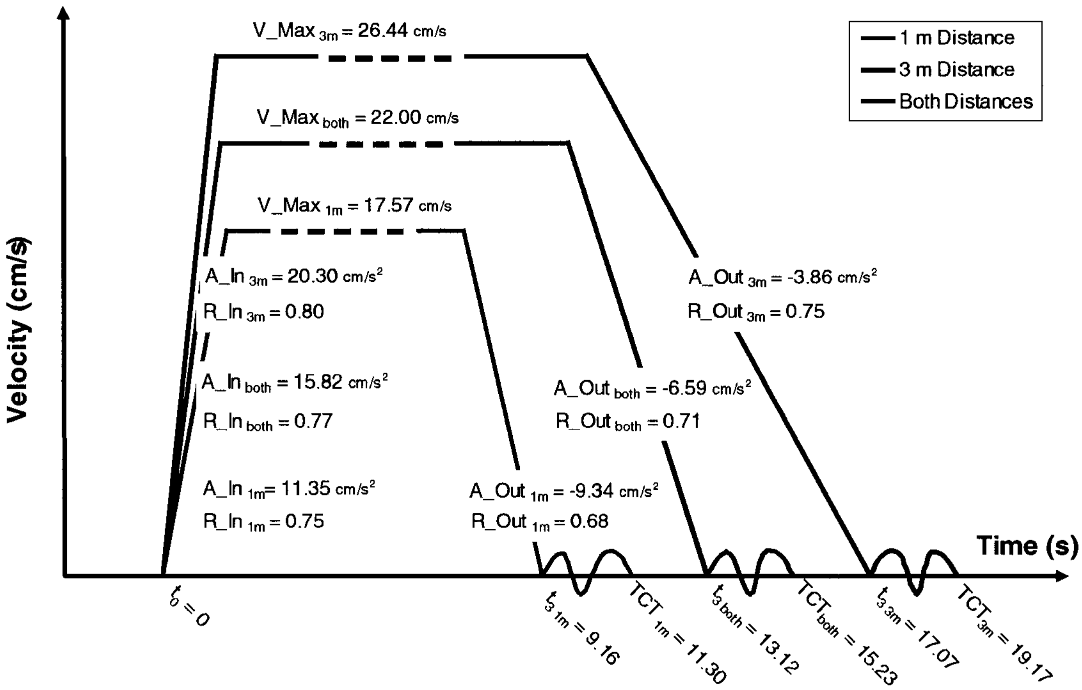

Figure 52. Comparison of Ramping Inputs by Task Distance.

skill or planning, suggesting that the deceleration was dictated by the upcoming target rather than planned by the operator. However, these differences may be due in part to an inherent difference in the ramp-in and ramp-out task; the ramp-in is hypothesized to be a more consciously-guided open-loop task, while the ramp-out may be a less-planned closed-loop task. Hence, further investigation is needed to confirm the actual cause of the differences between ramp-in and ramp-out performance.

The smoothness of the commands, as indicated by the R^2 values, was generally lower during ramp-out and were higher for the 3 m tasks than for the 1 m tasks. Regardless of distance, task correction times averaged about 2.1 seconds. Therefore, the accuracy of the initial target approach did not appear to be significantly affected by target distance. However, task completion times were significantly different due to target distance. The longer distance task allowed participants to achieve higher maximum velocities. Aside from the obvious dependence of movement times on rates and distances, the mean ramp-out absorbed 26% more time than the ramp-in for the 1 m tasks, 72% more time than the ramp-in for the 3 m tasks, and 53% more time than the ramp-in across all distances. The large ramp-out time for the 3 m tasks suggests that the differences in task completion time may be partly attributed to operator strategy rather than necessitated by the task. In all cases, the ramp-in appears to be assigned lower priority than the ramp-out.

6.3 Evaluation of Multi-Axis Performance

Multi-axis commanding was assessed by targeted movement tasks that were designed to require simultaneous movements along two or three axes. The multi-axis metrics also assessed speed, accuracy of initial approach, and the effects of task characteristics such as the ratio of task distances (required percent of multi-axis control) and the limiting axis. These multi-axis tasks required visual/spatial perception, psychomotor control, and situation awareness. In particular, the 3-D tasks required the operator to look at separate monitors to locate the target coordinates and to predict when the target would be acquired based on the current location and closing rate of the POR. Therefore, situation awareness was reflected in measures of accuracy. As with the ramping tasks, the target was often off-screen, so that the participant had to note the location mentally and update this information visually as the task progressed.

2-D task performance was affected by differences among participants and by the distance ratios that determined the required percent of multi-axis control. Task difficulty increased as the required percent of multi-axis control increased. The difficulty in controlling two axes simultaneously for longer periods of time resulted in longer completion times. Performance differences on the XZ tasks (increased correction times and task completion times) may be attributed to lower compatibility in the control-display mapping. Due to the physical definition of the 3-D VEGA environment, the XZ tasks were mapped on the starboard wall, while all other 1-D and 2-D tasks were mapped on the VEGA floor. Control movements in this plane were less intuitive, since X commands (pushing or pulling on the control knob) were displayed as horizontal movements (to the left or right). In all other tasks, the participant moved the knob to the left to move left, and to the right to move right.

The task requiring 100% multi-axis control was designed to investigate the ability of the operators to control straight-line motion (Strategy 2) in three-dimensional space. While participants were generally capable of simultaneously commanding two axes with reasonable effort, simultaneous control of three axes was not well managed. Participants tended to allocate attention to the target displayed in Monitor 3 (XY coordinates), and finished the task by moving to the Z target elevation (displayed in Monitor 1). This pattern of behavior was evidenced by the high lag times and correction times for the Z-axis inputs and the increased use of single-axis control for the 3-D tasks. The BORIS display setup used in the experiment may have contributed to these results. Participants appeared to have trouble scanning between the monitors for the 3-D visual cues. Hence, degraded performance in the 3-D tasks may be partially due to a lack of situation awareness. Monitor 3 provided a much larger view and a more defined target than Monitor 1. Additionally, the target information provided by Monitor 1 was only utilized on the seven 3-D tasks (out of the 37 total tasks presented during testing). Therefore, the operators were less accustomed to allocating attention to this monitor.

To investigate the control strategies from a human factors perspective, comparisons were made between the hypothesized and observed patterns of input. A preliminary hypothesis presented in this dissertation was that minimizing the number of axes simultaneously commanded reduces cognitive workload and the potential for error. Masliah and Milgram [2000] also noted a tendency for operators to try to simplify the task by limiting the number of axes controlled simultaneously. As hypothesized, this strategy may allow the operator to complete the task with greater accuracy. Support for this theory is provided by comparing the percentage of single-axis control with the task completion times in Figure 49. Participants could use up to 33.3% single-axis control and complete the tasks requiring 66.7% multi-axis control without a loss of efficiency. However, the percentage of single-axis control on the tasks requiring 100% multi-axis control directly represents inefficiency that would result in increased task completion times. Although participants averaged an acceptable 30% single-axis control on the tasks requiring 66.7%, and a highly unacceptable 25% single-axis control on the tasks requiring 100%, the average task completion time for the 66.7% tasks was significantly longer (34.6 s vs. 31.3 s) than that for the 100% tasks. This implies that the strategic use of single-axis control may have reduced the task complexity enough to allow completion of the task in a shorter time.

Corrections typically contributed to the percentage of single-axis control, since the majority of corrections were made one-axis-at-a-time. In most instances, the loss in time resulting from the use of single-axis control was compensated by the increase in accuracy. When participants attempted to complete the task using multi-axis commands, the target was often overshot. Participants who got close and then made final single-axis adjustments could complete the task as quickly or quicker than participants who used multi-axis adjustments. In summary, while multi-axis commanding is desirable to reduce arm oscillations and increase efficiency, it imposes a greater workload on the participant and may even be detrimental to translational accuracies. Conversely, while this strategy is acceptable for translational movements, tasks that require both position and orientation adjustments (such as aligning the POR for grappling) are much more difficult when inputting single-axis commands. One measure of operator skill may be the extent to which the operator can adjust to differences in the task demands and make appropriate choices regarding the use of multi-axis commanding.

The selected multi-axis metrics were sensitive to changes over time that could indicate skill acquisition. Task completion times and the use of single-axis control decreased significantly, lag times were shorter, and the number of excessive accelerations decreased from replicate A to replicate B. This implies improved control and increased accuracy on the tasks. The highest accuracy (lowest correction time) was achieved for movements along the Y-axis. Z-axis accuracy was obviously lowest, since participants typically delayed these movements until the end of the task. However, X-axis accuracy might have been affected by inherent differences in the mechanical design of the THC. X-axis inputs were made by pushing or pulling on the controller knob, while Y- and Z-axis inputs were made by deflecting the knob to the left and right or up and down. This necessitated a different grip on the knob. Additionally, the travel distance of the knob was shorter along the X-axis such that a deflection in X produced a movement of greater velocity than the same deflection in Y or Z.

Task completion time proved to be sensitive to performance differences in both the ramping and multi-axis tasks. Completion time was significantly affected by differences in target distance, participants, and replicate. This metric played a prominent role in classification of the participants with respect to both ramping and multi-axis performance. The resulting classifications were successful in providing a reasonable classification of RMS operator performance as very poor, poor, fair, good, or very good. These five classes may be comparable to the current five-point evaluation scale employed by the NASA GRT instructors.

Further research using a broader range of performers should help verify the utility of the performance metrics developed in this study. While the specific results are valid for the group of novice operators utilized in this study, great caution should be used in applying these conclusions to other operators. However, the experimental methodology developed herein represents a major contribution, and should be useful in the acquisition of expert data that is critical to the establishment of the criteria that separate the levels of performance.

6.4 Recommendations

As mentioned, verification of the utility of the metrics will require an examination of the performance of operators who possess a broader range of skills. While the data collected in this research were useful in evaluating the sensitivity of the proposed metrics, they provided insufficient information to truly differentiate "good" performance from "poor" performance. The operator classification was made relative to the performance of the twelve novice operators tested in this study. Expert data are needed to determine the true parameters of skilled performance. Only then can one see where these particular operators fall along the broader performance spectrum. Use of the expert data can determine the appropriate criteria for optimality to be used when sorting participants based on performance. The operator classification should also be verified by comparison against the subjective GRT evaluation. The "very good" to "very poor" performance classifications might easily be converted to facilitate comparison to the five-point rating scale utilized by the GRT evaluation.

Future studies should apply the complete methodology to the testing of any subsequent participants, as the proposed metrics may be differentially affected by skill level. It is anticipated that "expert" data may exhibit much less variability and might be characterized by different aspects than those that characterized the novice performance.

While the 1-D tasks sufficiently isolated ramping performance, an attempt should be made to provide a more realistic task to evaluate multi-axis performance. The results of this study were constrained by controls needed to allow testing of the experimental hypotheses. The tasks would be greatly improved by providing the operator with a clear and unambiguous target in 3-D space. However, selection of optimal camera views is essential to provide sufficient visual cues. Ultimately, the methodology should be extended to include rotational motion. Additional RMS performance metrics should be developed that evaluate the ability of operators to control 6-DOF movements.

REFERENCES

Belanger, F., Jaar, G., & Cyril, X. (2000). The Canadian space robotics operations and training simulator. *Canadian Aeronautics and Space Journal*, *46*(2), 100-105.

Bloomer, E.C. (2001). *International Space Station Robotic Overview Training Manual (Robotic OV C 21002).* Document No. TD0102. Houston, TX: National Aeronautics and Space Administration, Johnson Space Center.

Canadian Space Agency (CSA). (1999). *SSRMS Success Stories.* Retrieved May 21, 2002 from http://www.space.gc.ca/space/apogee/1999/fall_en/areas/success_stories.htm.

Eddy, D.R., Schiflett, S.G., Schlegel, R.E., & Shehab, R.L. (1998). Cognitive performance aboard the Life and Microgravity Spacelab. *Acta Astronautica*, *43*(3-6), 193-210.

Endsley, M.R. (1995a). Measurement of situation awareness in dynamic systems. *Human Factors*, *37*(1), 65-84.

Endsley, M.R. (1995b). Toward a theory of situation awareness in dynamic systems. *Human Factors*, *37*(1), 32-64.

Gilliland, K., & Schlegel, R.E. (1993). *Readiness to Perform Testing: A Critical Analysis of the Concept and Current Practices* (Final Report DOT/FAA/AM-93-13). Washington, DC: Office of Aviation Medicine, Federal Aviation Administration.

Gilliland, K., Schlegel, R.E., & Nesthus, T.E. (1999). *Effects of Antihistamine, Age, and Gender on Task Performance* (Final Report DOT/FAA/AM-99/20). Washington, DC: Office of Aviation Medicine, Federal Aviation Administration.

Goonetilleke, R.S., Drury, C.G., & Sharit, J. (1995). Evaluation of control strategies in a complex space-vehicle control task: Effects of training type. *Advances in Human Factors / Ergonomics*, *20*(B), 311-316.

Hair, J.F., Anderson, R.E., Tatham, R.L., & Black, W.C. (1998). *Multivariate data analysis (5th ed.).* Upper Saddle River, NJ: Prentice Hall, Inc.

Institute of Electrical and Electronics Engineers (IEEE). (2001). *The Shuttle Remote Manipulator System – The Canadarm.* Retrieved November 12, 2001 from http://www.ieee.ca/millennium/canadarm/canadarm_technical.html

Johnson, D.E. (1998). *Applied multivariate methods for data analysts.* Pacific Grove, CA: Brooks/Cole Publishing Company.

Kane, R.L., & Kay, G.G. (1992). Computerized assessment in neuropsychology: A review of tests and test batteries. *Neuropsychology Review*, *3*, 1-118.

Khoury, G.J., Morphew, M.E., & Balmer, D.V. (1999). *Remote Manipulator System Critical Task Inventory for Self-monitoring Performance Tool Pilot Study* (Report No. HSYS-REP-0005). Houston, TX: Johnson Engineering.

Kim, W.S. (1993). Graphical operator interface for space telerobotics. In *Proceedings of the 1993 IEEE International Conference on Robotics and Automation, Volume 3* (pp. 761-768). Piscataway, NJ: Institute of Electrical and Electronics Engineers, Inc.

Kroemer, K.H.E., Kroemer, H.B., & Kroemer-Elbert, K.E. (1994). *Ergonomics: How to design for ease and efficiency.* Englewood Cliffs, NJ: Prentice-Hall Inc.

Lapointe, J.F., & Robert, J.M. (2000). Using VR for efficient training of forestry machine operators. *Education and Information Technologies*, *5*(4), 237-250.

McCartney, P.A. (2002). *BORIS User's Guide, SimPack v Release.* Houston, TX: National Aeronautics and Space Administration Johnson Space Center Automation, Robotics, and Simulation Division.

Macedo, J.A., Kaber, D.B., Endsley, M.R., Powanusorn, P., & Myung, S. (1998). The effect of automated compensation for incongruent axes on teleoperator performance. *Human Factors*, *40*(4), 542-553.

Manzey, D., Lorenz, B., Heuer, H., & Sangals, J. (2000). Impairments of manual tracking performance during spaceflight: More converging evidence from a 20-day space mission. *Ergonomics*, *43*(5), 589-609.

Manzey, D., Lorenz, B., & Poljakov, V. (1998). Mental performance in extreme environments: Results from a performance monitoring study during a 438-day spaceflight. *Ergonomics*, *41*(4), 537-559.

Masliah, M.R., & Milgram, P. (2000). Measuring the allocation of control in a 6 degree-of-freedom docking experiment. In *Proceedings of the CHI 2000 Conference on Human Factors in Computing Systems*, (pp. 25-32). New York, NY: ACM Press.

Morphew, M.E., Balmer, D.V., & Khoury, G.J. (2001). Human performance in space. *Ergonomics in Design*, *9*(4), 6-11.

National Aeronautics and Space Administration (NASA). (2002a). *NASA Human Spaceflight - International Space Station Assembly.* Retrieved May 20, 2002 from http://spaceflight.nasa.gov/station/assembly/elements/mss/.

National Aeronautics and Space Administration (NASA). (2002b). *NASA Human Spaceflight - International Space Station Year 1.* Retrieved October 24, 2002 from http://spaceflight.nasa.gov/station/crew/year1/index.html.

National Aeronautics and Space Administration (NASA). (2002c). *Generic Robotics Training (Robo Kine OV C 21001).* A Powerpoint™ presentation. Houston, TX: National Aeronautics and Space Administration, Johnson Space Center.

Nguyen, P.K., & Hughes, P.C. (1994). Teleoperation: From the space shuttle to the space station. In *Progress in Astronautics and Aeronautics: An American Institute of Aeronautics and Astronautics Series* (pp. 353-410). New York, NY: Academic Press.

Sanders, M.S., & McCormick, E.J. (1992). *Human factors in engineering and design (7th ed.).* New York, NY: McGraw-Hill, Inc.

Sauerwein, T.A., & Molino, J.A. (1993). Simulating the replacement of spacecraft modules by means of a telerobot. In *Proceedings of the Human Factors and Ergonomics Society 37th Annual Meeting, Volume 1* (pp. 43-46). Santa Monica, CA: Human Factors and Ergonomics Society.

Schlegel, R.E., & Gilliland, K. (1990). *Evaluation of the Criterion Task Set – Part I: CTS Performance and SWAT Data – Baseline Conditions (U)* (Final Report AAMRL-TR-90-007). WPAFB, OH: Harry G. Armstrong Aerospace Medical Research Laboratory.

Schlegel, R.E., Gilliland, K., & Shehab, R.L. (2002). *The Development and Validation of Remote Manipulator System (RMS) Operator Proficiency and Training Effectiveness Metrics.* NASA Research Grant NRA 01-OPBR-07.

Schlegel, R.E., Shehab, R.L., & Gilliland, K. (2000). *Integrated Crew Performance Assessment and Training.* NASA Research Grant NAG 9-1280.

Schlegel, R.E., Shehab, R.L., Gilliland, K., Eddy, D.R., & Schiflett, S.G. (1995). *Microgravity Effects on Cognitive Performance Measures: Practice Schedules to Acquire and Maintain Performance Stability* (Final Report AL/CF-TR-1994-0040). Brooks AFB, TX: Armstrong Laboratory.

Shah, J., & Darzi, A. (2001). Simulation and skills assessment. In *Proceedings of the IEEE International Workshop on Medical Imaging and Augmented Reality* (pp. 5-9). Piscataway, NJ: Institute of Electrical and Electronics Engineers, Inc.

Shehab, R.L., & Schlegel, R.E. (2000). Applying quality control charts to the analysis of single-subject data sequences. *Human Factors, 42*(4), 604-616.

Smart, K. (2000). *American Society for Gravitational and Space Biology - Human Performance During ISS Operations.* Retrieved October 22, 2002 from http://agsgb.indstate.edu/newsletter/v16_3/human_performance.html.

Taylor, K., & Trevelyan, J. (1998, July 28). *A telerobot on the World Wide Web* [Presented at the 1995 National Conference of the Australian Robot Association]. Retrieved November 9, 2000 from http://telerobot.mech.uwa.edu.au/ROBOT/telerobo.htm.

Tendick, F., Downes, M., Goktekin, T., Cavusoglu, M.C., Feygin, D., Wu, X., Eyal, R., Hegarty, M., & Way, L.W. (2000). A virtual environment testbed for training laparoscopic surgical skills. *Presence: Teleoperators & Virtual Environments*, *9*(3), 236-255.

Uhlarik, J., & Comerford, D.A. (2002). *A review of situation awareness literature relevant to pilot surveillance functions* (Report No. DOT/FAA/AM-02/3). Washington, DC: Office of Aerospace Medicine, Federal Aviation Administration.

Van Erp, J.B.F., & Oving, A.B. (2002). Control performance with three translational degrees of freedom. *Human Factors*, *44*(1), 144-156.

Vidulich, M.A. (2003). Mental workload and situation awareness: Essential concepts for aviation psychology practice. In P.S. Tsang & M.A. Vidulich (Eds.), *Principles and practice of aviation psychology* (pp. 115-146). Mahweh, NJ: Lawrence Erlbaum Associates, Inc.

Wilkinson, S. (2002). Reverse engines! Virtual land ahead! *Popular Science*, *261*(1), 30-31.

Witzke, W.O., Witzke, D.B., Hoskins, J.D., Mastrangelo, M.J., Chu, U.B., George, I.M., & Park, A.E. (2001). A criterion-referenced approach to assessing perioperative skills in a VR environment. In *Proceedings of the IEEE Conference on Advanced Learning Technologies* (pp. 291-294). Piscataway, NJ: Institute of Electrical and Electronics Engineers, Inc.

Zak, H., & Das, H. (1995). Towards a training methodology for skilled teleoperation. *IEEE Transactions on Systems, Man, and Cybernetics*, *25*(2), 313-327.

Zhai, S. & Milgram, P. (1998). Quantifying coordination in multiple DOF movement and its application to evaluating 6 DOF input devices. In *CHI '98 Proceedings of the Conference on Human Factors in Computing Systems* (pp. 320-327). New York, NY: ACM Press / Addison-Wesley Publishing Co.

APPENDIX A

INFORMED CONSENT FORM

Appendix A: Informed Consent Form

Informed Consent Form

For participation in a research project conducted under the auspices of
The University of Oklahoma - Norman Campus

Title of the project: The Development and Evaluation of Remote Manipulator System (RMS) Proficiency and Training Effectiveness Metrics

Investigators: Robert E. Schlegel, Professor, School of Industrial Engineering, 325-3721
Kirby Gilliland, Professor, Department of Psychology, 325-4511
Randa L. Shehab, Associate Professor, Industrial Engineering, 325-3721
Tamy L. Fry, Student, School of Industrial Engineering, tamyfry@ou.edu
Casmir Agbaraji, Student, School of Industrial Engineering, ciagbaraji@hotmail.com
Teryn Bray, Student, School of Industrial Engineering, terynbray@ou.edu
Daniel Walker, Student, School of Industrial Engineering, dwalker@ou.edu

The purpose of this research is to identify and develop ways to numerically evaluate the skills that are learned and used to control a robot arm in a three-dimensional space. The robot arm is shown on a computer video screen and is moved by using two hand controllers similar to a video game. The performance measures that are developed will be used by astronauts and their trainers to evaluate how well the astronauts are learning their tasks and how quickly their skills deteriorate without practice. The robot simulator (also known as the RMS or BORIS) will be implemented on a standard computer workstation and will consist of two computer video monitors and two hand controllers. Participants will be trained on the RMS simulator in a fashion similar to the training that NASA astronauts receive.

I understand that I must be at least 18 years of age to participate in this research and that I will be paid at a rate of $8/hour plus an additional $2/hour bonus for completing the experiment for up to 10 hours spread across approximately one month. By participating in this study, I will be contributing to the development of tools that can be used to improve the training of astronauts and make space operations safer.

I understand that I may expect minimal physical and/or mental discomfort equivalent to that encountered when playing video games on a computer, including eye fatigue and hand/arm fatigue. I understand that the university has no responsibility for any injury that may occur from participation in this study. I understand that no compensation or medical treatment will be provided for any injuries incurred during the course of the study. If I am aware of any condition that would be made worse by this activity, I will refrain from participating in this study.

I understand that I am free to refuse to participate in any procedure or to refuse to answer any question at any time without prejudice to me. I understand that I am free to withdraw my consent and to withdraw from the research at any time without prejudice to me. I also understand that if I choose to withdraw from the research, I will be paid for the time I have contributed.

I understand that by agreeing to participate in this research and signing this form I do not waive any of my legal rights.

I understand that total confidentiality of my identity is assured throughout this research. I understand that the research investigators named above will answer any of my questions relating to the research procedures at any time. If I have questions regarding my rights as a research participant, I understand that I may call the Institutional Review Board at 405-325-8110.

This is to certify that I, ____, hereby agree to participate as a volunteer in a scientific experiment as part of a research program at the University of Oklahoma under the supervision of Drs. Robert E. Schlegel, Kirby Gilliland, and Randa L. Shehab. I understand that my participation is voluntary and that I may withdraw at any time without penalty or loss of benefits.

______________________ ______________________________

Date Signature

APPENDIX B

PARTICIPANT SURVEY

Appendix B: Participant Survey

Participant Survey

Age: ________ Gender: M F Dominant Hand: Left Right

Occupation: ______________________ First Language: ____________

College Major: ____________________ Class (Fr,So,Jr,Sr,Gr): ________

Is your vision 20/20 or corrected to 20/20? Yes No

Do you wear eyeglasses or contact lenses? Yes No

Do you have any other vision condition that would influence computer use? Yes No

If yes, please explain. ______________________________

Describe any experience you have with robotics:

____

____

____

Describe any experience you have with robotic simulation programs:

____

____

____

Please rate the following:

	Low				High
Interest in robotic arm training:	1	2	3	4	5
Interest in robotic arm simulation:	1	2	3	4	5

Describe your experience with each of the following:

- Gymnastics ______________________
- Diving (pool or sky) ______________________
- Other sports (specify) ______________________
- Dance ______________________
- Driving a standard transmission vehicle ______________________
- Aircraft piloting ______________________
- Video games (specify):
  - Puzzle games ______________________
  - Sports games ______________________
  - Adventure games ______________________
- Operation of heavy machinery (forklift, crane) ______________________
- Other activities involving hand controls ______________________
- Remote controlled devices (cars, planes) ______________________
- Computers
  - Business applications ______________________
  - Gaming ______________________

APPENDIX C

DEBRIEFING QUESTIONNAIRE

Appendix C: Debriefing Questionnaire

Debriefing Questionnaire

We are interested in understanding your experience as a participant in this experiment. This questionnaire will take approximately 15 minutes to fill out. Please be very honest in all your responses and don't be afraid of offending the research team. Your thoughts and comments are needed to help us improve our research. All of your responses will be treated as confidential.

1. What is your overall impression of being a participant in this experiment?

2. What was your motivation to participate?

3. Did the experimenters adequately accommodate your schedule?

4. How were you treated by the experimental staff? Please be honest.

5. What was (were) your most preferred task(s)? Why?

6. What was (were) your least preferred task(s)? Why?

7. Did you prefer the internal or external command frame? Why?

Appendix C: Debriefing Questionnaire

8. Did you receive enough instructions about the tasks? If not, what additional instructions do you recommend?

9. Were you adequately trained for the tasks? If not, what additional training would you recommend?

10. Did you develop any strategies to improve your performance? Please specify.

11. Do you have any comments about the testing environment (e.g., lighting, disturbances from other participants, experimenters, etc.)?

12. How did you feel during the testing (energetic, bored, etc)?

13. Outside of the lab, did you spend any time thinking about the simulator or other aspects of the study? Please specify.

14. Would you be interested in participating in future NASA research studies?

APPENDIX D

TEST INSTRUCTIONS

Participant Test Instructions

During each test session, you will perform a total of 37 targeted movement tasks. There are twelve 1-D tasks in which you will move the end effector (EE) along a single axis (X, Y, or Z), eighteen 2-D tasks in which movements are made along two axes (X and Y, or X and Z, or Y and Z), and seven 3-D tasks, in which movements are made along three axes (X and Y and Z). These tasks will help us evaluate your ability to command smooth hand controller inputs and simultaneously control motion along multiple axes. You will be assessed on smoothness of commanded inputs, speed, use of multi-axis control, and the ability to minimize cross-coupling of control axes (control movement in unwanted directions). The entire test session should take approximately one hour to complete.

Three different monitor views will be presented in the display. The largest monitor (on the right) will provide the standard EE camera view. The top left monitor will provide a view from Camera 2, and the bottom left monitor will display the view from the window in the forward wall. These views can help you verify your final target position.

At the start of each task, the EE camera crosshairs will be located at the intersection of a set of gridlines. The experimenter will specify the location of the target (intersection of gridlines) with respect to the start location by stating the direction and distance to move in each direction. For a 2-D task, the experimenter might say "The target is located three meters in the positive X direction, and one meter in the negative Y direction." All directions are given with respect to the hand controller frame. There are three possible control-display mappings based on the command frame and orientation of the end effector. A diagram of the mappings will be located at the workstation for your reference. The experimenter will indicate which mapping applies for each task. Before you begin, the experimenter will ask you to point to the designated target location on (or slightly off) the display. In addition, you will be asked to state the control inputs that you will use to move to the target, such as "I will move the controller forward and to the left."

Your task is to move to the target

- using smooth hand controller inputs
- as quickly as possible
- using multi-axis control
- while minimizing cross-coupling (control movement in unwanted directions).

Plan your motion to stop when the crosshairs are located within the target boundaries. Once you are within the target boundaries, you have completed the task. If the crosshairs are outside of the target boundaries, you must adjust the position until the crosshairs are within the boundaries. Please remove your hand from the controls to indicate that you are finished. The experimenter may make adjustments before you begin the next task.

1-D Tasks

Try to make pure X, Y, or Z inputs to the controller to move in only the desired direction. If the crosshairs drift in a direction you are not commanding, do not try to correct the drift. Figure 1 illustrates final crosshair positions that are "okay" and "not okay" for completing the 1-D tasks.

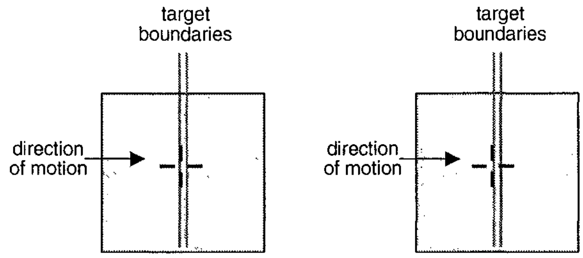

☑ **okay** ⃠ **not okay**

Figure 1. Examples of final crosshair positions that are okay and not okay for the 1-D tasks. To complete each 1-D task, the crosshairs perpendicular to the direction of motion must be completely inside the target (gridline) boundaries.

2-D Tasks

Try to make inputs to the controller to achieve multi-axis motion to improve your time. However, be careful not to command unwanted motion in the third axis. Figure 2 shows final crosshair positions that are "okay" and "not okay" for completing the 2-D tasks.

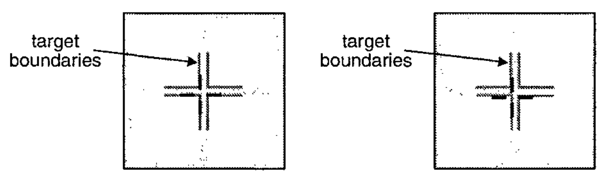

☑ **okay** ⃠ **not okay**

Figure 2. Examples of final crosshair positions that are okay and not okay for the 2-D tasks. To complete each 2-D task, all of the crosshairs must be completely inside the target (gridline intersection) boundaries.

3-D Tasks

Try to make inputs to the controller to achieve multi-axis motion to improve your time. The task is successfully completed when the crosshairs in Monitor 3 are within the target boundaries, as in Figure 2, **AND** the tip of the EE is level with the horizontal bars of the crosshairs in Monitor 1, as shown in Figure 3.

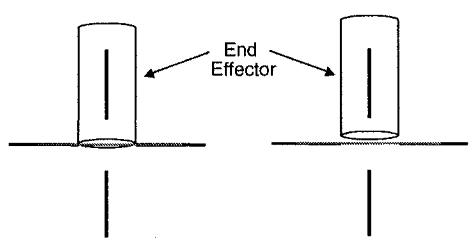

☑ **okay** ⃠ **not okay**

Figure 3. Example of final EE positions that are okay and not okay for the 3-D tasks. To complete each 3-D task, all of the crosshairs must be completely inside the target (gridline intersection) boundaries, and the EE tip must be level with the crosshairs displayed in Monitor 1.

APPENDIX E

STUDY DIRECTIONS

RMS Study Directions

Move to the target

- using smooth hand controller movements
- as quickly as possible
- using multi-axis control
- while minimizing cross-coupling (control movement in unwanted directions).

Hand Controller Frame

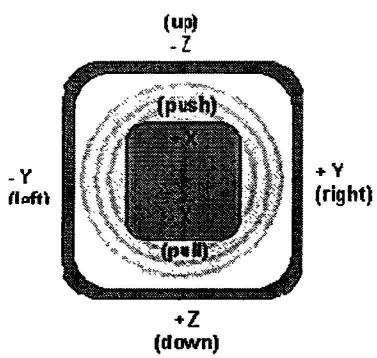

Control-Display Mappings

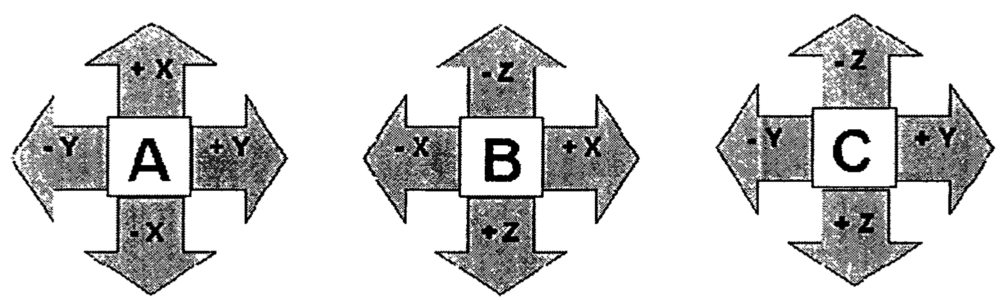

APPENDIX F

TASK DIALOGUES USED DURING TESTING

1-D Task Dialogue:

You will now complete a set of six 1-D tasks. Move to the designated target gridline quickly using smooth commands. Try to input pure X, Y, or Z commands to avoid cross-coupling. If the crosshairs drift off the line parallel to your commanded motion, do not be concerned. Complete the task, and I will correct your position before the next task if necessary.

For this set of tasks, refer to Mapping _____.
Target ____ is located _____ meter(s) in the (+, -) ____ direction.

Q1: Where is the target on the screen?
Q2: What inputs will you use to reach the target?

2-D Task Dialogue:

You will now complete a set of three 2-D tasks. Move to the designated target intersection quickly using smooth, multi-axis commands and avoid cross-coupling. All portions of the crosshairs must be within the target boundaries to complete the task.

For this set of tasks, refer to Mapping _____.
Target ____ is located _____ meter(s) in the (+, -) _____ direction, and _____ meter(s) in the (+, -) _____ direction.

Q1: Where is the target on the screen?
Q2: What inputs will you use to reach the target?

3-D Task Dialogue:

The next task is a 3-D task. To complete this task, move to Target 1 using Monitor 3 to verify the XY location, and the crosshairs in Monitor 1 to find the Z elevation. Remember to move quickly using smooth, multi-axis commands and avoid cross-coupling. To complete the task, the crosshairs must be within the target boundaries in Monitor 3, and the tip of the EE must be level with the horizontal crosshairs in Monitor 1.

For this set of tasks, refer to Mapping _____.
Target 1 is located ______ meter(s) in the (+, -) **X** direction, _____ meter(s) in the (+, -) **Y** direction, and ____ meter(s) in the (+, -) **Z** direction.

Q1: Where is the target on the screen?
Q2: What inputs will you use to reach the target?

APPENDIX G

TASK MOVEMENT PATTERNS AND SEQUENCE DETAILS

Appendix G: Task Movement Patterns and Sequence Details

1-D (Ramping) Task Patterns

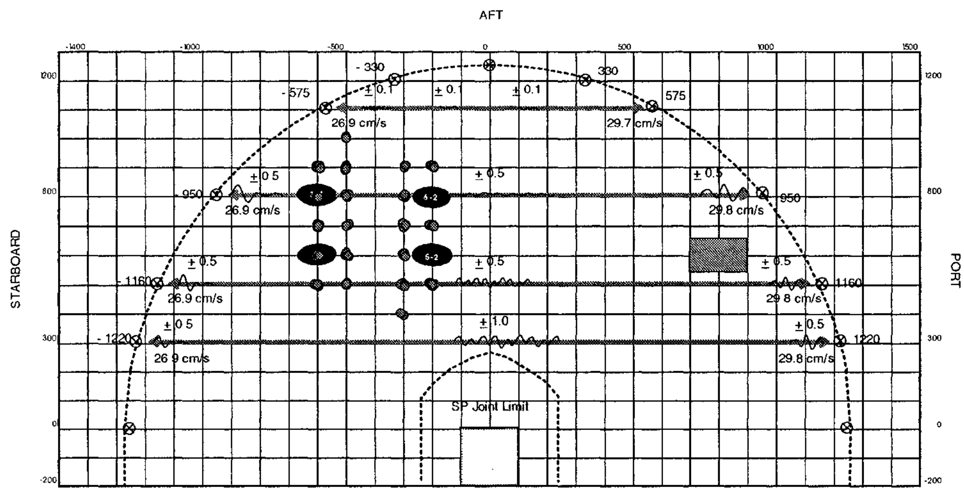

2-D (Multi-Axis) Task Patterns

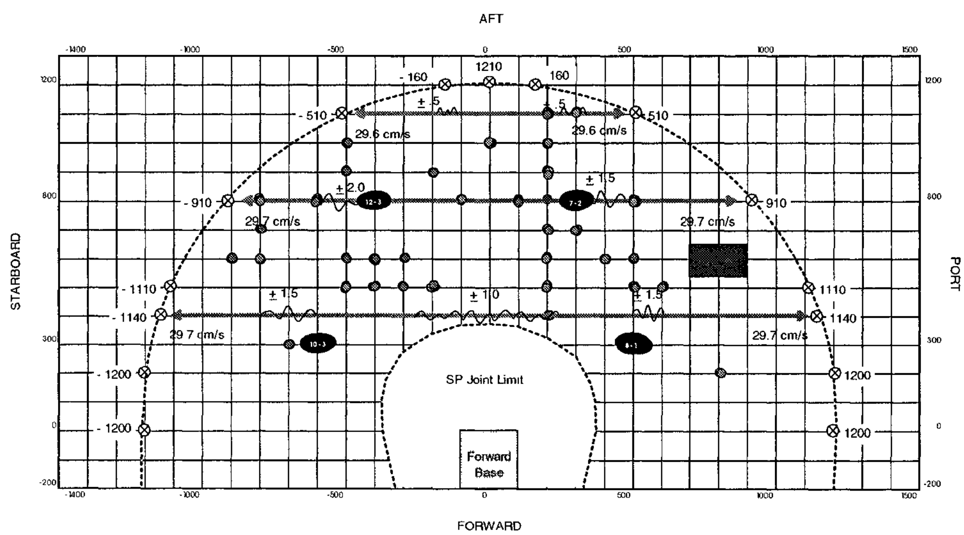

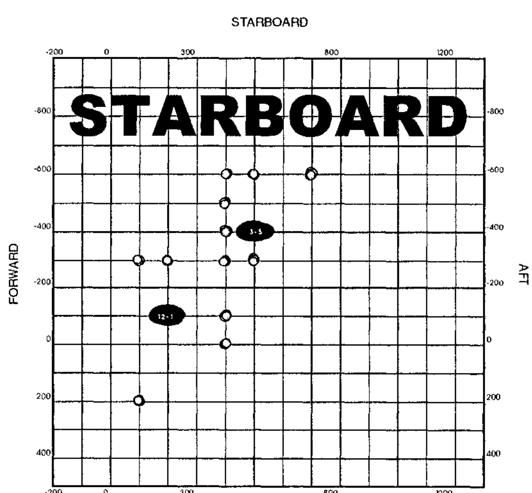

Appendix G: Task Movement Patterns and Sequence Details

1-D Task Order and Start Codes

													Start Code	
Sequence 1	Y	X	-3X	3Y	-X	3X	-Z	Z	-3Y	-Y	-3Z	3Z	1	3
Sequence 2	X	-3X	3Y	-X	3X	Y	Z	-3Y	-Y	-3Z	3Z	-Z	1	3
Sequence 3	-3X	3Y	-X	3X	Y	X	-3Y	-Y	-3Z	3Z	-Z	Z	1	3
Sequence 4	3Y	-X	3X	Y	X	-3X	-Y	-3Z	3Z	-Z	Z	-3Y	4	3
Sequence 5	-X	3X	Y	X	-3X	3Y	-3Z	3Z	-Z	Z	-3Y	-Y	4	3
Sequence 6	3X	Y	X	-3X	3Y	-X	3Z	-Z	Z	-3Y	-Y	-3Z	4	2
Sequence 7	-Y	Z	-3Z	-3Y	-Z	3Z	-X	X	3Y	Y	-3X	3X	3	1
Sequence 8	Z	-3Z	-3Y	-Z	3Z	-Y	X	3Y	Y	-3X	3X	-X	3	1
Sequence 9	-3Z	-3Y	-Z	3Z	-Y	Z	3Y	Y	-3X	3X	-X	X	3	1
Sequence 10	-3Y	-Z	3Z	-Y	Z	-3Z	Y	-3X	3X	-X	X	3Y	2	1
Sequence 11	-Z	3Z	-Y	Z	-3Z	-3Y	-3X	3X	-X	X	3Y	Y	2	1
Sequence 12	3Z	-Y	Z	-3Z	-3Y	-Z	3X	-X	X	3Y	Y	-3X	2	4

Internal Command Frame

1-D Start Points, Joint Angles, and Display Variables

Start Point	Code	Joint Angles						Monitor 1	Camera 2
769, -600, 0, -90, 0, 0	1	-32.1	45.7	-79.0	-56.7	-0.0	32.1	- 66.7 P +07.4 T 1.00 Zoom	
769, -200, 0, -90, 0, 0	2	-7.4	59.3	-103.2	-46.1	0.0	7.4	No Crosshairs	
569, -200, 0, -90, 0, 0	3	-9.8	72.8	-124.9	-37.9	0.0	9.8	Monitor 2	Window View
569, -600, 0, -90, 0, 0	4	-39.6	57.0	-99.1	-47.9	-0.0	39.6		
								Monitor 3	EE Camera
								+00.0 P +0.00 T 1.00 Zoom	

Appendix G: Task Movement Patterns and Sequence Details

2-D Task Order

	2D-1			2D-2			2D-3			2D-4			2D-5			2D-6		
Sequence 1	3X 3Y	3X Y	X -3Y	2X 3Y	3X -3Y	-3X 2Y	3Y Z	-3Y -3Z	-3Y -2Z	3Y 3Z	-Y -3Z	-2Y -3Z	-3X Z	3X -3Z	-X 3Z	-3X 3Z	3X -2Z	2X -3Z
Sequence 2	3X Y	X -3Y	2X 3Y	3X -3Y	-3X 2Y	3X 3Y	-3Y -3Z	-3Y -2Z	3Y 3Z	-Y -3Z	-2Y -3Z	3Y Z	3X -3Z	-X 3Z	-3X 3Z	3X -2Z	2X -3Z	-3X Z
Sequence 3	X -3Y	2X 3Y	3X -3Y	-3X 2Y	3X 3Y	3X Y	-3Y -2Z	3Y 3Z	-Y -3Z	-2Y -3Z	3Y Z	-3Y -3Z	-X 3Z	-3X 3Z	3X -2Z	2X -3Z	-3X Z	3X -3Z
Sequence 4	2X 3Y	3X -3Y	-3X 2Y	3X 3Y	3X Y	X -3Y	3Y 3Z	-Y -3Z	-2Y -3Z	3Y Z	-3Y -3Z	-3Y -2Z	-3X 3Z	3X -2Z	2X -3Z	-3X Z	3X -3Z	-X 3Z
Sequence 5	-Y -3Z	-2Y -3Z	3Y Z	-3Y -3Z	-3Y -2Z	3Y 3Z	3X -2Z	2X -3Z	-3X Z	3X -3Z	-X 3Z	-3X 3Z	3X -3Y	-3X 2Y	3X 3Y	3X Y	X -3Y	2X 3Y
Sequence 6	-2Y -3Z	3Y Z	-3Y -3Z	-3Y -2Z	3Y 3Z	-Y -3Z	2X -3Z	-3X Z	3X -3Z	-X 3Z	-3X 3Z	3X -2Z	-3X 2Y	3X 3Y	3X Y	X -3Y	2X 3Y	3X -3Y
Sequence 7	3Y Z	-3Y -3Z	-3Y -2Z	3Y 3Z	-Y -3Z	-2Y -3Z	-3X Z	3X -3Z	-X 3Z	-3X 3Z	3X -2Z	2X -3Z	3X 3Y	3X Y	X -3Y	2X 3Y	3X -3Y	-3X 2Y
Sequence 8	-3Y -3Z	-3Y -2Z	3Y 3Z	-Y -3Z	-2Y -3Z	3Y Z	3X -3Z	-X 3Z	-3X 3Z	3X -2Z	2X -3Z	-3X Z	3X Y	X -3Y	2X 3Y	3X -3Y	-3X 2Y	3X 3Y
Sequence 9	-X 3Z	-3X 3Z	3X -2Z	2X -3Z	-3X Z	3X -3Z	X -3Y	2X 3Y	3X -3Y	-3X 2Y	3X 3Y	3X Y	-3Y -2Z	3Y 3Z	-Y -3Z	-2Y -3Z	3Y Z	-3Y -3Z
Sequence 10	-3X 3Z	3X -2Z	2X -3Z	-3X Z	3X -3Z	-X 3Z	2X 3Y	3X -3Y	-3X 2Y	3X 3Y	3X Y	X -3Y	3Y 3Z	-Y -3Z	-2Y -3Z	3Y Z	-3Y -3Z	-3Y -2Z
Sequence 11	3X -2Z	2X -3Z	-3X Z	3X -3Z	-X 3Z	-3X 3Z	3X -3Y	-3X 2Y	3X 3Y	3X Y	X -3Y	2X 3Y	-Y -3Z	-2Y -3Z	3Y Z	-3Y -3Z	-3Y -2Z	3Y 3Z
Sequence 12	2X -3Z	-3X Z	3X -3Z	-X 3Z	-3X 3Z	3X -2Z	-3X 2Y	3X 3Y	3X Y	X -3Y	2X 3Y	3X -3Y	-2Y -3Z	3Y Z	-3Y -3Z	-3Y -2Z	3Y 3Z	-Y -3Z

Floor - External Command Frame (xy task combinations)
Floor - Internal Command Frame (yz task combinations)
Starboard Wall - External Command Frame (xz task combinations)

2-D Task Start Codes

	S1	S2	S3	S4
H	5	5	6	5
I	5	5	8	5
L	6	6	7	7
M	7	6	5	6
J	9	10	20	19
K	19	10	18	9

	S5	S6	S7	S8
L	6	5	6	6
M	6	7	7	6
J	10	18	9	10
K	10	20	19	10
H	5	8	5	5
I	5	6	5	5

	S9	S10	S11	S12
J	20	19	10	18
K	18	9	10	20
H	6	5	5	8
I	8	5	5	6
L	7	7	6	5
M	5	6	6	7

2-D Task Start Points, Joint Angles, and Display Variables

Start Point	Code	Joint Angles					
269, -600, 0, -90, 0, 0	5	-57.2	69.0	-119.1	-39.9	0.1	57.2
269, 500, 0, -90, 0, 0	6	71.8	75.5	-128.7	-36.7	0.0	-71.8
769, 300, 0, -90, 0, 0	7	28.3	57.0	-99.4	-47.7	0.0	-28.3
769, -400, 0, -90, 0, 0	8	-20.9	54.1	-94.1	-50.0	-0.0	20.9
500, -1000, -369, 0, -90, 0	9	-51.9	49.7	-73.1	23.5	-38.1	0.0
300, -1000, 30, 0, -90, 0	10	-62.7	31.7	-87.4	55.7	-27.3	-0.1
500, -1000, -130, 0, -90, 0	18	-51.9	18.7	-70.6	51.9	-38.1	0.0
500, -1000, 30, 0, -90, 0	19	-51.9	26.2	-74.3	48.1	-38.1	-0.1
600, -1000, -269, 0, -90, 0	20	-47.4	40.2	-66.6	26.5	-42.6	-0.5

Monitor 1	Camera 2
- 66.7 P +07.4 T 1.00 Zoom	
No Crosshairs	
Monitor 2	Window View
Monitor 3	EE Camera
+00.0 P +0.00 T 1.00 Zoom	

3-D Task Order

Sequence	Task Order 1	2	3	4	5	6	7
1	- X Y 3Z	3X 3Y 3Z	3X -Y -2Z	X -3Y -Z	3X Y -Z	2X 3Y Z	X -2Y -3Z
2	3X 3Y 3Z	3X -Y -2Z	X -3Y -Z	3X Y -Z	2X 3Y Z	X -2Y -3Z	- X Y 3Z
3	3X -Y -2Z	X -3Y -Z	3X Y -Z	2X 3Y Z	X -2Y -3Z	- X Y 3Z	3X 3Y 3Z
4	X -3Y -Z	3X Y -Z	2X 3Y Z	X -2Y -3Z	- X Y 3Z	3X 3Y 3Z	3X -Y -2Z
5	3X Y -Z	2X 3Y Z	X -2Y -3Z	- X Y 3Z	3X 3Y 3Z	3X -Y -2Z	X -3Y -Z
6	2X 3Y Z	X -2Y -3Z	- X Y 3Z	3X 3Y 3Z	3X -Y -2Z	X -3Y -Z	3X Y -Z
7	- X Y 3Z	3X 3Y 3Z	3X -Y -2Z	X -3Y -Z	3X Y -Z	2X 3Y Z	X -2Y -3Z
8	3X 3Y 3Z	3X -Y -2Z	X -3Y -Z	3X Y -Z	2X 3Y Z	X -2Y -3Z	- X Y 3Z
9	3X -Y -2Z	X -3Y -Z	3X Y -Z	2X 3Y Z	X -2Y -3Z	- X Y 3Z	3X 3Y 3Z
10	X -3Y -Z	3X Y -Z	2X 3Y Z	X -2Y -3Z	- X Y 3Z	3X 3Y 3Z	3X -Y -2Z
11	3X Y -Z	2X 3Y Z	X -2Y -3Z	- X Y 3Z	3X 3Y 3Z	3X -Y -2Z	X -3Y -Z
12	2X 3Y Z	X -2Y -3Z	- X Y 3Z	3X 3Y 3Z	3X -Y -2Z	X -3Y -Z	3X Y -Z

Note: None start with task F. Sequence 1-6 repeats for 7-12.

3-D Task Start Points and Display Variables

Task Code	Directions			Start Code	start	end	Monitor 1
A	3X	Y	- Z	11	469, -500, 100	769, -400, 0	Camera 2
B	X	- 3Y	- Z	12	669, -100, 100	769, -400, 0	- 66.7 P + 07.4 T 1.00 Zoom
C	- X	Y	3Z	13	869, -500, -300	769, -400, 0	Monitor 2
D	3X	- Y	- 2Z	14	469, -300, 200	769, -400, 0	Window View
E	2X	3Y	Z	15	569, -700, -100	769, -400, 0	Monitor 3
F	X	- 2Y	- 3Z	16	669, -200, 300	769, -400, 0	EE Camera
G	3X	3Y	3Z	17	469, -700, -300	769, -400, 0	0.00 P 00.0 T 1.00 Zoom

3-D Task Start Codes and Joint Angles

Start Point	Code	Joint Angles					
469, -500, 100, -90, 0, 0	11	-38.4	58.4	-116.7	-31.6	0.0	38.4
669, -100, 100, -90, 0, 0	12	-0.0	58.9	-117.9	-31.0	0.0	0.0
869, -500, -300, -90, 0, 0	13	-24.2	53.8	-61.8	-82.0	-0.0	24.2
469, -300, 200, -90, 0, 0	14	-22.2	53.6	-129.9	-13.7	-0.0	22.2
569, -700, -100, -90, 0, 0	15	-44.5	56.8	-87.0	-59.8	0.0	44.5
669, -200, 300, -90, 0, 0	16	-8.4	38.7	-111.7	-16.9	-0.0	8.4
469, -700, -300, -90, 0, 0	17	-49.4	69.6	-85.3	-74.3	0.0	49.4

APPENDIX H

RUN SEQUENCES

Appendix H: Run Sequences

Sequence	task	Start	number	task	start	task code												
1	set	No.	of axes	plane	code	1	2	3	4	5	6	start point	task sequence					
O	1D-E	1	1	a	1	b	a	j	h	d	g	769, -600, 0, -90, 0, 0	Y	X	-3X	3Y	-X	3X
C	3D-3	2	3	a	13	c	--	--	--	--	--	869, -500, -300, -90, 0, 0	-X Y 3Z	--	--	--	--	--
G	3D-7	3	3	a	17	g	--	--	--	--	--	469, -700, -300, -90, 0, 0	3X 3Y 3Z	--	--	--	--	--
H	XY-1	4	2	a	5	a	m	p	--	--	--	269, -600, 0, -90, 0, 0	3X 3Y	3X Y	X -3Y	--	--	--
D	3D-4	5	3	a	14	d	--	--	--	--	--	469, -300, 200, -90, 0, 0	3X -Y -2Z	--	--	--	--	--
I	XY-2	6	2	a	5	i	b	h	--	--	--	269, -600, 0, -90, 0, 0	2X 3Y	3X -3Y	-3X 2Y	--	--	--
L	YZ-1	7	2	c	6	o	f	j	--	--	--	269, 500, 0, -90, 0, 0	3Y Z	-3Y -3Z	-3Y -2Z	--	--	--
M	YZ-2	8	2	c	7	e	r	l	--	--	--	769, 300, 0, -90, 0, 0	3Y 3Z	-Y -3Z	-2Y -3Z	--	--	--
B	3D-2	9	3	a	12	b	--	--	--	--	--	669, -100, 100, -90, 0, 0	X -3Y -Z	--	--	--	--	--
N	1D-I	10	1	c	3	f	c	k	e	l	i	569, -200, 0, -90, 0, 0	-Z	Z	-3Y	-Y	-3Z	3Z
J	XZ-1	11	2	b	9	n	d	q	--	--	--	500, -1000, -369, 0, -90, 0	-3X Z	3X -3Z	-X 3Z	--	--	--
A	3D-1	12	3	a	11	a	--	--	--	--	--	469, -500, 100, -90, 0, 0	3X Y -Z	--	--	--	--	--
K	XZ-2	13	2	b	19	c	g	k	--	--	--	500, -1000, 30, 0, -90, 0	-3X 3Z	3X -2Z	2X -3Z	--	--	--
E	3D-5	14	3	a	15	e	--	--	--	--	--	569, -700, -100, -90, 0, 0	2X 3Y Z	--	--	--	--	--
F	3D-6	15	3	a	16	f	--	--	--	--	--	669, -200, 300, -90, 0, 0	X -2Y -3Z	--	--	--	--	--

Sequence	task	Start	number	task	start	task code												
5	set	No.	of axes	plane	code	1	2	3	4	5	6	start point	task sequence					
M	YZ-2	1	2	c	6	f	j	e	--	--	--	269, 500, 0, -90, 0, 0	-3Y -3Z	-3Y -2Z	3Y 3Z	--	--	--
A	3D-1	2	3	a	11	a	--	--	--	--	--	469, -500, 100, -90, 0, 0	3X Y -Z	--	--	--	--	--
L	YZ-1	3	2	c	6	r	l	o	--	--	--	269, 500, 0, -90, 0, 0	-Y -3Z	-2Y -3Z	3Y Z	--	--	--
O	1D-E	4	1	a	4	d	g	b	a	j	h	569, -600, 0, -90, 0, 0	-X	3X	Y	X	-3X	3Y
E	3D-5	5	3	a	15	e	--	--	--	--	--	569, -700, -100, -90, 0, 0	2X 3Y Z	--	--	--	--	--
F	3D-6	6	3	a	16	f	--	--	--	--	--	669, -200, 300, -90, 0, 0	X -2Y -3Z	--	--	--	--	--
C	3D-3	7	3	a	13	c	--	--	--	--	--	869, -500, -300, -90, 0, 0	-X Y 3Z	--	--	--	--	--
J	XZ-1	8	2	b	10	g	k	n	--	--	--	300, -1000, 30, 0, -90, 0	3X -2Z	2X -3Z	-3X Z	--	--	--
K	XZ-2	9	2	b	10	d	q	c	--	--	--	300, -1000, 30, 0, -90, 0	3X -3Z	-X 3Z	-3X 3Z	--	--	--
G	3D-7	10	3	a	17	g	--	--	--	--	--	469, -700, -300, -90, 0, 0	3X 3Y 3Z	--	--	--	--	--
D	3D-4	11	3	a	14	d	--	--	--	--	--	469, -300, 200, -90, 0, 0	3X -Y -2Z	--	--	--	--	--
I	XY-2	12	2	a	5	m	p	i	--	--	--	269, -600, 0, -90, 0, 0	3X Y	X -3Y	2X 3Y	--	--	--
H	XY-1	13	2	a	5	b	h	a	--	--	--	269, -600, 0, -90, 0, 0	3X -3Y	-3X 2Y	3X 3Y	--	--	--
B	3D-2	14	3	a	12	b	--	--	--	--	--	669, -100, 100, -90, 0, 0	X -3Y -Z	--	--	--	--	--
N	1D-I	15	1	c	3	l	i	f	c	k	e	569, -200, 0, -90, 0, 0	-3Z	3Z	-Z	Z	-3Y	-Y

Sequence	task	Start	number	task	start	task code												
9	set	No.	of axes	plane	code	1	2	3	4	5	6	start point	task sequence					
J	XZ-1	1	2	b	20	q	c	g	--	--	--	600, -1000, -269, 0, -90, 0	-X 3Z	-3X 3Z	3X -2Z	--	--	--
D	3D-4	2	3	a	14	d	--	--	--	--	--	469, -300, 200, -90, 0, 0	3X -Y -2Z	--	--	--	--	--
N	1D-I	3	1	c	3	l	k	f	i	e	c	569, -200, 0, -90, 0, 0	-3Z	-3Y	-Z	3Z	-Y	Z
K	XZ-2	4	2	b	18	k	n	d	--	--	--	500, -1000, 130, 0, -90, 0	2X -3Z	-3X Z	3X -3Z	--	--	--
B	3D-2	5	3	a	12	b	--	--	--	--	--	669, -100, 100, -90, 0, 0	X -3Y -Z	--	--	--	--	--
H	XY-1	6	2	a	6	p	i	b	--	--	--	269, 500, 0, -90, 0, 0	X -3Y	2X 3Y	3X -3Y	--	--	--
A	3D-1	7	3	a	11	a	--	--	--	--	--	469, -500, 100, -90, 0, 0	3X Y -Z	--	--	--	--	--
E	3D-5	8	3	a	15	e	--	--	--	--	--	569, -700, -100, -90, 0, 0	2X 3Y Z	--	--	--	--	--
O	1D-E	9	1	a	1	h	b	j	g	d	a	769, -600, 0, -90, 0, 0	3Y	Y	-3X	3X	-X	X
F	3D-6	10	3	a	16	f	--	--	--	--	--	669, -200, 300, -90, 0, 0	X -2Y -3Z	--	--	--	--	--
C	3D-3	11	3	a	13	c	--	--	--	--	--	869, -500, -300, -90, 0, 0	-X Y 3Z	--	--	--	--	--
I	XY-2	12	2	a	8	h	a	m	--	--	--	769, -400, 0, -90, 0, 0	-3X 2Y	3X 3Y	3X Y	--	--	--
G	3D-7	13	3	a	17	g	--	--	--	--	--	469, -700, -300, -90, 0, 0	3X 3Y 3Z	--	--	--	--	--
M	YZ-2	14	2	c	5	l	o	f	--	--	--	269, -600, 0, -90, 0, 0	-2Y -3Z	3Y Z	-3Y -3Z	--	--	--
L	YZ-1	15	2	c	7	j	e	r	--	--	--	769, 300, 0, -90, 0, 0	-3Y -2Z	3Y 3Z	-Y -3Z	--	--	--

Sequence	task	Start	number	task	start	task code												
2	set	No.	of axes	plane	code	1	2	3	4	5	6	start point	task sequence					
O	1D-E	1	1	a	1	a	j	h	d	g	b	769, -600, 0, -90, 0, 0	X	-3X	3Y	-X	3X	Y
H	XY-1	2	2	a	5	m	p	i	--	--	--	269, -600, 0, -90, 0, 0	3X Y	X -3Y	2X 3Y	--	--	--
G	3D-7	3	3	a	17	g	--	--	--	--	--	469, -700, -300, -90, 0, 0	3X 3Y 3Z	--	--	--	--	--
I	XY-2	4	2	a	5	b	h	a	--	--	--	269, -600, 0, -90, 0, 0	3X -3Y	-3X 2Y	3X 3Y	--	--	--
N	1D-I	5	1	c	3	c	k	e	l	i	f	569, -200, 0, -90, 0, 0	Z	-3Y	-Y	-3Z	3Z	-Z
D	3D-4	6	3	a	14	d	--	--	--	--	--	469, -300, 200, -90, 0, 0	3X -Y -2Z	--	--	--	--	--
B	3D-2	7	3	a	12	b	--	--	--	--	--	669, -100, 100, -90, 0, 0	X -3Y -Z	--	--	--	--	--
A	3D-1	8	3	a	11	a	--	--	--	--	--	469, -500, 100, -90, 0, 0	3X Y -Z	--	--	--	--	--
L	YZ-1	9	2	c	6	f	j	e	--	--	--	269, 500, 0, -90, 0, 0	-3Y -3Z	-3Y -2Z	3Y 3Z	--	--	--
M	YZ-2	10	2	c	6	r	l	o	--	--	--	269, 500, 0, -90, 0, 0	-Y -3Z	-2Y -3Z	3Y Z	--	--	--
E	3D-5	11	3	a	15	e	--	--	--	--	--	569, -700, -100, -90, 0, 0	2X 3Y Z	--	--	--	--	--
F	3D-6	12	3	a	16	f	--	--	--	--	--	669, -200, 300, -90, 0, 0	X -2Y -3Z	--	--	--	--	--
J	XZ-1	13	2	b	10	d	q	c	--	--	--	300, -1000, 30, 0, -90, 0	3X -3Z	-X 3Z	-3X 3Z	--	--	--
K	XZ-2	14	2	b	10	g	k	n	--	--	--	300, -1000, 30, 0, -90, 0	3X -2Z	2X -3Z	-3X Z	--	--	--
C	3D-3	15	3	a	13	c	--	--	--	--	--	869, -500, -300, -90, 0, 0	-X Y 3Z	--	--	--	--	--

Appendix H: Run Sequences

Sequence 6	task set	Start No.	number of axes	task plane	start code	task code 1	2	3	4	5	6	start point	task sequence					
M	YZ-2	1	2	c	7	j	e	r	--	--	--	269, -600, 0, -90, 0, 0	-3Y -2Z	3Y 3Z	-Y -3Z	--	--	--
E	3D-5	2	3	a	15	e	--	--	--	--	--	569, -700, -100, -90, 0, 0	2X 3Y Z	--	--	--	--	--
L	YZ-1	3	2	c	5	l	o	f	--	--	--	769, 300, 0, -90, 0, 0	-2Y -3Z	3Y Z	-3Y -3Z	--	--	--
F	3D-6	4	3	a	16	f	--	--	--	--	--	669, -200, 300, -90, 0, 0	X -2Y -3Z	--	--	--	--	--
C	3D-3	5	3	a	13	c	--	--	--	--	--	869, -500, -300, -90, 0, 0	-X Y 3Z	--	--	--	--	--
O	1D-E	6	1	a	4	g	b	a	j	h	d	569, -600, 0, -90, 0, 0	3X	Y	X	-3X	3Y	-X
G	3D-7	7	3	a	17	g	--	--	--	--	--	469, -700, -300, -90, 0, 0	3X 3Y 3Z	--	--	--	--	--
D	3D-4	8	3	a	14	d	--	--	--	--	--	469, -300, 200, -90, 0, 0	3X -Y -2Z	--	--	--	--	--
J	XZ-1	9	2	b	18	k	n	d	--	--	--	500, -1000, 130, 0, -90, 0	2X -3Z	-3X Z	3X -3Z	--	--	--
B	3D-2	10	3	a	12	b	--	--	--	--	--	669, -100, 100, -90, 0, 0	X -3Y -Z	--	--	--	--	--
K	XZ-2	11	2	b	20	q	c	g	--	--	--	600, -1000, -269, 0, -90, 0	-X 3Z	-3X 3Z	3X -2Z	--	--	--
I	XY-2	12	2	a	6	p	i	b	--	--	--	269, 500, 0, -90, 0, 0	X -3Y	2X 3Y	3X -3Y	--	--	--
H	XY-1	13	2	a	8	h	a	m	--	--	--	769, -400, 0, -90, 0, 0	-3X 2Y	3X 3Y	3X Y	--	--	--
A	3D-1	14	3	a	11	a	--	--	--	--	--	469, -500, 100, -90, 0, 0	3X Y -Z	--	--	--	--	--
N	1D-I	15	1	c	2	i	f	c	k	e	l	769, -200, 0, -90, 0, 0	3Z	-Z	Z	-3Y	-Y	-3Z

Sequence 10	task set	Start No.	number of axes	task plane	start code	task code 1	2	3	4	5	6	start point	task sequence					
J	XZ-1	1	2	b	19	c	g	k	--	--	--	500, -1000, 30, 0, -90, 0	-3X 3Z	3X -2Z	2X -3Z	--	--	--
N	1D-I	2	1	c	2	k	f	i	e	c	l	769, -200, 0, -90, 0, 0	-3Y	-Z	3Z	-Y	Z	-3Z
B	3D-2	3	3	a	12	b	--	--	--	--	--	669, -100, 100, -90, 0, 0	X -3Y -Z	--	--	--	--	--
A	3D-1	4	3	a	11	a	--	--	--	--	--	469, -500, 100, -90, 0, 0	3X Y -Z	--	--	--	--	--
E	3D-5	5	3	a	15	e	--	--	--	--	--	569, -700, -100, -90, 0, 0	2X 3Y Z	--	--	--	--	--
K	XZ-2	6	2	b	9	n	d	q	--	--	--	500, -1000, -369, 0, -90, 0	-3X Z	3X -3Z	-X 3Z	--	--	--
I	XY-2	7	2	a	5	a	m	p	--	--	--	269, -600, 0, -90, 0, 0	3X 3Y	3X Y	X -3Y	--	--	--
F	3D-6	8	3	a	16	f	--	--	--	--	--	669, -200, 300, -90, 0, 0	X -2Y -3Z	--	--	--	--	--
C	3D-3	9	3	a	13	c	--	--	--	--	--	869, -500, -300, -90, 0, 0	-X Y 3Z	--	--	--	--	--
H	XY-1	10	2	a	5	i	b	h	--	--	--	269, -600, 0, -90, 0, 0	2X 3Y	3X -3Y	-3X 2Y	--	--	--
L	YZ-1	11	2	c	7	e	r	l	--	--	--	769, 300, 0, -90, 0, 0	3Y 3Z	-Y -3Z	-2Y -3Z	--	--	--
G	3D-7	12	3	a	17	g	--	--	--	--	--	469, -700, -300, -90, 0, 0	3X 3Y 3Z	--	--	--	--	--
O	1D-E	13	1	a	1	b	j	g	d	a	h	769, -600, 0, -90, 0, 0	Y	-3X	3X	-X	X	3Y
M	YZ-2	14	2	c	6	o	f	j	--	--	--	269, 500, 0, -90, 0, 0	3Y Z	-3Y -3Z	-3Y -2Z	--	--	--
D	3D-4	15	3	a	14	d	--	--	--	--	--	469, -300, 200, -90, 0, 0	3X -Y -2Z	--	--	--	--	--

Sequence 3	task set	Start No.	number of axes	task plane	start code	task code 1	2	3	4	5	6	start point	task sequence					
D	3D-4	1	3	a	14	d	--	--	--	--	--	469, -300, 200, -90, 0, 0	3X -Y -2Z	--	--	--	--	--
O	1D-E	2	1	a	1	j	h	d	g	b	a	769, -600, 0, -90, 0, 0	-3X	3Y	-X	3X	Y	X
H	XY-1	3	2	a	6	p	i	b	--	--	--	269, 500, 0, -90, 0, 0	X -3Y	2X 3Y	3X -3Y	--	--	--
B	3D-2	4	3	a	12	b	--	--	--	--	--	669, -100, 100, -90, 0, 0	X -3Y -Z	--	--	--	--	--
I	XY-2	5	2	a	8	h	a	m	--	--	--	769, -400, 0, -90, 0, 0	-3X 2Y	3X 3Y	3X Y	--	--	--
A	3D-1	6	3	a	11	a	--	--	--	--	--	469, -500, 100, -90, 0, 0	3X Y -Z	--	--	--	--	--
E	3D-5	7	3	a	15	e	--	--	--	--	--	569, -700, -100, -90, 0, 0	2X 3Y Z	--	--	--	--	--
N	1D-I	8	1	c	3	k	e	l	i	f	c	569, -200, 0, -90, 0, 0	-3Y	-Y	-3Z	3Z	-Z	Z
F	3D-6	9	3	a	16	f	--	--	--	--	--	669, -200, 300, -90, 0, 0	X -2Y -3Z	--	--	--	--	--
C	3D-3	10	3	a	13	c	--	--	--	--	--	869, -500, -300, -90, 0, 0	-X Y 3Z	--	--	--	--	--
L	YZ-1	11	2	c	7	j	e	r	--	--	--	769, 300, 0, -90, 0, 0	-3Y -2Z	3Y 3Z	-Y -3Z	--	--	--
G	3D-7	12	3	a	17	g	--	--	--	--	--	469, -700, -300, -90, 0, 0	3X 3Y 3Z	--	--	--	--	--
M	YZ-2	13	2	c	5	l	o	f	--	--	--	269, -600, 0, -90, 0, 0	-2Y -3Z	3Y Z	-3Y -3Z	--	--	--
K	XZ-2	14	2	b	18	k	n	d	--	--	--	500, -1000, 130, 0, -90, 0	2X -3Z	-3X Z	3X -3Z	--	--	--
J	XZ-1	15	2	b	20	q	c	g	--	--	--	600, -1000, -269, 0, -90, 0	-X 3Z	-3X 3Z	3X -2Z	--	--	--

Sequence 7	task set	Start No.	number of axes	task plane	start code	task code 1	2	3	4	5	6	start point	task sequence					
C	3D-3	1	3	a	13	c	--	--	--	--	--	869, -500, -300, -90, 0, 0	-X Y 3Z	--	--	--	--	--
G	3D-7	2	3	a	17	g	--	--	--	--	--	469, -700, -300, -90, 0, 0	3X 3Y 3Z	--	--	--	--	--
M	YZ-2	3	2	c	6	e	r	l	--	--	--	269, 500, 0, -90, 0, 0	3Y 3Z	-Y -3Z	-2Y -3Z			
D	3D-4	4	3	a	14	d	--	--	--	--	--	469, -300, 200, -90, 0, 0	3X -Y -2Z	--	--	--	--	--
L	YZ-1	5	2	c	7	o	f	j	--	--	--	769, 300, 0, -90, 0, 0	3Y Z	-3Y -3Z	-3Y -2Z			
K	XZ-2	6	2	b	19	c	g	k	--	--	--	500, -1000, 30, 0, -90, 0	-3X 3Z	3X -2Z	2X -3Z			
J	XZ-1	7	2	b	9	n	d	q	--	--	--	500, -1000, -369, 0, -90, 0	-3X Z	3X -3Z	-X 3Z			
B	3D-2	8	3	a	12	b	--	--	--	--	--	669, -100, 100, -90, 0, 0	X -3Y -Z	--	--	--	--	--
N	1D-I	9	1	c	3	e	c	l	k	f	i	569, -200, 0, -90, 0, 0	-Y	Z	-3Z	-3Y	-Z	3Z
H	XY-1	10	2	a	5	a	m	p	--	--	--	269, -600, 0, -90, 0, 0	3X 3Y	3X Y	X -3Y			
A	3D-1	11	3	a	11	a	--	--	--	--	--	469, -500, 100, -90, 0, 0	3X Y -Z	--	--	--	--	--
I	XY-2	12	2	a	5	i	b	h	--	--	--	269, -600, 0, -90, 0, 0	2X 3Y	3X -3Y	-3X 2Y			
E	3D-5	13	3	a	15	e	--	--	--	--	--	569, -700, -100, -90, 0, 0	2X 3Y Z	--	--	--	--	--
F	3D-6	14	3	a	16	f	--	--	--	--	--	669, -200, 300, -90, 0, 0	X -2Y -3Z	--	--	--	--	--
O	1D-E	15	1	a	1	d	a	h	b	j	g	769, -600, 0, -90, 0, 0	-X	X	3Y	Y	-3X	3X

Appendix H: Run Sequences

Sequence 11	task set	Start No.	number of axes	task plane	start code	task code 1	2	3	4	5	6	start point	task sequence					
N	1D-I	1	1	c	2	f	i	e	c	l	k	769, -200, 0, -90, 0, 0	-Z	3Z	-Y	Z	-3Z	-3Y
K	XZ-2	2	2	b	10	d	q	c	--	--	--	300, -1000, 30, 0, -90, 0	3X -3Z	-X 3Z	-3X 3Z	--	--	--
A	3D-1	3	3	a	11	a	--	--	--	--	--	469, -500, 100, -90, 0, 0	3X Y -Z	--	--	--	--	--
J	XZ-1	4	2	b	10	g	k	n	--	--	--	300, -1000, 30, 0, -90, 0	3X -2Z	2X -3Z	-3X Z	--	--	--
E	3D-5	5	3	a	15	e	--	--	--	--	--	569, -700, -100, -90, 0, 0	2X 3Y Z	--	--	--	--	--
F	3D-6	6	3	a	16	f	--	--	--	--	--	669, -200, 300, -90, 0, 0	X -2Y -3Z	--	--	--	--	--
O	1D-E	7	1	a	1	j	g	d	a	h	b	769, -600, 0, -90, 0, 0	-3X	3X	-X	X	3Y	Y
C	3D-3	8	3	a	13	c	--	--	--	--	--	869, -500, -300, -90, 0, 0	-X Y 3Z	--	--	--	--	--
G	3D-7	9	3	a	17	g	--	--	--	--	--	469, -700, -300, -90, 0, 0	3X 3Y 3Z	--	--	--	--	--
I	XY-2	10	2	a	5	m	p	i	--	--	--	269, -600, 0, -90, 0, 0	3X Y	X -3Y	2X 3Y	--	--	--
D	3D-4	11	3	a	14	d	--	--	--	--	--	469, -300, 200, -90, 0, 0	3X -Y -2Z	--	--	--	--	--
H	XY-1	12	2	a	5	b	h	a	--	--	--	269, -600, 0, -90, 0, 0	3X -3Y	-3X 2Y	3X 3Y	--	--	--
L	YZ-1	13	2	c	6	r	l	o	--	--	--	269, 500, 0, -90, 0, 0	-Y -3Z	-2Y -3Z	3Y Z	--	--	--
M	YZ-2	14	2	c	6	f	j	e	--	--	--	269, 500, 0, -90, 0, 0	-3Y -3Z	-3Y -2Z	3Y 3Z	--	--	--
B	3D-2	15	3	a	12	b	--	--	--	--	--	669, -100, 100, -90, 0, 0	X -3Y -Z	--	--	--	--	--

Sequence 4	task set	Start No.	number of axes	task plane	start code	task code 1	2	3	4	5	6	start point	task sequence					
B	3D-2	1	3	a	12	b	--	--	--	--	--	669, -100, 100, -90, 0, 0	X -3Y -Z	--	--	--	--	--
I	XY-2	2	2	a	5	a	m	p	--	--	--	269, -600, 0, -90, 0, 0	3X 3Y	3X Y	X -3Y	--	--	--
O	1D-E	3	1	a	4	h	d	g	b	a	j	569, -600, 0, -90, 0, 0	3Y	-X	3X	Y	X	-3X
A	3D-1	4	3	a	11	a	--	--	--	--	--	469, -500, 100, -90, 0, 0	3X Y -Z	--	--	--	--	--
E	3D-5	5	3	a	15	e	--	--	--	--	--	569, -700, -100, -90, 0, 0	2X 3Y Z	--	--	--	--	--
F	3D-6	6	3	a	16	f	--	--	--	--	--	669, -200, 300, -90, 0, 0	X -2Y -3Z	--	--	--	--	--
H	XY-1	7	2	a	5	i	b	h	--	--	--	269, -600, 0, -90, 0, 0	2X 3Y	3X -3Y	-3X 2Y	--	--	--
M	YZ-2	8	2	c	7	o	f	j	--	--	--	769, 300, 0, -90, 0, 0	3Y Z	-3Y -3Z	-3Y -2Z	--	--	--
C	3D-3	9	3	a	13	c	--	--	--	--	--	869, -500, -300, -90, 0, 0	-X Y 3Z	--	--	--	--	--
G	3D-7	10	3	a	17	g	--	--	--	--	--	469, -700, -300, -90, 0, 0	3X 3Y 3Z	--	--	--	--	--
L	YZ-1	11	2	c	6	e	r	l	--	--	--	269, 500, 0, -90, 0, 0	3Y 3Z	-Y -3Z	-2Y -3Z	--	--	--
K	XZ-2	12	2	b	9	n	d	q	--	--	--	500, -1000, -369, 0, -90, 0	-3X Z	3X -3Z	-X 3Z	--	--	--
D	3D-4	13	3	a	14	d	--	--	--	--	--	469, -300, 200, -90, 0, 0	3X -Y -2Z	--	--	--	--	--
N	1D-I	14	1	c	3	e	l	i	f	c	k	569, -200, 0, -90, 0, 0	-Y	-3Z	3Z	-Z	Z	-3Y
J	XZ-1	15	2	b	19	c	g	k	--	--	--	500, -1000, 30, 0, -90, 0	-3X 3Z	3X -2Z	2X -3Z	--	--	--

Sequence 8	task set	Start No.	number of axes	task plane	start code	task code 1	2	3	4	5	6	start point	task sequence					
G	3D-7	1	3	a	17	g	--	--	--	--	--	469, -700, -300, -90, 0, 0	3X 3Y 3Z	--	--	--	--	--
D	3D-4	2	3	a	14	d	--	--	--	--	--	469, -300, 200, -90, 0, 0	3X -Y -2Z	--	--	--	--	--
B	3D-2	3	3	a	12	b	--	--	--	--	--	669, -100, 100, -90, 0, 0	X -3Y -Z	--	--	--	--	--
M	YZ-2	4	2	c	6	r	l	0	--	--	--	269, 500, 0, -90, 0, 0	-Y -3Z	-2Y -3Z	3Y Z	--	--	--
L	YZ-1	5	2	c	6	f	j	e	--	--	--	269, 500, 0, -90, 0, 0	-3Y -3Z	-3Y -2Z	3Y 3Z	--	--	--
A	3D-1	6	3	a	11	a	--	--	--	--	--	469, -500, 100, -90, 0, 0	3X Y -Z	--	--	--	--	--
E	3D-5	7	3	a	15	e	--	--	--	--	--	569, -700, -100, -90, 0, 0	2X 3Y Z	--	--	--	--	--
K	XZ-2	8	2	b	10	g	k	n	--	--	--	300, -1000, 30, 0, -90, 0	3X -2Z	2X -3Z	-3X Z	--	--	--
J	XZ-1	9	2	b	10	d	q	c	--	--	--	300, -1000, 30, 0, -90, 0	3X -3Z	-X 3Z	-3X 3Z	--	--	--
F	3D-6	10	3	a	16	f	--	--	--	--	--	669, -200, 300, -90, 0, 0	X -2Y -3Z	--	--	--	--	--
N	1D-I	11	1	c	3	c	l	k	f	i	e	569, -200, 0, -90, 0, 0	Z	-3Z	-3Y	-Z	3Z	-Y
H	XY-1	12	2	a	5	m	p	i	--	--	--	269, -600, 0, -90, 0, 0	3X Y	X -3Y	2X 3Y	--	--	--
C	3D-3	13	3	a	13	c	--	--	--	--	--	869, -500, -300, -90, 0, 0	-X Y 3Z	--	--	--	--	--
I	XY-2	14	2	a	5	b	h	a	--	--	--	269, -600, 0, -90, 0, 0	3X -3Y	-3X 2Y	3X 3Y	--	--	--
O	1D-E	15	1	a	1	a	h	b	j	g	d	769, -600, 0, -90, 0, 0	X	3Y	Y	-3X	3X	-X

Sequence 12	task set	Start No.	number of axes	task plane	start code	task code 1	2	3	4	5	6	start point	task sequence					
N	1D-I	1	1	c	2	i	e	c	l	k	f	769, -200, 0, -90, 0, 0	3Z	-Y	Z	-3Z	-3Y	-Z
E	3D-5	2	3	a	15	e	--	--	--	--	--	569, -700, -100, -90, 0, 0	2X 3Y Z	--	--	--	--	--
F	3D-6	3	3	a	16	f	--	--	--	--	--	669, -200, 300, -90, 0, 0	X -2Y -3Z	--	--	--	--	--
C	3D-3	4	3	a	13	c	--	--	--	--	--	869, -500, -300, -90, 0, 0	-X Y 3Z	--	--	--	--	--
K	XZ-2	5	2	b	20	q	c	g	--	--	--	600, -1000, -269, 0, -90, 0	-X 3Z	-3X 3Z	3X -2Z	--	--	--
J	XZ-1	6	2	b	18	k	n	d	--	--	--	500, -1000, 130, 0, -90, 0	2X -3Z	-3X Z	3X -3Z	--	--	--
G	3D-7	7	3	a	17	g	--	--	--	--	--	469, -700, -300, -90, 0, 0	3X 3Y 3Z	--	--	--	--	--
D	3D-4	8	3	a	14	d	--	--	--	--	--	469, -300, 200, -90, 0, 0	3X -Y -2Z	--	--	--	--	--
I	XY-2	9	2	a	6	p	i	b	--	--	--	269, 500, 0, -90, 0, 0	X -3Y	2X 3Y	3X -3Y	--	--	--
H	XY-1	10	2	a	8	h	a	m	--	--	--	769, -400, 0, -90, 0, 0	-3X 2Y	3X 3Y	3X Y	--	--	--
B	3D-2	11	3	a	12	b	--	--	--	--	--	669, -100, 100, -90, 0, 0	X -3Y -Z	--	--	--	--	--
O	1D-E	12	1	a	4	g	d	a	h	b	j	569, -600, 0, -90, 0, 0	3X	-X	X	3Y	Y	-3X
L	YZ-1	13	2	c	5	l	o	f	--	--	--	269, -600, 0, -90, 0, 0	-2Y -3Z	3Y Z	-3Y -3Z	--	--	--
A	3D-1	14	3	a	11	a	--	--	--	--	--	469, -500, 100, -90, 0, 0	3X Y -Z	--	--	--	--	--
M	YZ-2	15	2	c	7	j	e	r	--	--	--	769, 300, 0, -90, 0, 0	-3Y -2Z	3Y 3Z	-Y -3Z	--	--	--

APPENDIX I

SUBJECTIVE EVALUATION OF PARTICIPANT PERFORMANCE

Appendix I: Subjective Evaluation of Participant Performance

Participant	Ramping	Multi-Axis	Comments
101	poor	poor	Poor ramping. Very slow. Long lag times. Mostly single-axis control. Lots of corrections. Pulsing of controller.
106	poor	fair	Slow. Poor ramping. Some multi-axis, but mainly single or dual axis control. High number of large accelerations. Better on 2-D than 3-D tasks.
108	poor	poor	Ramping inconsistent. Long completion times. Many corrections. Attempted multi-axis, but poor control.
109	good	good	Smooth / controlled inputs. Ramping good. Consistent performance, but slow. Very good on 2-D tasks. Corrections mostly in Z on 3-D tasks.
110	poor	fair	No ramping. Heavy-handed on controller. High velocities. Many corrections. Short lag times and high percent of multi-axis, but inconsistent. Poor control.
111	poor	fair	No ramping. "Full throttle". Many corrections / pulsing of controller. Short lag times. Straight line path.
122	good	good	Smooth, proportional control (straight line). Most corrections in Z. Fast. Short lag times / completion times. Consistent. High accuracy.
123	fair	poor	Ramping inconsistent. High velocities / accelerations. Many corrections. Erratic path. Multi axis use better on 2-D tasks.
124	fair	fair	Inconsistent ramping. Many corrections. Attempts multi-axis, but inconsistent control. Long completion times on 3-D tasks. Good accuracy and completion times on 2-D tasks.
127	fair	good	Inconsistent ramping. Good multi-axis with decent control. Quick. Consistent. Good accuracy and completion times on 2-D tasks.
128	good	fair	Smooth, controlled ramping. Slow. Long lag times. Long completion times, but few corrections.
129	good	fair	Controlled ramping, but fast. Good multi-axis use, but inconsistent accuracy.